NUREG/IA-0160

International Agreement Report

Analysis of the Critical Flow Model in TRAC-BF1

Prepared by
M. Gómez, E. Valero, I. E. Parra

Department of Applied Mathematics and Statistics
Universidad Politécnica de Madrid
Spain

Office of Nuclear Regulatory Research
U.S. Nuclear Regulatory Commission
Washington, DC 20555–0001

May 1999

Prepared as part of
The Agreement on Research Participation and Technical Exchange
under the International Code Application and Maintenance Program (CAMP)

Published by
U.S. Nuclear Regulatory Commission

AVAILABILITY NOTICE

Availability of Reference Materials Cited in NRC Publications

NRC publications in the NUREG series, NRC regulations, and *Title 10, Energy,* of the *Code of Federal Regulations,* may be purchased from one of the following sources:

1. The Superintendent of Documents
   U.S. Government Printing Office
   P.O. Box 37082
   Washington, DC 20402–9328
   <http://www.access.gpo.gov/su_docs>
   202–512–1800

2. The National Technical Information Service
   Springfield, VA 22161–0002
   <http://www.ntis.gov/ordernow>
   703–487–4650

The NUREG series comprises (1) brochures (NUREG/BR-XXXX), (2) proceedings of conferences (NUREG/CP-XXXX), (3) reports resulting from international agreements (NUREG/IA-XXXX), (4) technical and administrative reports and books [(NUREG-XXXX) or (NUREG/CR-XXXX)], and (5) compilations of legal decisions and orders of the Commission and Atomic and Safety Licensing Boards and of Office Directors' decisions under Section 2.206 of NRC's regulations (NUREG-XXXX).

A single copy of each NRC draft report is available free, to the extent of supply, upon written request as follows:

Address: Office of the Chief Information Officer
Reproduction and Distribution
Services Section
U.S. Nuclear Regulatory Commission
Washington, DC 20555–0001
E–mail: <DISTRIBUTION@nrc.gov>
Facsimile: 301–415–2289

A portion of NRC regulatory and technical information is available at NRC's World Wide Web site:

<http://www.nrc.gov>

All NRC documents released to the public are available for inspection or copying for a fee, in paper, microfiche, or, in some cases, diskette, from the Public Document Room (PDR):

NRC Public Document Room
2120 L Street, N.W., Lower Level
Washington, DC 20555–0001
<http://www.nrc.gov/NRC/PDR/pdr1.htm>
1–800–397–4209 or locally 202–634–3273

Microfiche of most NRC documents made publicly available since January 1981 may be found in the Local Public Document Rooms (LPDRs) located in the vicinity of nuclear power plants. The locations of the LPDRs may be obtained from the PDR (see previous paragraph) or through:

<http://www.nrc.gov/NRC/NUREGS/SR1350/V9/lpdr/html>

Publicly released documents include, to name a few, NUREG-series reports; *Federal Register* notices; applicant, licensee, and vendor documents and correspondence; NRC correspondence and internal memoranda; bulletins and information notices; inspection and investigation reports; licensee event reports; and Commission papers and their attachments.

Documents available from public and special technical libraries include all open literature items, such as books, journal articles, and transactions, *Federal Register* notices, Federal and State legislation; and congressional reports. Such documents as theses, dissertations, foreign reports and translations, and non-NRC conference proceedings may be purchased from their sponsoring organization.

Copies of industry codes and standards used in a substantive manner in the NRC regulatory process are maintained at the NRC Library, Two White Flint North, 11545 Rockville Pike, Rockville, MD 20852–2738. These standards are available in the library for reference use by the public. Codes and standards are usually copyrighted and may be purchased from the originating organization or, if they are American National Standards, from—

American National Standards Institute
11 West 42nd Street
New York, NY 10036–8002
<http://www.ansi.org>
212–642–4900

DISCLAIMER

This report was prepared under an international cooperative agreement for the exchange of technical information. Neither the United States Government nor any agency thereof, nor any of their employees, makes any warranty, expressed or implied, or assumes any legal liability or responsibility for any third party's use, or the results of such use, of any information, apparatus, product, or process disclosed in this report, or represents that its use by such third party would not infringe privately owned rights.

NUREG/IA-0160

International Agreement Report

Analysis of the Critical Flow Model in TRAC-BF1

Prepared by
M. Gómez, E. Valero, I. E. Parra

Department of Applied Mathematics and Statistics
Universidad Politécnica de Madrid
Spain

Office of Nuclear Regulatory Research
U.S. Nuclear Regulatory Commission
Washington, DC 20555–0001

May 1999

Prepared as part of
The Agreement on Research Participation and Technical Exchange
under the International Code Application and Maintenance Program (CAMP)

Published by
U.S. Nuclear Regulatory Commission

ABSTRACT

Five Marviken Tests are modelled using TRAC-BF1. The code simulations are compared to Marviken data so as to analyse the capacity of TRAC-BF1 to reproduce subcooled and saturated blowdowns under critical conditions. Consequently, the critical flow model included in TRAC-BF1 will be validated.

Owing to the quasi-steady flow arising through the waste pipe, conserved quantities are useful to check the results accuracy. The influence of mesh refinement is also analysed.

Conclusions indicate that critical conditions must be imposed at the adequate sections to assure the calculations admissibility. However, the critical flow model introduces intrinsic errors that cannot be eliminated by means of mesh refinement.

TABLE OF CONTENTS

	Page
Abstract	iii
Executive Summary	xi
1. INTRODUCTION	1
1.1 Calculation of critical conditions	2
1.2 TRAC-BF1 critical flow model	4
2. EXPERIMENTS DESCRIPTION	9
3. CODE INPUT MODEL DESCRIPTION	11
3.1 Components and boundary conditions	11
3.2 Nodalization	11
3.3 Initial conditions	12
4. RESULTS	17
5. RUN STATISTICS	23
6. CONCLUDING REMARKS	24
7. REFERENCES	26
FIGURES	27

LIST OF FIGURES Pag.

FIGURE 1: Analytical pressure profiles at convergent nozzles 28
FIGURE 2:Comparison between analytical and numerical pressure profiles 28
FIGURE 3: Weight factor used in the transition zone 29
FIGURE 4: Basic computational cell upstream of the critical section 29
FIGURE 5: Initial temperature profiles at the vessel 29
FIGURE 6: Vessel and pipe nodalizations 30
FIGURE 7: Steam dome pressure evolution (Test 15) 31
FIGURE 8: Idem. (Test 21) 31
FIGURE 9: Idem. (Test 24) 32
FIGURE 10: Idem. (Test 10) 32
FIGURE 11: Idem. (Test 23) 33
FIGURE 12: Mass flow rate evolution (Test 15) 34
FIGURE 13: Idem. (Test 21) 34
FIGURE 14: Idem. (Test 24) 35
FIGURE 15: Idem. (Test 10) 35
FIGURE 16: Idem. (Test 23) 36
FIGURE 17: Void fraction evolution at last cell (Test 15)..... 37
FIGURE 18: Idem (Test 21) 37
FIGURE 19: Idem (Test 24) 38
FIGURE 20: Idem (Test 10) 38
FIGURE 21: Idem (Test 23) 39
FIGURE 22: Discharge pipe pressure profiles (4 cells, Test 15) 40
FIGURE 23: Discharge pipe pressure profiles (8 cells, Test 15) 40
FIGURE 24: Steam dome pressure evolution (Test 15, ICHOKE=0) 41
FIGURE 25: Mass flow rate evolution (Test 15, ICHOKE=0) 41
FIGURE 26: Discharge pipe pressure profiles (2 cells, Test 21) 42
FIGURE 27: Discharge pipe pressure profiles (4 cells, Test 21) 42

FIGURE 28: Steam dome pressure evolution (Test 21, ICHOKE=0) 43
FIGURE 29: Mass flow rate evolution (Test 21, ICHOKE=0) 43
FIGURE 30: Discharge pipe pressure profiles (2 cells, Test 24) 44
FIGURE 31: Discharge pipe pressure profiles (4 cells, Test 24) 44
FIGURE 32: Steam dome pressure evolution (Test 24, ICHOKE=0) 45
FIGURE 33: Mass flow rate evolution (Test 24, ICHOKE=0) 45
FIGURE 34: Discharge pipe pressure profiles (4 cells, Test 10) 46
FIGURE 35: Discharge pipe pressure profiles (8 cells, Test 10) 46
FIGURE 36: Steam dome pressure evolution (Test 10, ICHOKE=0) 47
FIGURE 37: Mass flow rate evolution (Test 10, ICHOKE=0) 47
FIGURE 38: Discharge pipe pressure profiles (2 cells, Test 23) 48
FIGURE 39: Discharge pipe pressure profiles (4 cells, Test 23) 48
FIGURE 40: Steam dome pressure evolution (Test 23, ICHOKE=0) 49
FIGURE 41: Mass flow rate evolution (Test 23, ICHOKE=0) 49
FIGURE 42: Initial dome pressure evolution (Test 15, diverse nodalizations) 50
FIGURE 43: Initial mass flux evolution (Test 15, diverse nodalizations)..... 50
FIGURE 44: Liquid total pressure along the pipe (Test 15, ICHOKE=1) 51
FIGURE 45: Idem. (Test 15, ICHOKE=0) 51
FIGURE 46: Stagnation enthalpy along the pipe (Test 15, ICHOKE=1) 52
FIGURE 47: Idem. (Test 15, ICHOKE=0) 52
FIGURE 48: Entropy along the pipe (Test 15, ICHOKE=1) 53
FIGURE 49: Idem (Test 15, ICHOKE=0) 53
FIGURE 50: Liquid total pressure along the pipe (Test 21, ICHOKE=1) 54
FIGURE 51: Idem. (Test 21, ICHOKE=0) 54
FIGURE 52: Stagnation enthalpy along the pipe (Test 21, ICHOKE=1) 55
FIGURE 53: Idem. (Test 21, ICHOKE=0) 55
FIGURE 54: Entropy along the pipe (Test 21, ICHOKE=1) 56
FIGURE 55: Idem (Test 21, ICHOKE=0) 56
FIGURE 56: Liquid total pressure along the pipe (Test 24, ICHOKE=1) 57

FIGURE 57: Idem. (Test 24, ICHOKE=0) 57
FIGURE 58: Stagnation enthalpy along the pipe (Test 24, ICHOKE=1) 58
FIGURE 59: Idem. (Test 24, ICHOKE=0) 58
FIGURE 60: Entropy along the pipe (Test 24, ICHOKE=1) 59
FIGURE 61: Idem (Test 24, ICHOKE=0) 59
FIGURE 62: Liquid total pressure along the pipe (Test 10, ICHOKE=1) 60
FIGURE 63: Idem. (Test 10, ICHOKE=0) 60
FIGURE 64: Stagnation enthalpy along the pipe (Test 10, ICHOKE=1) 61
FIGURE 65: Idem. (Test 10, ICHOKE=0) 61
FIGURE 66: Entropy along the pipe (Test 10, ICHOKE=1) 62
FIGURE 67: Idem (Test 10, ICHOKE=0) 62
FIGURE 68: Liquid total pressure along the pipe (Test 23, ICHOKE=1) 63
FIGURE 69: Idem. (Test 23, ICHOKE=0) 63
FIGURE 70: Stagnation enthalpy along the pipe (Test 23, ICHOKE=1) 64
FIGURE 71: Idem. (Test 23, ICHOKE=0) 64
FIGURE 72: Entropy along the pipe (Test 23, ICHOKE=1) 65
FIGURE 73: Idem (Test 24, ICHOKE=0) 65
FIGURE 74: TRAC execution time vs. real time (Test 15) 66
FIGURE 75: Time step vs. real time (Test 15) 66

LIST OF TABLES Pag.

TABLE 1: TRAC-BF1 critical flow model 8

TABLE 2: Characteristic parameters in Marviken Tests 10

TABLE 3: Typical input data 13

TABLE 4: Marviken 15, run statistics 23

EXECUTIVE SUMMARY

With the aim of verificating the critical flow model in TRAC-BF1, five blowdown experiments of the Marviken Test Series are modelled with such a thermalhydraulic code. The obtained results are compared with Marviken data and the HEM analytical correlation.

In order to study the maximum range of conditions, aside from two purely saturated blowdowns (Tests 10 and 23), three experiments presenting initial subcooled blowdown (Tests 15, 21 and 24) are chosen.

In a convergent nozzle (as those used in Marviken Tests) the critical condition appears as a turning point of the pressure profile arising at the outlet. However, the discretization used in the TRAC-BF1 numerical scheme fails to simulate this behaviour and the discretized pressure profiles can reach exterior pressures lower than the critical one. Consequently, critical conditions must be imposed on the numerical scheme externally.

In TRAC-BF1 this task is done by the subroutine CHOKE, which checks the fulfilment of critical conditions at externally determined sections. In this work the modelled tests are reproduced both with and without critical conditions imposed at the exit. The obtained results show the expected behaviour. On the one hand, when

CHOKE is inactive, the pressure profiles reach improperly the ambient pressure at the outlet and large errors arise in cells nearest to the pipe end. On the other hand, if critical pressure is imposed at the exit, the results are more exact. However, intrinsic errors, induced by CHOKE calculations, are unavoidable.

Experiments with different length to diameter ratios at the exit nozzle (from 0'3 in tests 23 and 24 to 3'6 in test 15), are chosen to study thermal disequilibrium effects. As a result, it is observed that those effects are not well modelled in TRAC-BF1 and, in general, critical flow is underestimated for subcooled blowdowns through short nozzles.

Diverse nozzle nodalizations are tried to study the influence of mesh refinement in TRAC-BF1 calculations. The cases analysed in this work indicate that increasing the number of cells improves the result. However, when subroutine CHOKE is active, the accuracy of global results is limited by inherent CHOKE errors in spite of mesh refinement.

In Marviken Tests, after a few seconds from the start, steady flow through the pipe can be considered. Therefore, some integral quantities must be conserved along pipe cells (mass flow rate, total enthalpy, entropy and liquid total pressure). In all cases studied here those quantities are checked to determine the results accuracy. As it has been mentioned above, errors accumulate at the pipe end, if CHOKE is inactive.

The general concluding remark of this work points out the need of activating the subroutine CHOKE at the adequate sections so as to obtain admissible results. Moreover, excessive mesh refinements do not improve code calculations beyond the limit imposed by CHOKE errors.

1. INTRODUCTION

The idea of critical velocity appears when the fluid motion is described by an hyperbolic system of conservation laws. Such a critical condition holds when the sound speed of the fluid coincides with the velocity of fluid particles and, as a result, the perturbations of motion variables (velocity and pressure) cannot go upstream.

The discharge of a vessel filled with liquid at high pressure and temperature is a practical situation where critical conditions can arise (LOCA phenomenon, fuel injection, ...). Usually, the flow through the nozzle is directly related with the difference between interior and exterior pressures. However, when the outer pressure falls below the critical value, either the fluid velocity equals the sound speed at some section or exceeds it. After that, as the information about the exterior pressure cannot travel upwards to the pipe inlet, the mass flux in the nozzle remains invariable and does not increase. So, the concept of critical flow can be defined practically as the maximum discharging flow attained for fixed vessel pressure and temperature.

In order to assess the capability of TRAC-BF1 code for modelling critical flows, five blowdown experiments of the Marviken Test Series have been chosen. Most of the time the blowdowns are saturated, but three of them also present initial stages of subcooled blowdown (tests 15, 21 and 24) and cover a wide range of inlet conditions. Furthermore, experiments with nozzles of different length to diameter

ratio (from 0.3 in tests 23 and 24 to 3.6 in tests 10 and 15), are chosen to analyse the code efficiency in simulating thermal disequilibrium effects.

The following section gives a brief introduction to critical solutions of analytical models. After that, the first chapter ends describing the discretized solutions introduced by the TRAC-BF1 numerical scheme, whose behaviour justifies a critical module were introduced in the code. The rest of the work is organised as follows: Chapters 2 and 3 contain respectively the description of the selected experiments and the corresponding code models. Chapter 4 is dedicated to expose the key results of the calculations. Some results about the run statistics of the calculations are included in Chapter 5. Finally, the principal concluding remarks are summed up in Chapter 6.

1.1 Calculation of critical conditions

For the motion through a pipe, the critical condition is set up mathematically cancelling out the first eigenvalue of the corresponding one-dimensional hyperbolic system, see, e.g., [1] and [2]. An equivalent condition is obtained when a steady solution passes through a singular point of the respective system of ordinary differential equations, [3] and [4]. For instance, if the flow in a convergent nozzle, through which a pressurised vessel is discharged, is modelled with the Homogeneous Equilibrium Model (HEM), the pressure profiles along the nozzle adopt the shape sketched in figure 1. All of these solutions possess a turning point. When such a

critical point arises at the outlet section, the corresponding solution is critical. Observe that, either the turning point is smooth with vertical tangent or it is a corner point. In the first case, the critical point arises in the mixture zone and the corresponding critical condition is similar to the classical criterion of gas dynamics: the fluid velocity coincides with the sound speed, $(\partial P / \partial \rho)_s^{1/2}$. In the second case, the bending point is discontinuous because of the existing discontinuity in the state equations along the saturation line, so the critical condition reduces to considering saturated liquid at the exit.

Similar conclusions are obtained for more complex and complete models, see, e.g., [3] where a general analysis of the problem is developed. However, to take into account thermal disequilibrium properly, a non-linear integral equation introducing delays in the generation of vapor must be added to the system of motion equations. As a consequence of that, the hyperbolic character of the fluid motion equations and the classical concept of critical condition are lost. In particular, supersaturated liquid can arise inside of the nozzle because of the delay in vapor generation. When a certain supersaturation degree is reached, the new phase appears and the mixture evolves quickly to attain either the saturation state or a metastable state compatible with the ambient conditions. In the first case, after the saturated conditions are approached, the mixture behaves near to equilibrium until critical conditions are reached. Then, if the exterior pressure is lower than the critical one, the ambient pressure is rapidly attained under metastable conditions.

In order to stress the differences between models, pressure profiles obtained with the disequilibrium model E.V.U.T. (Equal Velocity Unequal Temperature) are also sketched and compared to H.E.M. profiles in figure 1. Observe that, the disequilibrium solutions have not turning points as those arising at equilibrium curves. In those profiles, critical points are substituted by thin layers where ambient pressures are reached under metastable conditions. The position of these layers, which determines the "critical" mass flux in the disequilibrium model, are either the end of the metastable liquid region or the critical point of an equilibrium curve reached after the metastable layer inside of the pipe. Such an equilibrium curve is in general over the one corresponding to the equilibrium model and only appears for pipes with high length to diameter ratio. As a consequence of that, the "critical" non-equilibrium mass fluxes are greater than those calculated in the equilibrium model for either high inlet subcoolings or short nozzles.

1.2 TRAC-BF1 critical flow model

In TRAC-BF1 the six conservation equations of the two-fluid one-dimensional model are integrated numerically. The steady solutions of the corresponding numerical scheme present qualitative behaviour different from that explained in Section 1.1. To be exact, the numerical scheme does not have critical solutions as those described above for the equilibrium analytical model. Consequently, the critical condition must be imposed on the model externally.

In order to illustrate this assertion, the discharge through a convergent nozzle, modelled using the HEM approximation, is discretized following the TRAC-BF1 numerical scheme (see [5] and [6]). The steady solutions are obtained supposing constant magnitudes at successive time steps:

$$\rho_{j-1}A_{j-1/2}V_{j-1/2} = \rho_j A_{j+1/2}V_{j+1/2} = \phi, j = 1,\ldots,N, \tag{1}$$

$$\Delta P_{j+1/2} = P_j - P_{j+1} = \bar{\rho}_{j+1/2}\frac{\Delta\bar{x}_{j+1/2}}{\Delta x_j}V_{j+1/2}\left(V_{j+1/2} - V_{j-1/2}\right), j = 1,\ldots,N. \tag{2}$$

The notation is taken from references [5] and [6]. The parameter ϕ is the mass flow rate, which is a conserved quantity under steady conditions. In this model, ρ is the mean density of the mixture, $\alpha\rho_g + (1-\alpha)\rho_l$, and V is the common velocity of both phases. The discharging duct is divided into N computational cells, where the inlet and outlet cells are indexed under $j=1$ and $j = N$, respectively. The fractional indexes correspond to sections between cells.

Boundary conditions at the entrance and the exit must be included in the system:

$$P_0 = P_1 + \frac{1}{2}\bar{\rho}_{1/2}V_{1/2}^2, \tag{3}$$

$$P_{N+1} = P_a. \tag{4}$$

where the input data, P_0 and P_a, are respectively stagnation and exterior pressures.

Finally, a relation between the mean density of the mixture and pressure, which closes the system, is obtained from the equations of state and the hypothesis of isentropy:

$$\rho_j = \rho(P_j, s_0). \tag{5}$$

The following non-linear system can be obtained from equations (1), (2), (3) and (5):

$$\Delta P_{1/2} = \frac{\phi^2}{4A_{1/2}^2}\frac{\rho_0+\rho_1}{\rho_0^2}, \tag{6}$$

$$\Delta P_{j+1/2} = \frac{\phi^2}{4A_{j+1/2}}\frac{(\Delta x_j+\Delta x_{j+1})(\rho_j+\rho_{j+1})}{\Delta x_j \rho_j}\left(\frac{1}{\rho_j A_{j+1/2}} - \frac{1}{\rho_{j-1}A_{j-1/2}}\right), \quad j=1,\ldots,N, \tag{7}$$

where

$$\rho_j = \rho\left(P_0 - \sum_{i=0}^{j-1}\Delta P_{i+1/2}, S_0\right).$$

The above system is implicit because of the presence of ρ_{j+1} at the right members of Eqs. (6) and (7), which otherwise depend only on magnitudes calculated in lower order cells. Therefore, the system (6,7) possesses a lower triangular Jacobian matrix, whose diagonal elements are

$$J_{1/2,1/2} = 1 + \frac{\phi^2}{4A_{1/2}^2\rho_0^2}\frac{\partial\rho}{\partial P}(P_1, S_0), \tag{8}$$

$$J_{j+1/2,j+1/2} = 1 + \frac{\phi^2(\Delta x_j+\Delta x_{j+1})}{4A_{j+1/2}\Delta x_j\rho_j}\left(\frac{1}{\rho_j A_{j+1/2}} - \frac{1}{\rho_{j-1}A_{j-1/2}}\right)\frac{\partial\rho}{\partial P}(P_{j+1}, S_0), \quad j=1,\ldots,N. \tag{9}$$

As the modelized nozzle is convergent and the density is an increasing function of the pressure, the quantities (8) and (9) are strictly positive. Note that, if the nozzle

presents divergent zones, the above elements are also positive for fine nodalizations. Consequently, the system (6,7) possesses unique solution for every set of parameters, P_0, S_0 and ϕ, including the case of fine nodalizations in divergent channels. The components of such a solution are the pressure increments between consecutive cells, being all of them positive for convergent nozzles.

To sum up, if stagnation conditions, P_0 and s_0, and mass flux, ϕ, are given, pressure profiles as those sketched in figure 2 are obtained from equations (1), (2), (3) and (5). Two typical H.E.M. pressure profiles are also included in Fig. 2, so that the different behaviour of the two types of solutions is emphasized. Observe that, unlike the H.E.M. solutions, the numerical ones cannot present critical behaviour, i.e., they neither possess bending points nor present maximum existence intervals. Furthermore, the parameter ϕ and the pressure at the exit cell, P_{N+1}, are directly related and, as a result, the mass flow rate is determined by the exterior pressure through the boundary condition (4).

The numerically calculated mass flow rate, like that obtained analytically, grows as the exit pressure decreases. However, there are not critical limitations to pressures at the outlet in the numerical scheme, because the pressure profiles fit for reaching the ambient pressure whatever it is. Therefore, if the exterior pressure is under the critical value, the mass fluxes are overestimated by the numerical scheme of TRAC-BF1.

Consequently, in order to improve the TRAC-BF1 calculations, a subroutine of critical flow (CHOKE) is included in the code. At each time step, this subroutine checks whether the fluid velocity goes beyond the critical value. The sections of checking are selected externally activating the corresponding logical variable ICHOKE at the input data deck. The critical models used in TRAC-BF1 and their range of applicability are described in Table 1. The auxiliary figures 3 and 4 contain, respectively, the functional dependence on void fraction of a weight factor used in the range $0.01 \leq \alpha < 0.1$ and the computational cell upstream the critical section.

Table 1

TRAC-BF1 critical flow model

Void fraction at the critical section	Critical Velocity
$0 \leq \alpha < 0.01$	$\bar{a}_{crit} = max(a_s, a_H(0))$
$0.01 \leq \alpha < 0.1$	$\tilde{a}_{crit} = w a_H(0.1) + (1-w)\bar{a}_{crit}$
	(w plotted in Fig. 3)
$0.1 \leq \alpha < 0.999999$	$a_{crit} = a_H(\alpha)$
$0.999999 \leq \alpha < 1$	$a_{crit} = a_v$
$-a_S = \left(\frac{2(P_c - P_S(T_l) + \Delta P(a_S))}{\rho_l} + V_c^2 \right)^{1/2}$,	*see Fig. 4, ΔP given by the ALJ correlation, [7] y [8].* $V_c = 4 V_{mu} / \left(1 + \sqrt{A_l / A_v}\right)^2$
$-a_H(\alpha) = \left(\frac{\partial P}{\partial \rho} \right)_s^{1/2}$	*(mixture, depending on α)*
$-a_v = \left(\frac{\partial P}{\partial \rho} \right)_s^{1/2}$	*(pure steam, α=1)*

2. EXPERIMENTS DESCRIPTION

The experiments modelled in this work are extracted from the Series of Marviken Full Scale Critical Flow Tests. Those experiments were performed at Marviken Power Station (Sweden) and sponsored by a multinational consortium. The United States Nuclear Regulatory Commission (USNRC) participated in such a consortium and includes part of the data output in the validation matrix of its code assessment programs (ICAP, CAMP).

The principal characteristics of the experimental device used in these tests are summed up in Volumes 1 to 8 of [9]. Here, only the relevant parameters for the performed calculations are enumerated. Essentially, the experimental facility, which is reactor-sized, consists of: a pressurised vessel containing steam and water at high temperature, an exhaust pipe placed at the vessel bottom and a convergent nozzle ending the pipe. Each experiment initiates when the nozzle is suddenly opened, after that the pressures, temperatures and densities at various sections are measured during the subsequent blowdown.

In Marviken two type of experiments are done: totally saturated blowdowns and initially subcooled blowdowns. In the first case, before the experiments were initiated, the water was heated until the saturation temperature was uniformly reached in all the sections of the vessel. In the second case, initially the vessel presented

subcooled temperatures at the bottom whereas the conditions at the dome are saturated. Furthermore, various exit nozzles with length to diameter ratios under 4 are proven.

For this work five representative experiments of the Marviken programme are chosen: three sucooled tests (experiments 15, 21 and 24) and two saturated ones (tests 10 and 23). These experiments are performed with nozzles which cover widely the range of length to diameter ratios used in Marviken tests (from 0'3 in tests 23 and 24 to 3'6 in test 15). The other relevant parameters corresponding to the chosen experiments are summed up in table 2 and figure 5.

Table 2

Characteristic parameters in Marviken Tests

Test No.	**Test 15**	**Test 21**	**Test 24**	**Test 10**	**Test 23**
Mass of water (Mg.)	327	330	330	279	314
Mass of steam (Mg.)	0.6	0.6	0.63	1.8	0.65
Mass of saturated water (Mg.)	73.1	48.9	39.4	208	310.7
Vessel initial level (m.)	19.93	19.95	19.88	17.66	19.85
Initial steam dome pressure (MPa.)	5.04	4.94	4.96	4.97	4.96
Nozzle length to diameter ratio	3.6	1.5	0.3	3.1	0.3

3. CODE INPUT MODEL DESCRIPTON

A typical input data deck used for the Marviken simulations is shown in Table 3.

3.1 Components and boundary conditions

The vessel is modelled with a PIPE component as well as the discharge pipe together with the nozzle, which are included in a second PIPE component. In order to simulate the boundary conditions, two components are used: a FILL component with zero velocities modelling the closed end of the vessel, and a constant pressure BREAK component for modelling the break.

3.2 Nodalization

Firstly, the basic configuration defined in all the tests is being described. The PIPE component modelling the vessel is the same one in all the cases and it is shown in figure 6. This component is divided into 27 cells of different length (from .37 to 1.42m). The lengths of cells 5 and 6 differ in each test in order to locate the initial liquid level in the vessel on the common face to both cells (see figure 6).

The discharge pipe is always modelled with the first 17 cells of the second PIPE component with a minimum length of .025m and a maximum of 0.57m. (see

figure 6). The number of cells modelling the nozzle differs depending on the test (2 for short nozzles and 4 for the longest ones). Moreover, in order to analyse the code sensitivity to such a parameter, nozzle nodalizations both finer and coarser than the basic one are considered (see Fig. 6 for details).

3.3 Initial conditions

The initial pressure imposed in each cell of the PIPE components corresponds to the hydrostatic pressure calculated from the pressure at the steam dome. The liquid temperature profile is the experimental one (see figure 5) and the vapor temperature is the saturation one corresponding to the pressure at the steam dome. The void fraction is either 1 or 0 for the cells located respectively above or below the initial liquid level. The initial velocities are 1×10^{-5} m/s.

The blowdown is simulated at time zero by setting the BREAK pressure to the value 0.1 MPa. The time step is free with an initial value of 1×10^{-5}s.

Table 3

Typical input data

```
= MARVIKEN BLOWDOWN TEST 15 ON
**      IEOS      NTRACE       IST   NEXTR  MASPR  ICONT
OPTIONS    0         5         0    0    3    0
CHECKOUT 20000 0 0 0 0 0 0  0
**      DSTEP,  START TIMET
MAIN01     -1        1.50
**     STDYST      TRANSI       NCOMP       NJUN WATERPAK
MAIN02     1          0          4          3    0
** CONVER EPSO        EPSI        EPSS      IMPCON
MAIN03 1.0E-04      1.0E-05     1.0E-02        0
** ITER OITMAX       IITMAX   COURANT NTRX  NLEAKP NAXN  NDMPTR
MAIN04     8          0    100.   0    0     0   0
* CONTROL SYS        BORON   IAIR  NROT  NUMMPT   LEV1
MAIN05     0          0    0    0     0    0
** COMPONENTS  LIST  ORDER   CARDS
COMPLIST01   1 2 4 3
* TIME STEP DATA
*      DTMIN       DTMAX       TEND       RTWFP
*      EDINT      GRFINT      DMPINT      SEDINT
TIMESTEP011 1.E-4     .01        10.        10.0
TIMESTEP012  1.7       .5        10.       200.
*
TIMESTEP021 1.E-4     .01        50.       10.
TIMESTEP022  2.5       .5        10.      1000.
*
TIMESTEP031 1.E-4     .01        110.       10.
TIMESTEP032  2.       .1         45.      1000.
$
$
$$$$$$   PIPE HEADER CARD
PIPE01000  1 "    VESSEL PIPE                "
$$$$$$   PIPE PARAMETER CARD
*      NCELLS  NODES   JUN1   JUN2    MAT
PIPE01010    27     0     1     2     6
*        ICHF  IPVHT      RADIN        TH
PIPE01011     -1     0     2.5265E+00   1.62560000E-03
*          HOUTL      HOUTV      TOUTL      TOUTV
PIPE01012  .00000000E+00  .00000000E+00  .00000000E+02  .00000000E+02
*      IHTS   IWT
PIPE01050     0     0
*****    DX
PIPE01DX0  1.42000E+00  .78500E+00  .83000E+00  .97200E+00  .61300E+00
PIPE01DX1   .36900E+00  .96900E+00  .95100E+00  R02 .97500E+00
PIPE01DX2   .97700E+00  .96800E+00  R03 .97000E+00  .97400E+00  .98200E+00
PIPE01DX3  1.94000E+00  .97000E+00  .97400E+00  .96800E+00  .98400E+00
PIPE01DX4   .96400E+00  .45500E+00  .51500E+00  .37000E+00  .74000E+00 E
```

Table 3 (Continued)

```
*****   VOL
PIPE01VOL0 2.5090E+00   1.3870E+00  1.467E+00  9.499E+00  1.3119E+01
PIPE01VOL1 .78970E+01   2.0737E+01  2.0352E+01 R02 2.0866E+01
PIPE01VOL2 2.0909E+01   2.0716E+01 R03 2.0759E+01 2.0844E+01 2.1016E+01
PIPE01VOL3 4.1518E+01 2.0759E+01 2.0844E+01 2.0716E+01 2.1058E+01
PIPE01VOL4 2.0630E+01 9.737E+00 9.960E+00 2.895E+00 .626E+00 E
*****   FA
PIPE01FA0 R04 1.767E+00 R21 2.14008E+01 1.7349E+01
PIPE01FA1   1.327E+00 .444146E+00 E
*****   FKLOS
PIPE01FKLOS0 R28  .00000000E+00 E
*****   RKLOS
PIPE01RKLOS0 R28  .00000000E+00 E
*****   GRAV
PIPE01GRAV0 R28   -1.00000000E+00 E
*****   HD
PIPE01HD0 R28     0. E
*****   EPSD
PIPE01EPSD0 R28  .00000000E+00 E
*****   ICHOKE
PIPE01ICHOKE0   R28  0 E
*****   ICCFL
PIPE01ICCFL0 R28   0 E
*****   ALP
PIPE01ALP0      R05 1.0E+00     R22  0.0000E+00 E
*****   VL
PIPE01VL0      R06 1.000E-05  R03 .6500E+00  .6400E+00
PIPE01VL1      R03 .6500E+00  .6400E+00   R08 .6200E+00
PIPE01VL2      R03 .6100E+00  .7600E+00 9.8900E+00 2.955E+01 E
*****   VV
PIPE01VV0      R28 1.000E-05 E
*****   TL
PIPE01TL0   R05  5.34250E+02   5.33850E+02 5.3425E+02 5.34850E+02
PIPE01TL1       5.33150E+02   5.33650E+02 5.3365E+02 5.34150E+02
PIPE01TL2       5.28650E+02   5.13850E+02 5.0815E+02 5.08750E+02
PIPE01TL3       5.08450E+02   5.07450E+02 5.0835E+02 5.08550E+02
PIPE01TL4       5.08850E+02   5.06450E+02 5.0695E+02 5.06650E+02
PIPE01TL5       5.06250E+02   5.05950E+02 5.0565E+02 E
*****   TV
PIPE01TV0 R27    5.3516E+02 E
*****   P
PIPE01P0   R05  4.85000E+06  4.85130E+06 4.8550E+06 4.8586E+06
PIPE01P1       4.86230E+06  4.86600E+06 4.8697E+06 4.8734E+06
PIPE01P2       4.87710E+06  4.88100E+06 4.8849E+06 4.8888E+06
PIPE01P3       4.89510E+06  4.90290E+06 4.9067E+06 4.9106E+06
PIPE01P4       4.91450E+06  4.91850E+06 4.9224E+06 4.9242E+06
PIPE01P5       4.92600E+06  4.88750E+06 4.5710E+06 E
******  ILEV1
*PIPE01640 R06 0  1  R23 0 E
```

Table 3 (Continued)

```
****** ALPA
*PIPE01650 R06 1.E+00  1.E+00 R23 0.E+00 E
****** ALPB
*PIPE01660 R06 1.E+00  0.E+00 R23 0.E+00 E
****** DZLV1
*PIPE01670 R06 0.E+00  0.810E+00 R23 0.E+00 E
******VLEV1
*PIPE01680 R06 0.E+00  0.0E+00 R23 0.E+00 E
$
$
$$$$$$  PIPE HEADER CARD
PIPE02000 2 "   DISCHARGE PIPE          "
$$$$$$  PIPE PARAMETER CARD
*     NCELLS NODES  JUN1  JUN2   MAT
PIPE02010   22    0    2    3    6
*       ICHF IPVHT     RADIN        TH
PIPE02011    -1    0    .3760E+00    1.62560000E-03
*          HOUTL     HOUTV     TOUTL     TOUTV
PIPE02012 .00000000E+00 .00000000E+00 2.98000000E+02 2.98000000E+02
*     IHTS   IWT
PIPE02050    0    0
*****   DX
PIPE02DX0 .5700E+00 R02 .0600E+00 R04 .4950E+00 R02 .0600E+00
PIPE02DX1 R04 .44450E+00 .2750E+00 R02 .350E+00 .0250E+00 .156E+00
PIPE02DX2 R04 .450E+00 E
*****   VOL
PIPE02VOL0 .25320E+00 R02 2.66500E-02 R04 .21990E+00 2.6650E-02
PIPE02VOL1 2.7653E-02 R04 .21240E+00 .12670E+00 R02 .1555E+00
PIPE02VOL2 1.5168E-02   6.6139E-02  .1323E+00 R03 .08884E+00 E
*****   FA
PIPE02FA0 R09 .444146E+00 R05 .4780E+00 R04 .444146E+00 .4041E+00
PIPE02FA1 R04 .19635E+00 E
*****   FKLOS
PIPE02FKLOS0 R23  .00000000E+00 E
*****   RKLOS
PIPE02RKLOS0 R23  .00000000E+00 E
*****   GRAV
PIPE02GRAV0 R23  -1.00000000E+00 E
*****   HD
PIPE02HD0 R23     0. E
*****   EPSD
PIPE02EPSD0 R23  .00000000E+00 E
*****   ICHOKE
PIPE02ICHOKE0  1 0 R15 0    R05 0  1 E
*****   ICCFL
PIPE02ICCFL0 R23    0 E
*****   ALP
PIPE02ALP0      R22 0.0000E+00 E
```

Table 3 (Continued)

```
*****   VL
PIPE02VL0      2.955E+01 2.963E+01   2.972E+01  2.973E+01  2.972E+01
PIPE02VL1      2.970E+01  2.968E+01  2.967E+01  2.966E+01
PIPE02VL2  R02 2.754E+01   2.752E+01  2.751E+01  R05 2.960E+01
PIPE02VL3      3.252E+01 R04  66.93E+00 E
*****   VV
PIPE02VV0      R23  1.000E-05 E
*****   TL
PIPE02TL0       5.0728E+02   5.0908E+02    5.0923E+02  5.0903E+02
PIPE02TL1       5.0868E+02   5.0833E+02    5.0797E+02  5.0778E+02
PIPE02TL2       5.0773E+02   5.0755E+02    5.0724E+02  5.0692E+02
PIPE02TL3       5.0660E+02   5.0635E+02    5.0638E+02
PIPE02TL4      R07 5.0663E+02  E
*****   TV
PIPE02TV0 R22    5.3516E+02 E
*****   P
PIPE02P0        4.5713E+06   4.5694E+06    4.5694E+06  4.5716E+06
PIPE02P1        4.5741E+06   4.5766E+06    4.5788E+06  4.5793E+06
PIPE02P2        4.6293E+06   4.6311E+06    4.6333E+06  4.6353E+06
PIPE02P3        4.5880E+06   4.5891E+06    4.5905E+06  4.5919E+06
PIPE02P4        4.5920E+06   4.5180E+06    3.1122E+06  3.1140E+06
PIPE02P5        3.1158E+06   3.1176E+06 E
$
$
$$$$$$   BREAK HEADER CARD
BREAK03000  3 "   BLOWDOWN BREAK                "
*        JUN1  IBROP   NBTB   ISAT  ICOMT
BREAK03010     3     0     0     0     0
*            DXIN      VOLIN      ALPIN       TIN
BREAK03011 .45000000E+00 .0884E+00 1.00000000E+00  3.730000E+02
*            PIN,
BREAK03012 .10000000E+06
$
$$$$$$   FILL HEADER CARD
FILL04000  4 " INLET FILL                    "
*        JUN1  IFTY   IFTR   NFTX  ICOMT
FILL04010     1     1     0     0     0
*            DXIN      VOLIN      ALPIN       VIN
FILL04011  1.4200000E+00 2.50900E+00  1.00000000E+00 .0000000+00
*            TIN       PIN     BORCIN
CHECKOUT 20000 0 0 0 0   0 7
FILL04012  5.3516000E+02  4.85000000E+06
```

4. RESULTS

The results obtained in the performed calculations are summarized in figures 7 to 71. In a first group (Figs. 7 to 11), the evolution of vessel pressure is represented for the five analysed experiments. The figures from 12 to 16 contain the corresponding evolutions of mass flow rate. In these graphs, experimental data are compared with TRAC-BF1 results obtained using the basic nodalizations (see section 3) and with the subroutine CHOKE both active and inactive at the exit. Moreover, theoretical critical mass fluxes, calculated using the HEM model for experimental stagnation conditions, are included in the second group of figures.

When critical conditions are imposed at the exit (ICHOKE=1), the obtained results are acceptable. However, the calculated mass flow rates are under the experimental values. Such an underestimate is specially noticeable in tests 23 and 24 and during the subcooled stages of tests 15 and 21, where the HEM correlation gives the maximum underestimate too. The main reason for this behaviour is that thermal disequilibrium, that is of great importance in subcooled blowdowns and discharges through short nozzles, is poorly evaluated by TRAC-BF1 and neglected by the HEM correlation.

In order to confirm the previous observations, the evolutions of the calculated void fractions at the exit cell are plotted in figures 17 to 21. The initial subcooled

stages of tests 15, 21 and 24 are characterized by void fractions less than 0.1 in the curves corresponding to ICHOKE=1. In those regions, subroutine CHOKE corrects the HEM critical model, used in the remaining regimes, with the Alamgir, Lienhard and Jones (ALJ) correlation, see [7] and [8]. To be exact, a weighted average between the result corrected with the above correlation and the HEM critical velocity corresponding to α=0.1 is taken in the transition zone ($0.01<\alpha<0.1$, table 1). The ALJ correlation could introduce essential errors in the calculations, because it was developed using data corresponding to very rapid depressurizations (greater than 400 MPa/s). However, for subcooled blowdowns, the steady flow through the discharging pipe usually implies pressure undershoots reached at the pipe end after a slow depressurization (less than 300 MPa/s. in the tests modelled here).

On the other hand, note that the void fraction at the critical node is greater than 0.1 during all the test 23 and the latter stages of the test 24. It means that the HEM correlation is being used by CHOKE. As the nozzles employed in these tests are very short, there are foreseeable thermal disequilibria which have not been taken into account.

In order to compare the results obtained when subroutine CHOKE is either active (ICHOKE=1) or inactive (ICHOKE=0), calculations performed with ICHOKE=0 are also included in the figures from 7 to 21. As a general rule, the mass flow rates are overestimated if critical conditions are not imposed externally.

Explanation of this behaviour has been given in section 1.2: the pressure profiles obtained with the TRAC-BF1 numerical scheme adapt to reach the exterior pressure, even if it is subcritical. Note, for instance, the excessive values attained by the exit void fraction when CHOKE is inactive. Consequently, calculated pressure gradients and mass fluxes are greater than the adequate critical values.

It has been mentioned (section 1.2) that TRAC-BF1 models cannot attain a critical behaviour in a natural way, so the subroutine CHOKE is needed. However, refining the mesh near the critical section may apparently improve the results, even if CHOKE is not active. To verify this assertion in the cases analysed here, some calculations have been performed with different nozzle refinements and ICHOKE=0. The results are summarized in the figures from 22 to 41, that are grouped in series of four corresponding to the five modelled tests. Pressure profiles along the discharging nozzles, calculated with CHOKE both active and inactive, are plotted for various time steps and using two different nodalizations in the two leading figures of each group. The two last figures of each set contain respectively the evolutions of the steam dome pressure and the mass flow rate calculated with ICHOKE=0 for the different pipe nodalizations described in figure 6. Calculations performed with ICHOKE=1 have also been done, but in such a case the magnitude evolutions hardly vary with nodalization and the corresponding curves have not been included. However, in order to check the influence of subroutine CHOKE, results corresponding to CHOKE both

active and inactive are compared in figures 42 and 43 for the finest nodalizations of Test 15.

As it is expected, the pressure profiles along the nozzle reach the exterior pressure (0.1 Mpa) when they are calculated with ICHOKE=0. While restricting the exit velocities with the subroutine CHOKE implies that pressure cannot fall under the corresponding limit pressure. Moreover, as it has been anticipated in section 1.2, the mass fluxes calculated without critical limitations are generally greater than the experimental ones.

It is also observed that, when CHOKE is inactive, the finer is the nozzle nodalization the smaller is the calculated mass flux through the pipe. To explain this behaviour, first observe that the second member of Eq. (7) is very small when the corresponding cells are filled with subcooled liquid. Consequently, the pressure jump arises basically at the cells nearest to the exit and after the saturated conditions are reached. Thus refining the mesh implies bringing near the outlet the point where the saturation pressure is reached the first time. As a consequence of that, the subcooled mass flow rate drops, approaching from above the result obtained with the HEM correlation (saturated liquid at the exit, see section 1.1). Remember that HEM neglects thermal disequilibrium and, as a result, underestimates the critical mass flow rates under subcooled conditions. So, when the mesh is fine enough, calculated mass

fluxes can be occasionally under the experimental data (see subcooled stages of the tests 15, 21 and 24, Figs. 25, 29 and 33).

On the other hand, for saturated blowdowns, if CHOKE is inactive, errors are distributed along the discharging nozzle and the mass flux is always overestimated independently of mesh refinement. However, if the nozzle nodalization is refined, the erroneous pressure gradients are accumulated at the exit, lowering the mass flow rates and improving the results.

In any case, there is a "natural" mass flux limitation when CHOKE is inactive. Such a restraint is weaker than the H.E.M. critical condition, but approaches it from above when the mesh is refined. Therefore, for fine nodalizations, this mesh-dependent limit must be taken into account when critical conditions different from the H.E.M. correlation are employed. Observe, for instance, in figures 42 and 43, the earliest stages of Marviken Test 15 calculated with fine nodalizations at the exit. Note that, activating CHOKE has no influence in the results, because the numerical restraint to the mass flux is stronger than that imposed by the subroutine CHOKE (which in this case corresponds to the A.L.J. correlation, [7] and [8]).

Finally, in order to check the results accuracy, the evolution of some conserved quantities are calculated at given nodes along the pipe. The underlying idea is that pipe flow can be considered frictionless and stationary and, as a result, there is

some quantities that must be uniformly conserved along the pipe: Mass flow rate, entropy and stagnation enthalpy of the mixture and total pressure in the liquid phase. Actually entropy grows when both slip and mass transfer between phases exist, however the slip between phases is very small in the cases analysed here.

The results relative to each experiment are presented in six consecutive figures (see Figs. from 44 to 73). In each graph, the evolution of a conserved quantity at four different nodes is plotted (mass flow rate is excluded, because it hardly varies in any of the performed calculations). Three figures of each group show calculations done with ICHOKE=1, the remaining three are obtained with ICHOKE=0. In all cases, apart from two intermediate cells, the inlet and outlet cells are taken as checking nodes.

The results indicate the acceptable accuracy of the code when CHOKE is active. The small drop of stagnation enthalpy and entropy at the exit cells could be produced by the errors originated in the subroutine CHOKE and the TRAC-BF1 inability to simulate a critical behaviour.

However, if CHOKE is inactive, a considerable increase in the liquid total pressure and appreciable decreases in stagnation enthalpy and entropy are observed at the outermost cells. Such variations in quantities which must be conserved denote the

inaccuracy of the corresponding results, which actually violate the condition of nondecreasing entropy.

5. RUN STATISTICS

The runs are performed on a SUN station 4, model 100 computer with TRAC-BF1/MOD1 version NRC 0.4. The run statistics for test 15 are given on table 4, and figures 74 and 75 show typical plots of the Courant limited time step and CPU time versus real time. It is shown that either activating CHOKE or not hardly has influenee in the computational cost. However, it is observed that the mean time step corresponding to CHOKE=1 is appreciably longer than the one obtained for CHOKE=0. Statistics corresponding to the rest of the tests are very similar and are not included for the sake of brevity.

Table 4

Marviken 15, run statistics

ICHOKE	0	1
Real time (s)	62	82
Time step number	6392	8364
Mean time step	.082	.144
CPU time (s)	2.912	3.162
CPU time/real time	.047	.039

6. CONCLUDING REMARKS

Five blowdown experiments of the Marviken Test Series have been modelled with the TRAC-BF1 thermalhydraulic code. Three of them present an initial stage of subcooled blowdown, the remaining two cases are totally saturated blowdowns.

The general conclusions obtained from the comparative study between the code results, the experimental data and the HEM correlation are summarized below:

First, provided that the TRAC-BF1 numerical scheme is unable to reproduce critical solutions in a natural way, an externally imposed critical condition is needed. In TRAC-BF1, such a condition is supplied by the subroutine CHOKE, developed on the basis of HEM correlation and other semiempirical models. These models can introduce essential errors in TRAC-BF1 calculations, which are, however, acceptable enough when CHOKE is active.

Second, both the analytical model discretized in TRAC-BF1 and the CHOKE critical correlation fail to reproduce the thermal disequilibrium arising in the transition from monophasic liquid to boiling mixture. Therefore, the critical mass flow rates are underestimated in subcooled blowdowns and discharges through very short nozzles.

Third, when the subroutine CHOKE is not active, the pressure profiles can fall under subcritical pressures at the exit. Therefore, if the exterior pressure is subcritical, TRAC-BF1 generally overestimates the pressure gradients and the mass fluxes at the nozzle. The previous effect can be balanced by the code inability to model thermal disequilibrium and, as a result, the calculated mass fluxes are occasionally under the experimental data specially for subcooled blowdowns.

Four, provided that critical conditions are not imposed, refining the mesh near the critical section could apparently improve the results. However, owing to the improper pressure drop at the exit, such an improvement is very limited for saturated blowdowns. On the other hand, there is a natural TRAC restriction to the calculated mass flux, even if CHOKE is inactive. Such a limitation is mesh dependent and must be taken into account when critical conditions weaker than H.E.M. correlation are used.

Five, the verification along the pipe of some conserved quantities shows clearly the erroneous behaviour of the code when the ambient pressure is subcritical and CHOKE is inactive. The computational results actually violate the condition of nondecreasing entropy. Errors are concentrated at the cells nearest to the critical section, this suggests that in more complex installations errors could propagate after the critical section if CHOKE is not adequately activated.

7. REFERENCES

1. Trapp J. A., Ransom V.H., 1982. A choked-flow calculation criterion for nonhomogeneous, nonequilibrium, two-phase flows. *Int. J. Multiphase flow* 8, No.6, 669-681.
2. Sami S.M., Duong T., 1989 A transient model for predicting nonhomogeneous critical two-phase flows. *Nuclear Technology* 85, 98-108.
3. Bilicki Z., Dafermos C., Kestin J., Majda G., Zeng D.L., 1987. Trajectories and singular points in steady-state models of two-phase flows. *Int. J. Multiphase flow* 13, No,4,511-533.
4. Bilicki Z., Kestin J.,1990. Physical aspects of the relaxation model in two-phase flow. *Proc. R. Soc. Lond.* A 428, 379-397.
5. TRAC-BF1/MOD1: An Advanced Best-Estimate Computer Program for BWR Accident Analysis. NUREG/CR-4356 , EGG-2626, 1992.
6. TRAC-BF1/MOD1: Models and Correlations. NUREG/CR-4391, EGG-2680, 1992.
7. Alamgir Md., Lienhard J.H., 1981. Correlation of Pressure Undershoot During Hot-Water Despressurization. ASME J. Heat Transfer 103, 52-55.
8. Jones, O.C., 1980. Flashing Inception in Flowing Liquids, ASME J. Heat Transfer 102, 439-444.
9. EPRI Final Report NP-2370, 1982. The Marviken Full Scale Critical Flow Tests. Volumes 1 to 35.

FIGURES

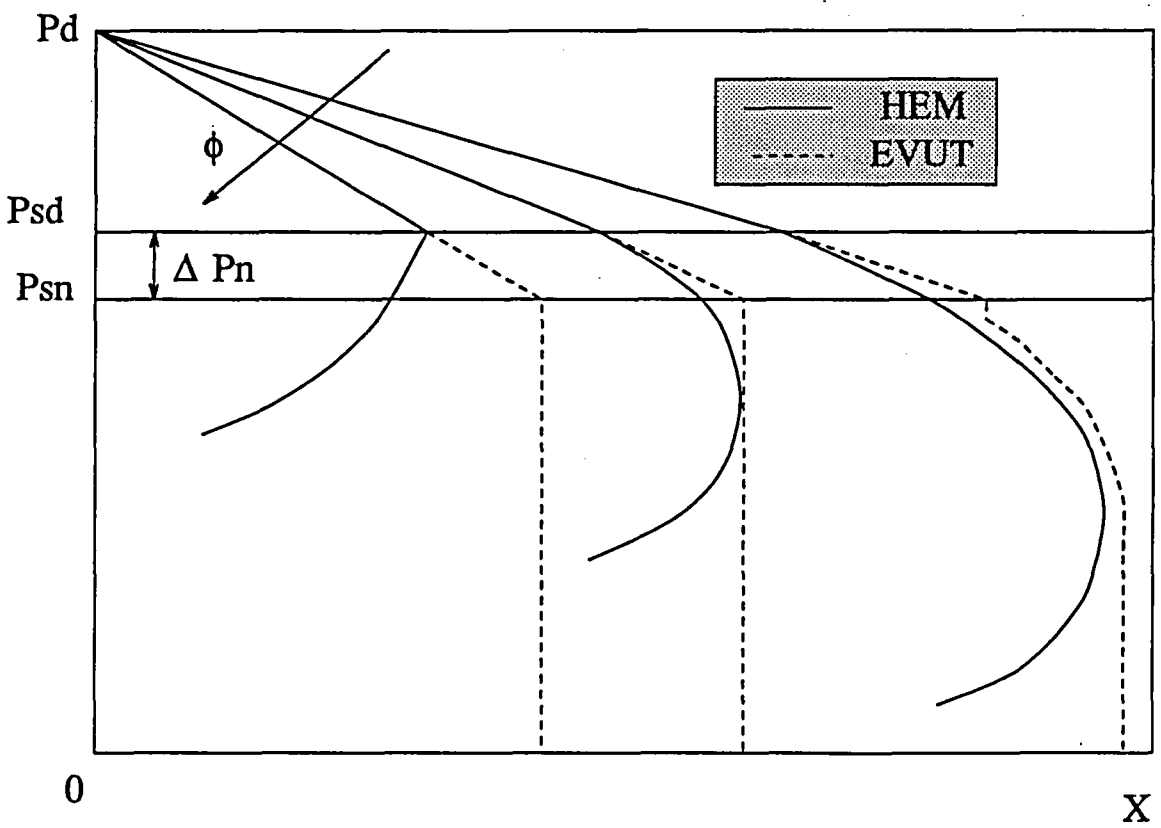

Figure 1. Analytical pressure profiles at convergent nozzles

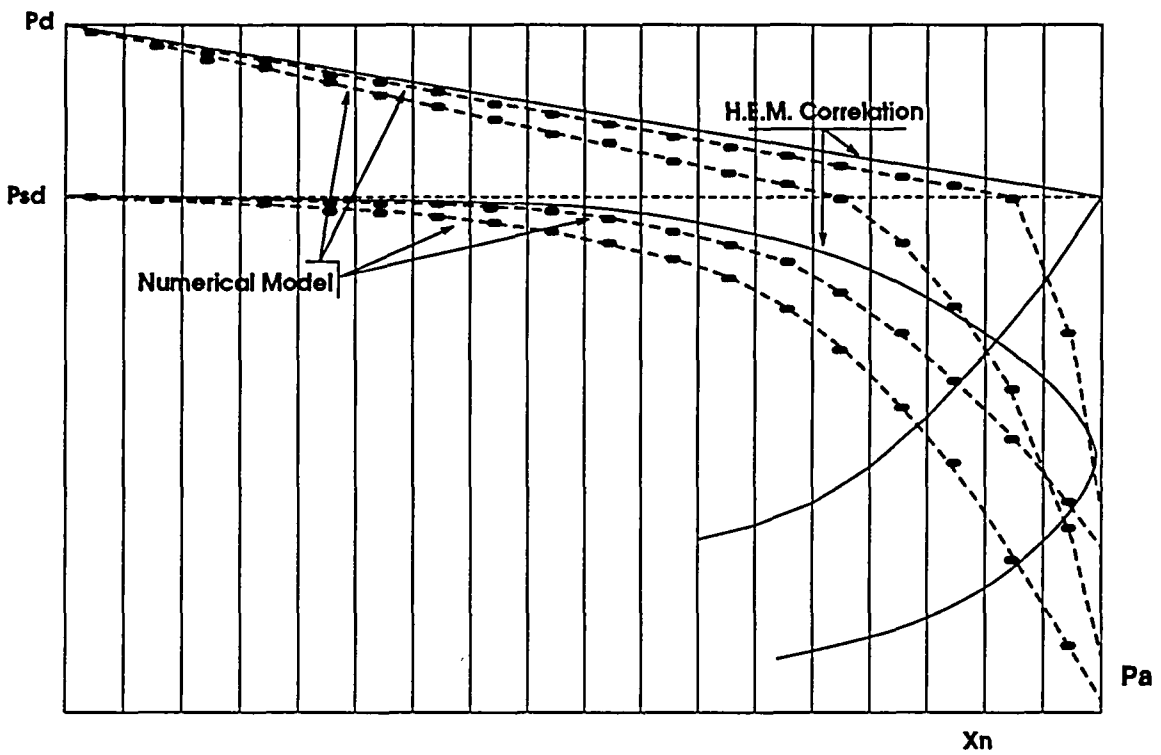

Figure 2. Comparison between analytical and numerical pressure profiles

Weight factor used in the transition zone

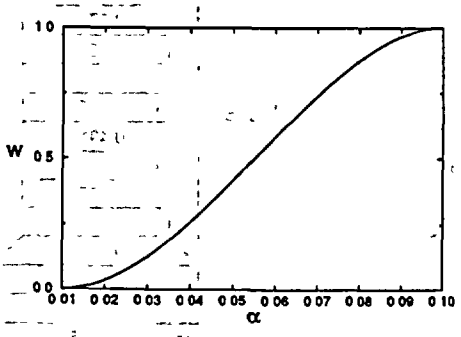

Figure 3

Basic computational cell upstream of the critical section

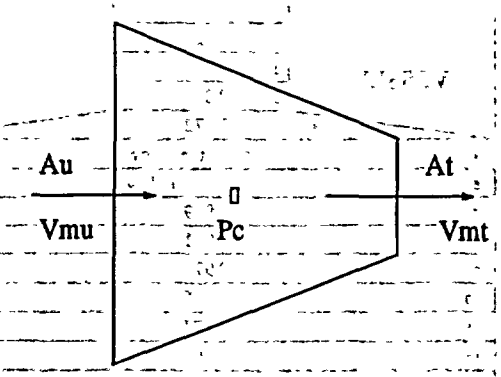

Figure 4

Initial temperature profiles at the vessel

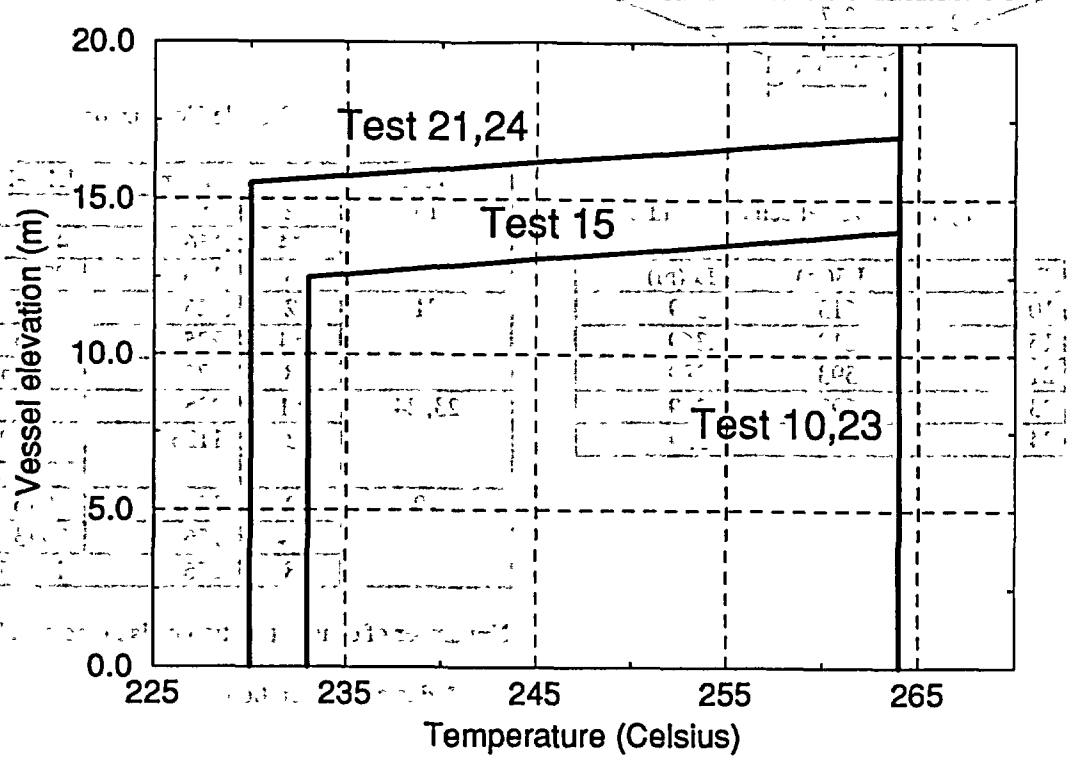

Figure 5

Vessel and pipe nodalizations

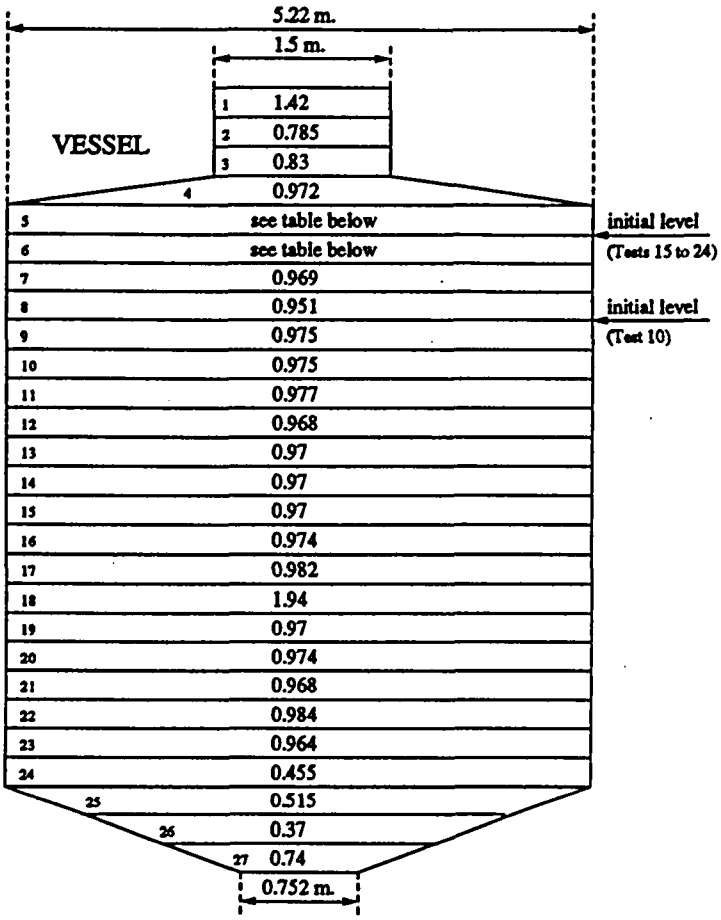

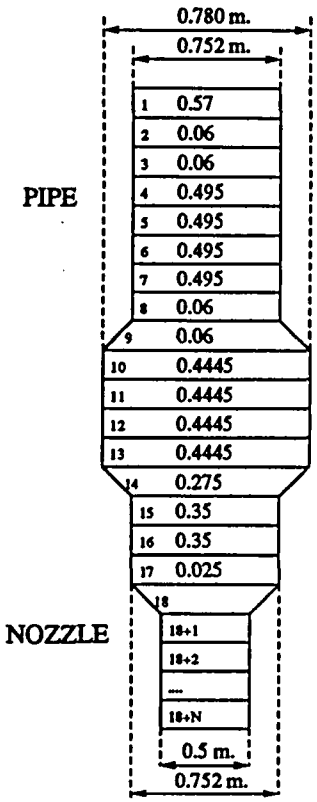

Lengths of vessel cells 5 and 6

Test	L5(m)	L6(m)
10	.613	.369
15	.613	.369
21	.593	.389
23	.693	.289
24	.643	.339

Nozzle Nodalizations

Test	N	L18(m)	L18+I (I:1...N) (m)
15	2	.156	.90
	*4	.156	.45
	8	.156	.275
21	2	.225	.365
	*4	.225	.1825
	8	.225	.09125
23, 24	*1	.225	.166
	3	.1125	L19=.1125 L20,L21=.083
10	2	.156	.7946
	*4	.156	.3973
	8	.156	.19865

N=number of constant section cells in the nozzle

* Basic configuration

Figure 6

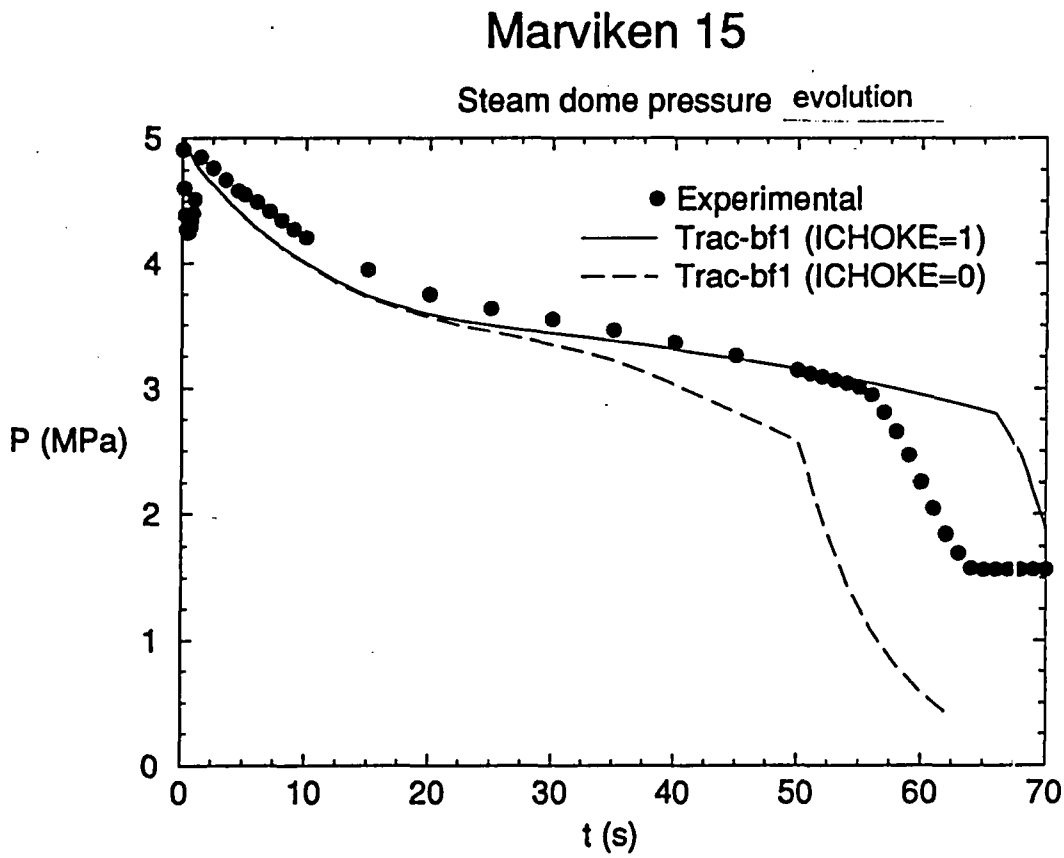

Figure 7

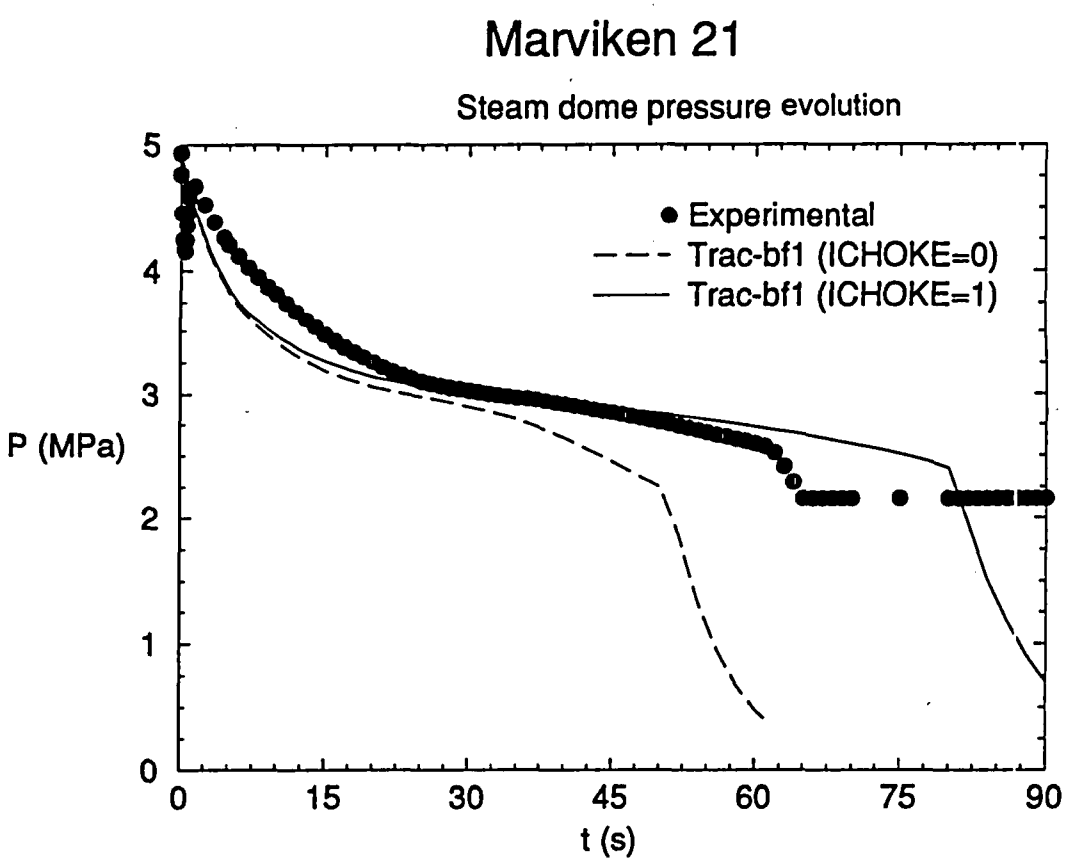

Figure 8

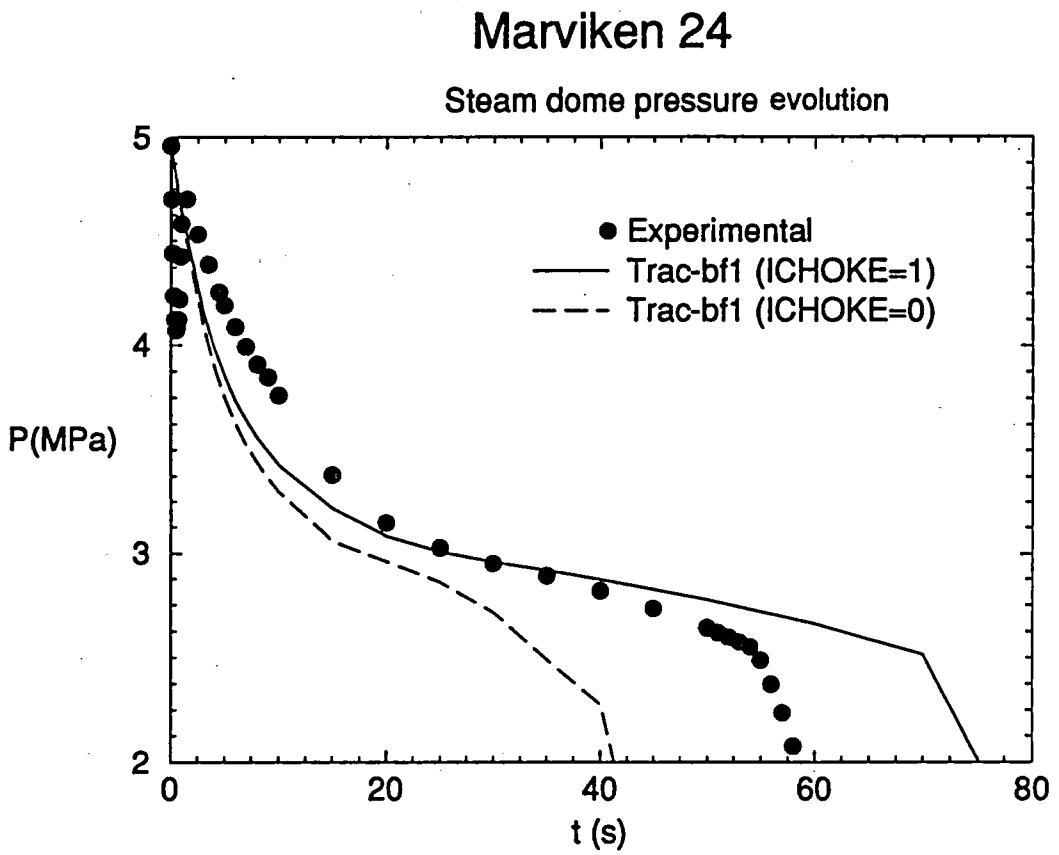

Figure 9

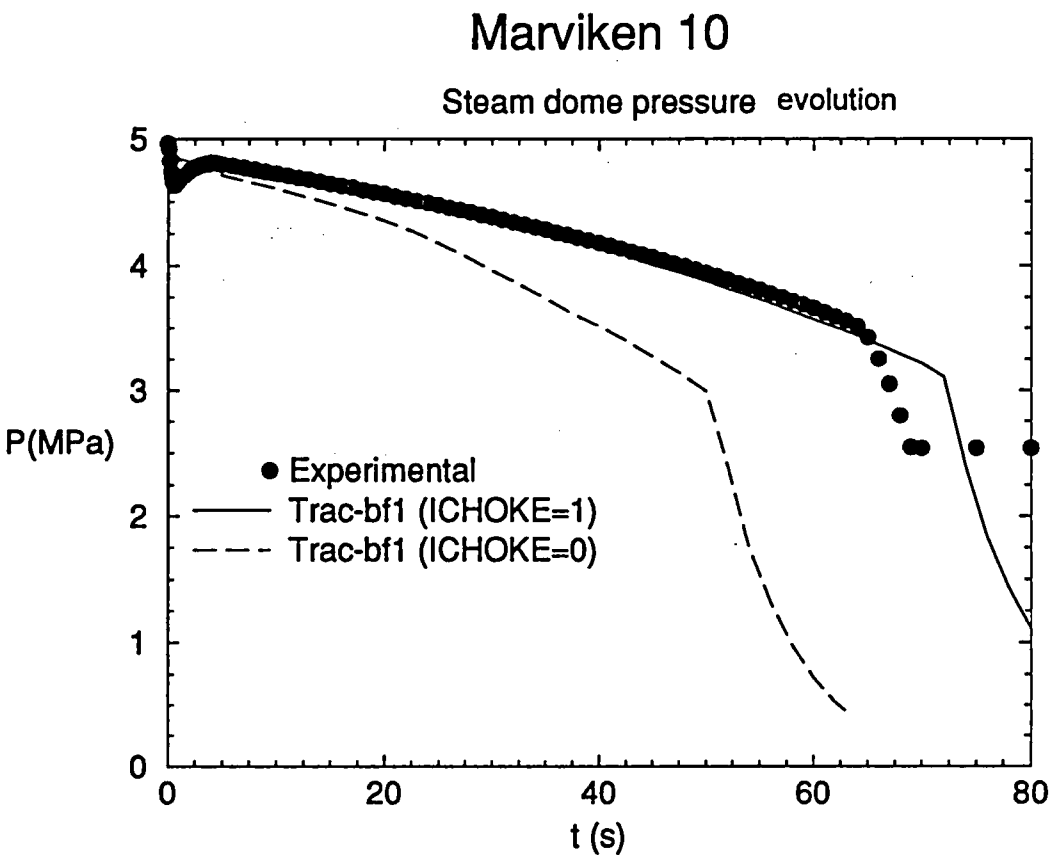

Figure 10

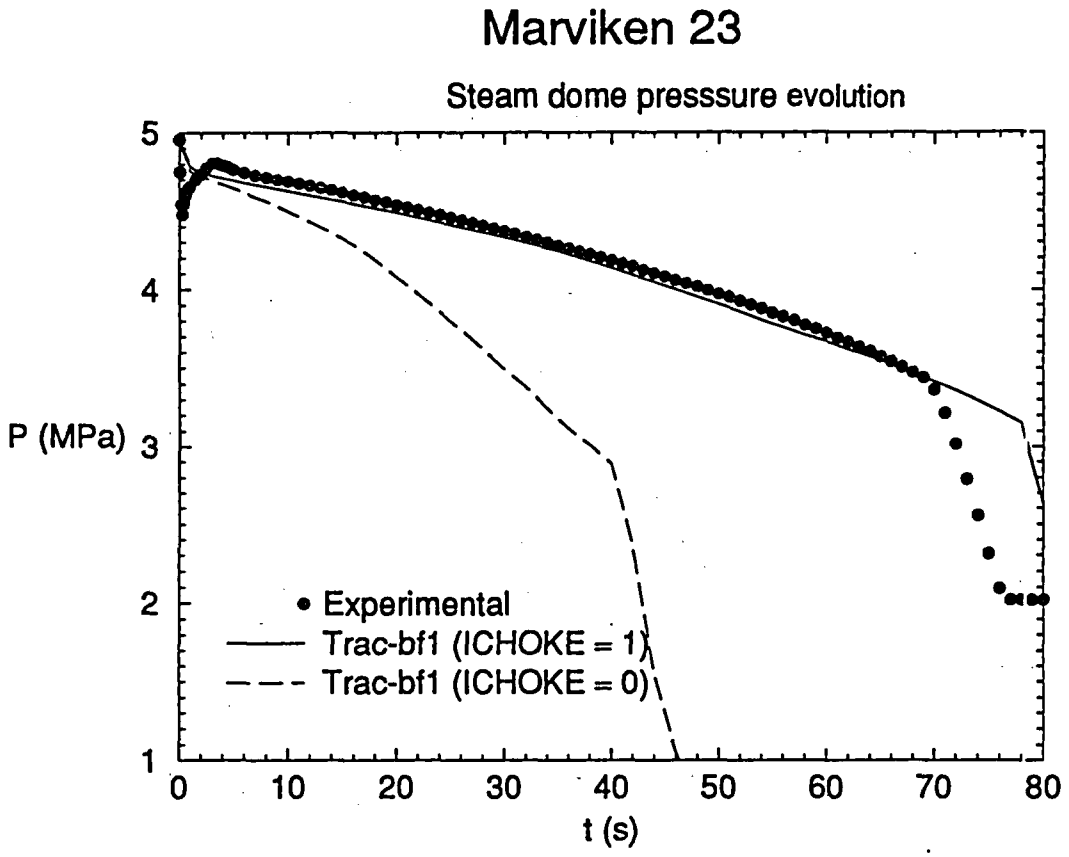
Marviken 23
Steam dome presssure evolution
P (MPa)
5
4
3
2
1
0
10
20
30
40
50
60
70
80
t (s)
Experimental
Trac-bf1 (ICHOKE = 1)
Trac-bf1 (ICHOKE = 0)

Figure 11

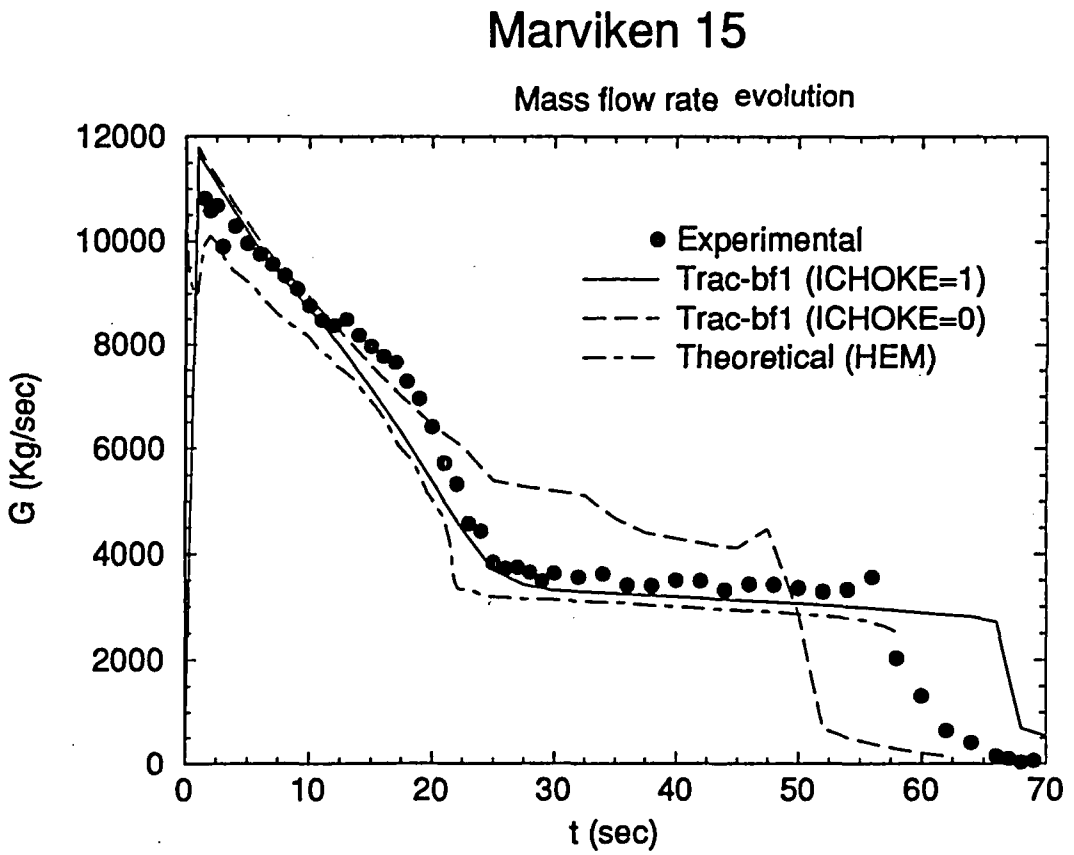

Figure 12

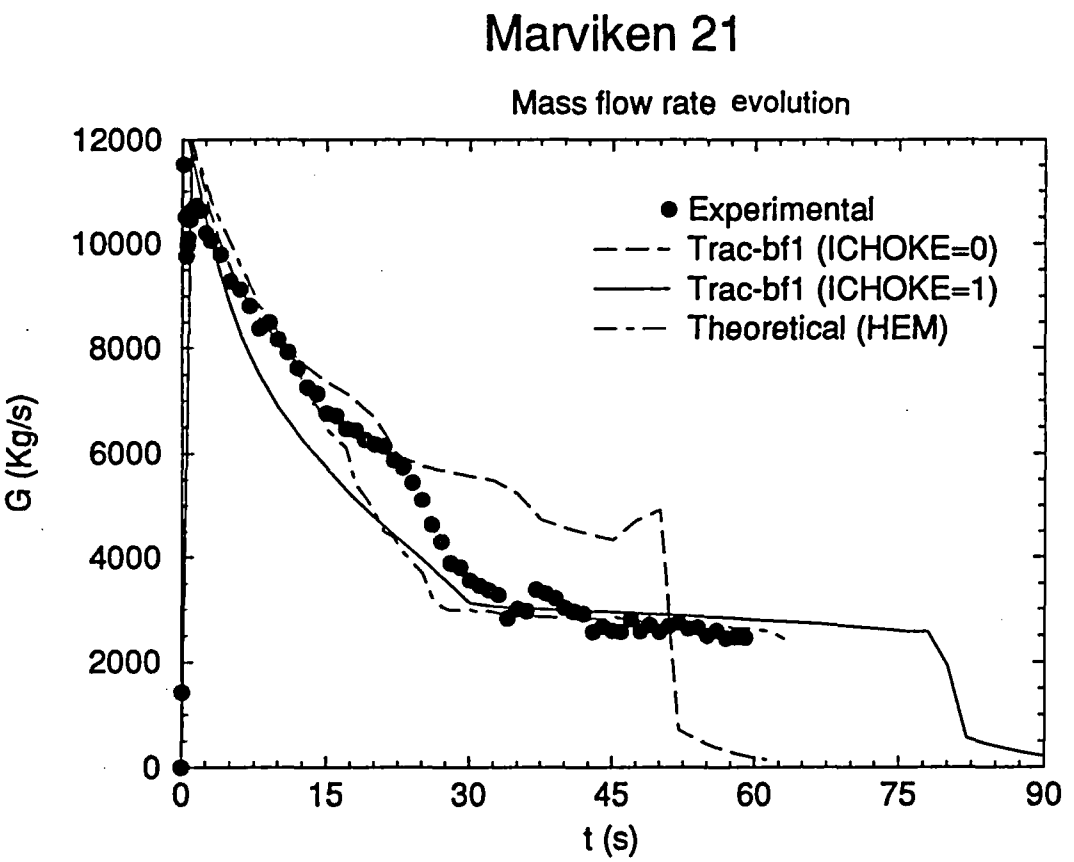

Figure 13

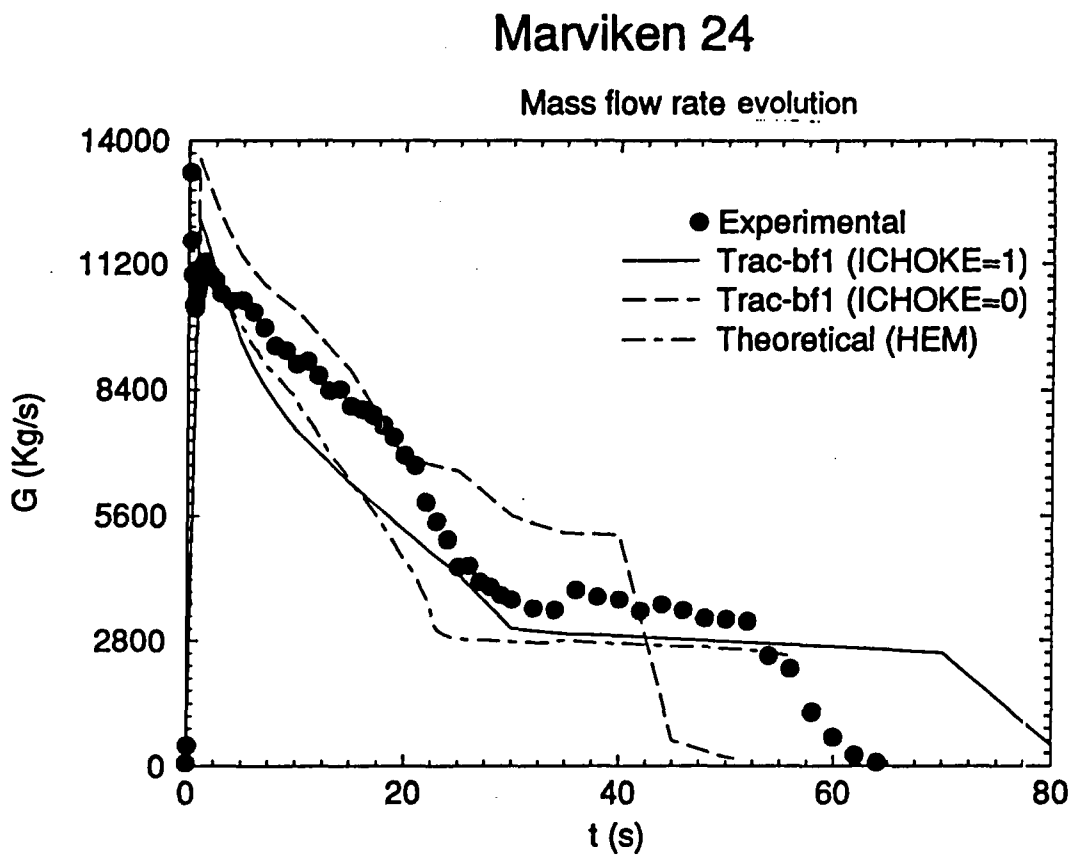

Figure 14

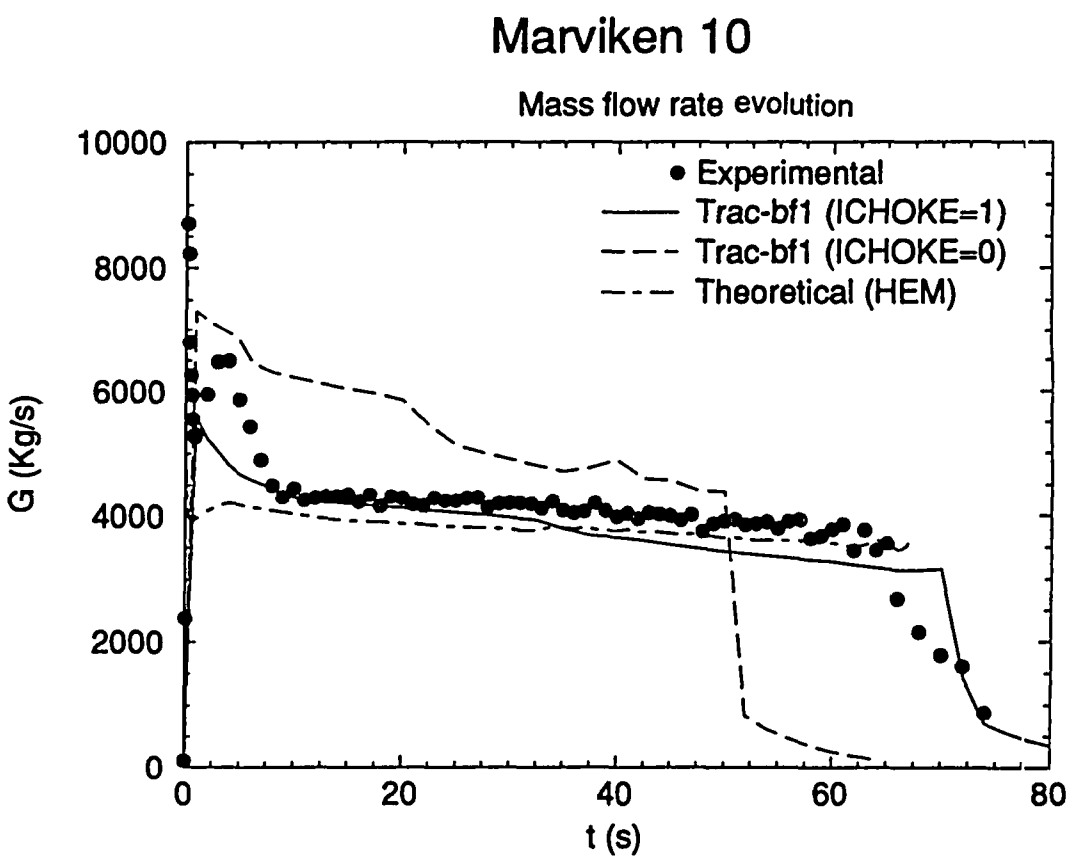

Figure 15

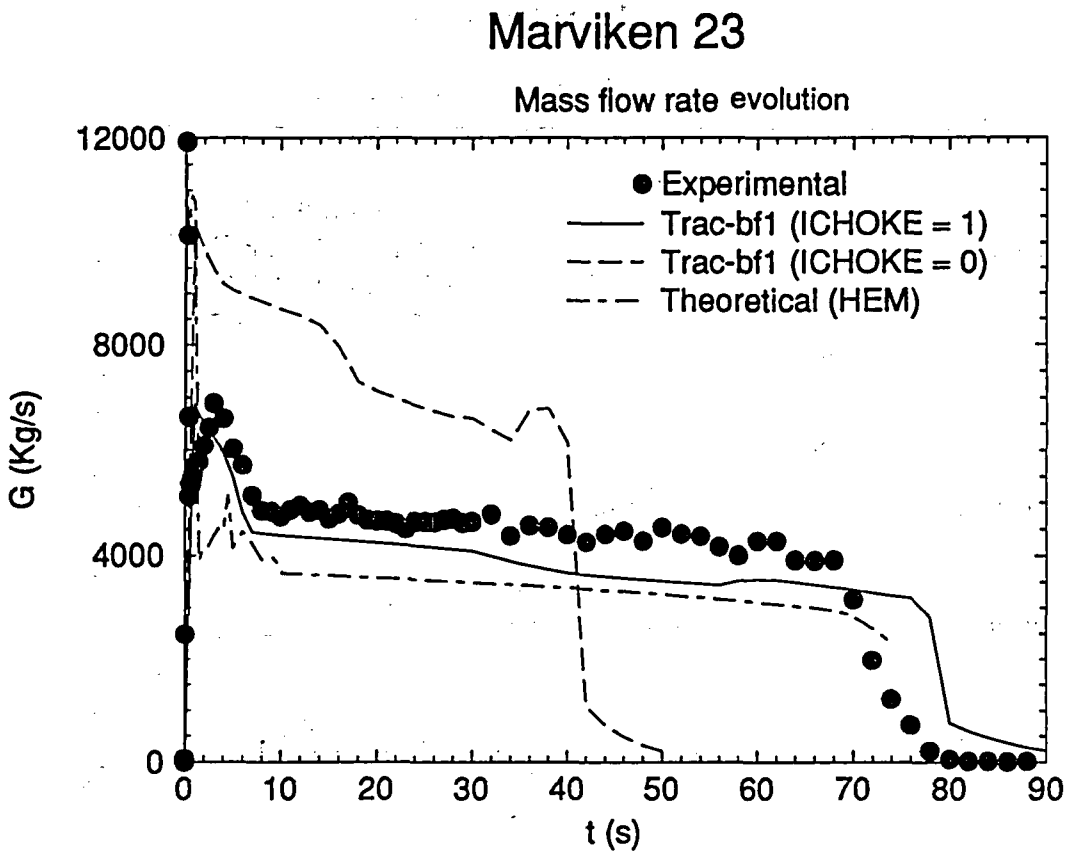
Marviken 23
Mass flow rate evolution
Experimental
Trac-bf1 (ICHOKE = 1)
Trac-bf1 (ICHOKE = 0)
Theoretical (HEM)
G (Kg/s)
12000
8000
4000
0
0
10
20
30
40
50
60
70
80
90
t (s)

Figure 16

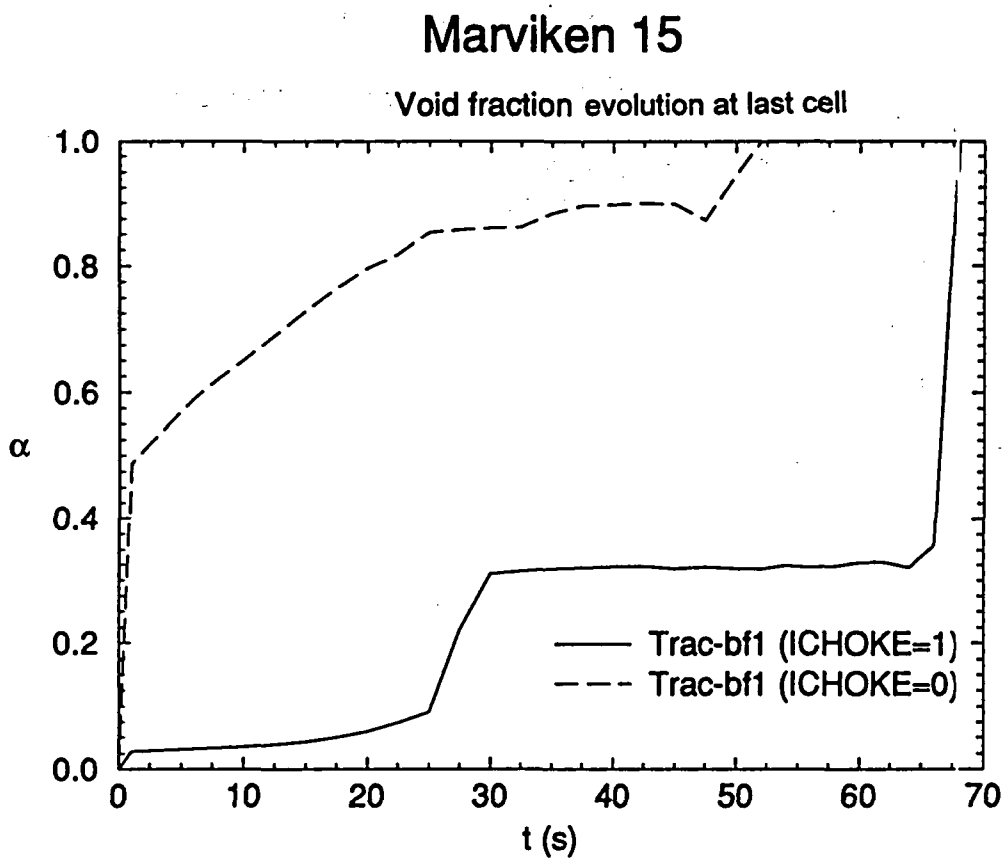

Figure 17

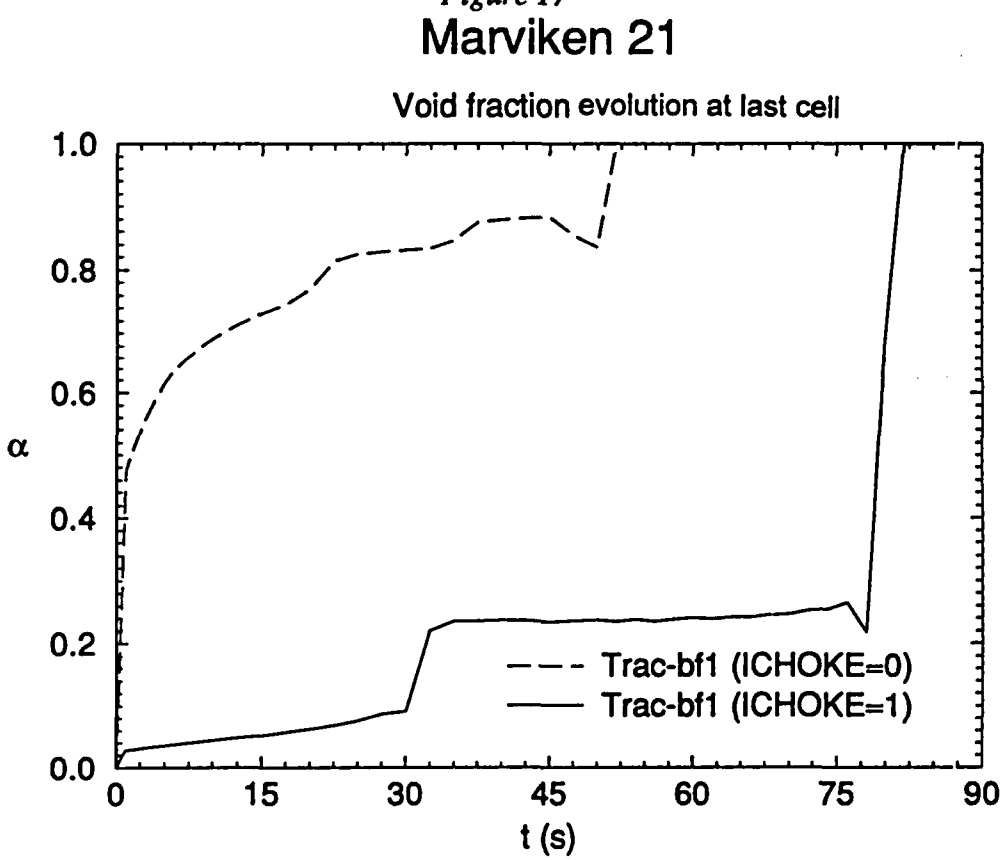

Figure 18

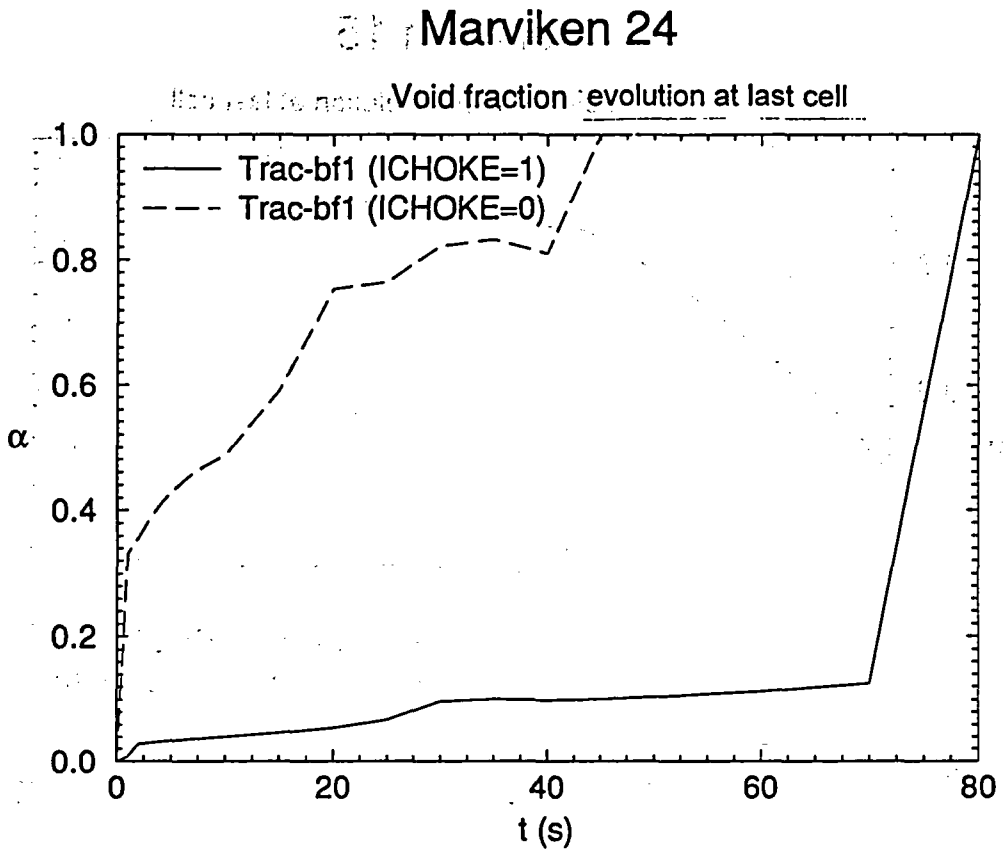

Figure 19

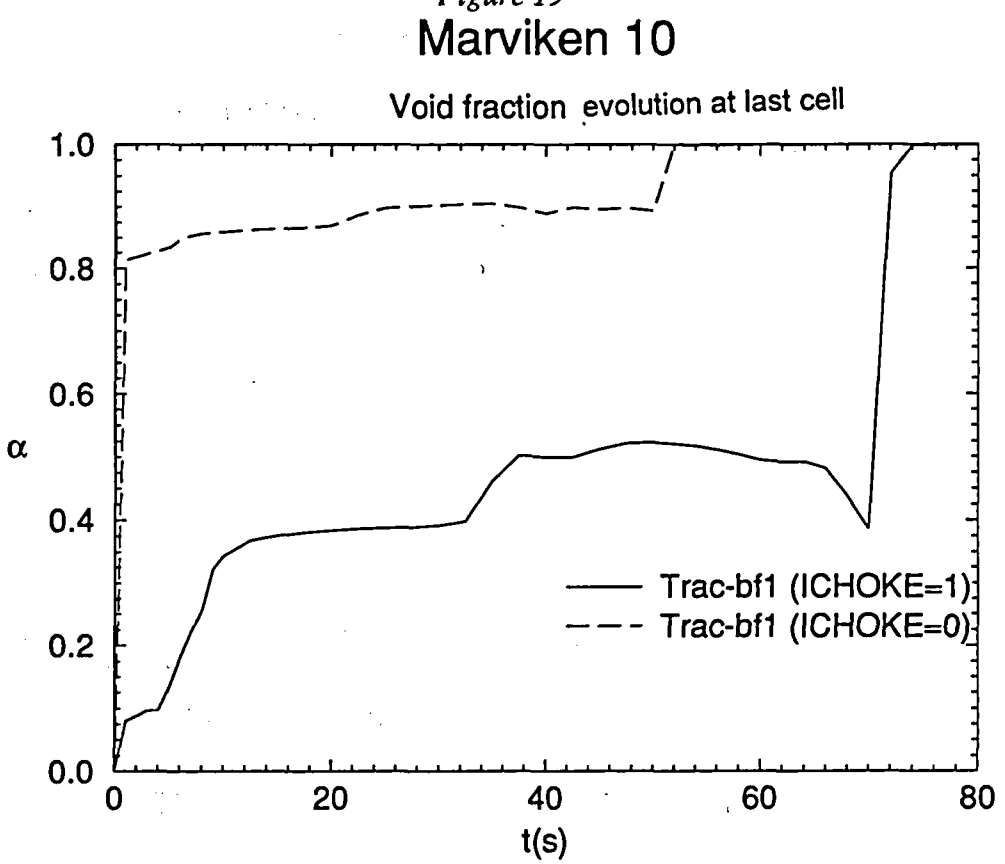

Figure 20

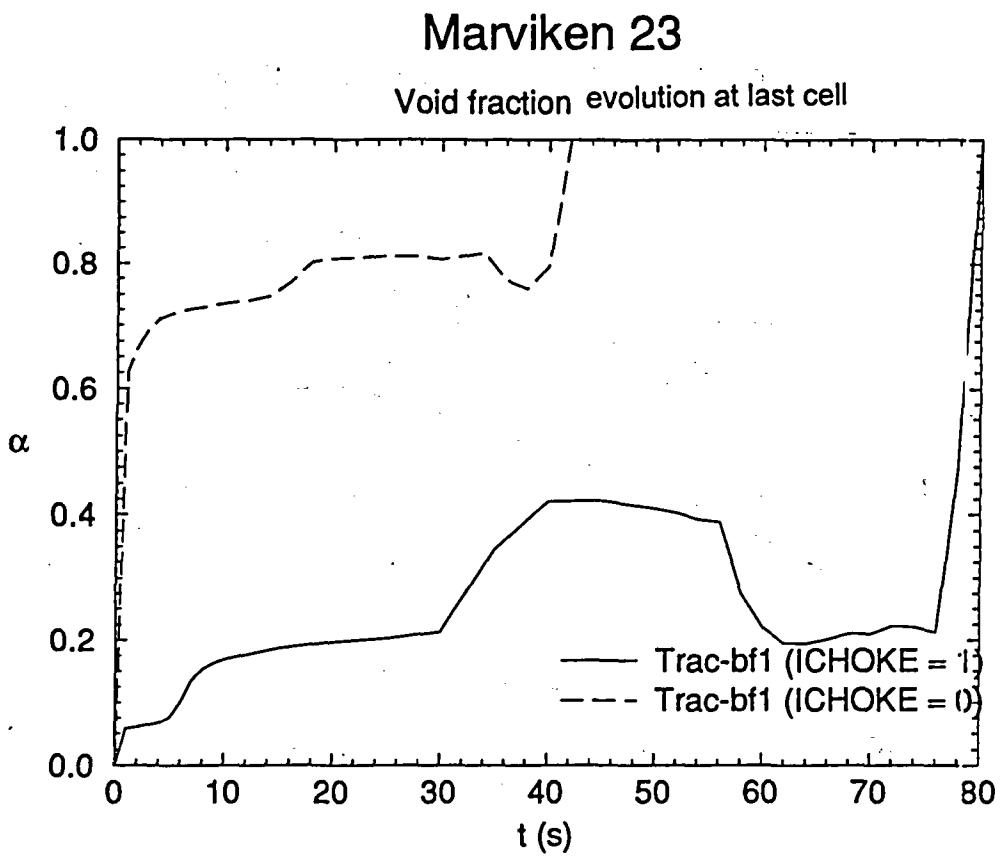
Marviken 23
Void fraction evolution at last cell
1.0
0.8
0.6
0.4
0.2
0.0
α
0
10
20
30
40
50
60
70
80
t (s)
Trac-bf1 (ICHOKE = 1)
Trac-bf1 (ICHOKE = 0)

Figure 21

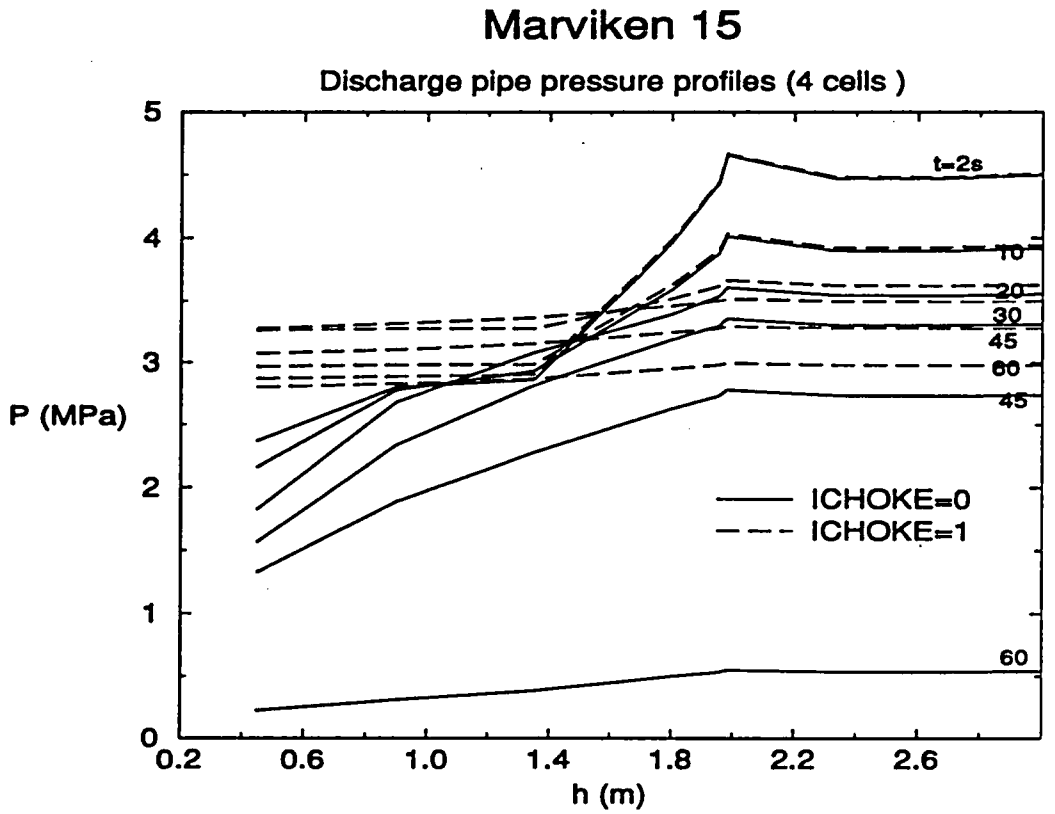

Figure 22

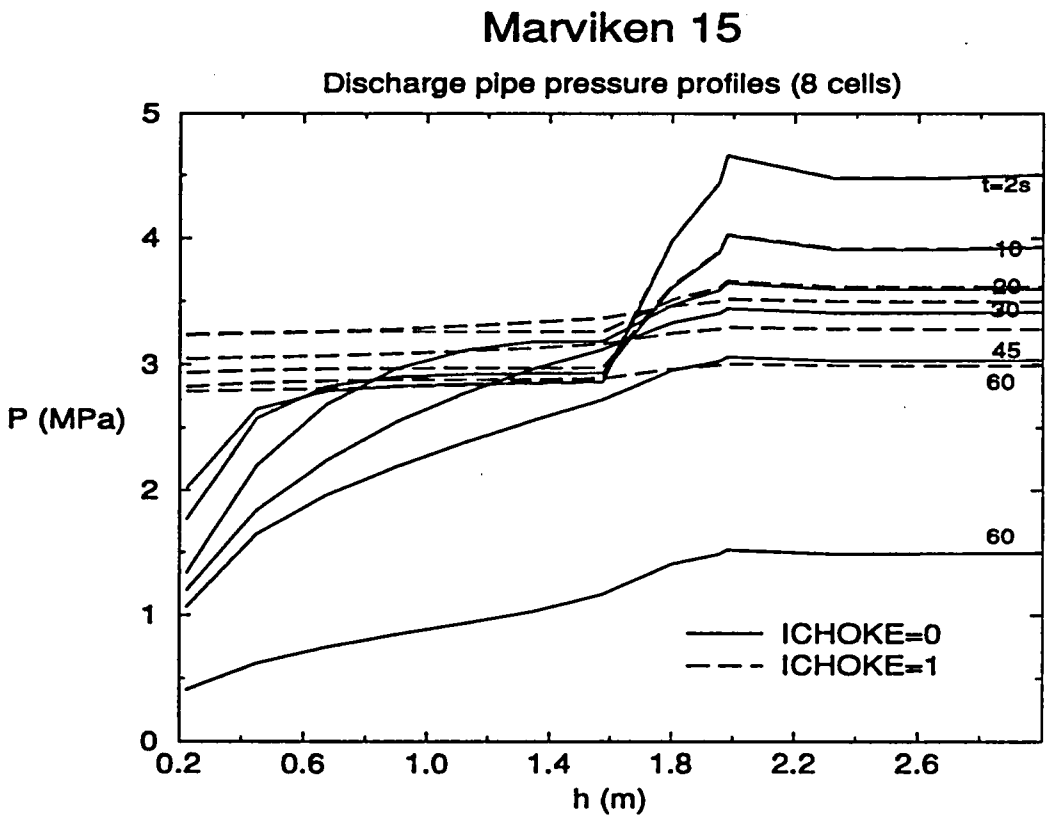

Figure 23

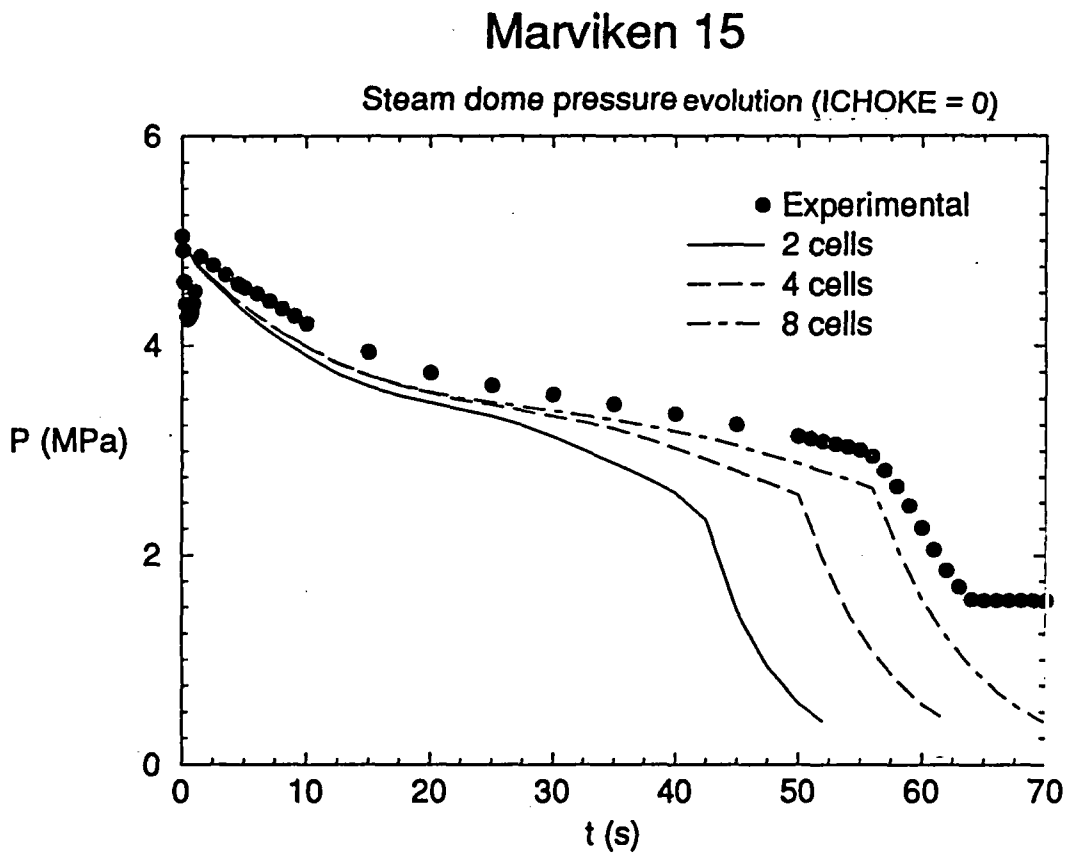

Figure 24

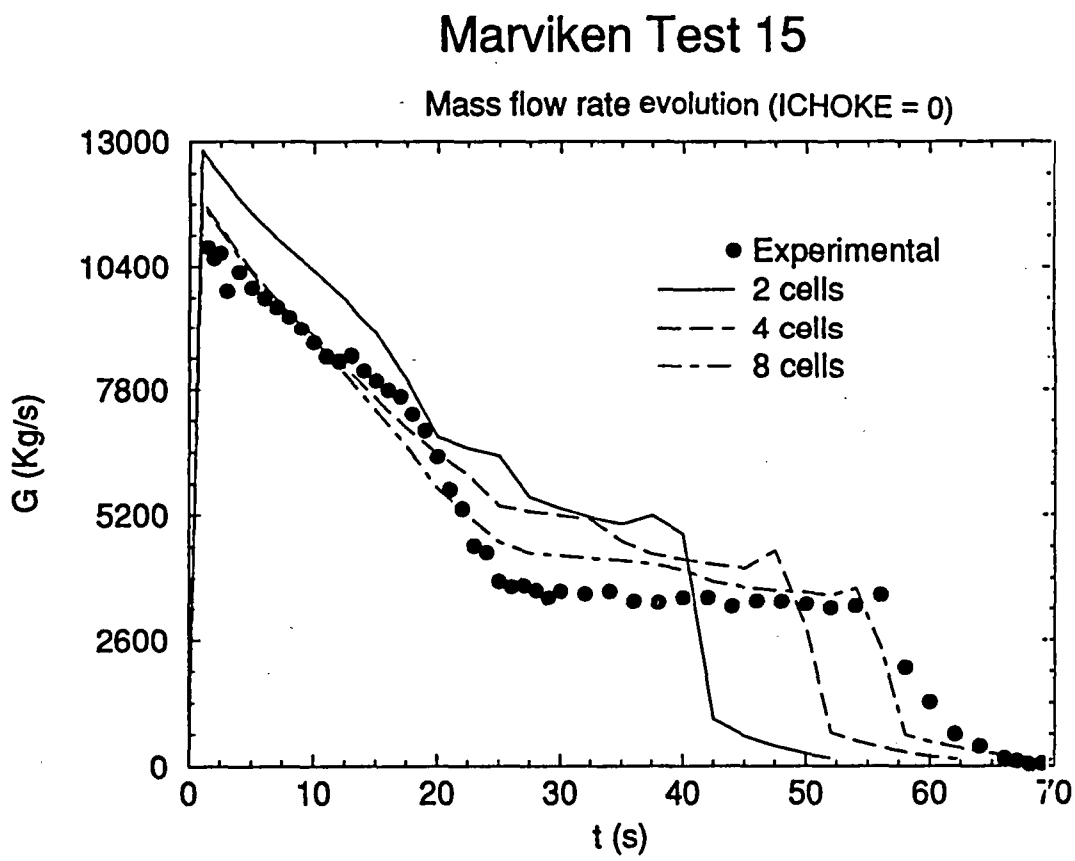

Figure 25

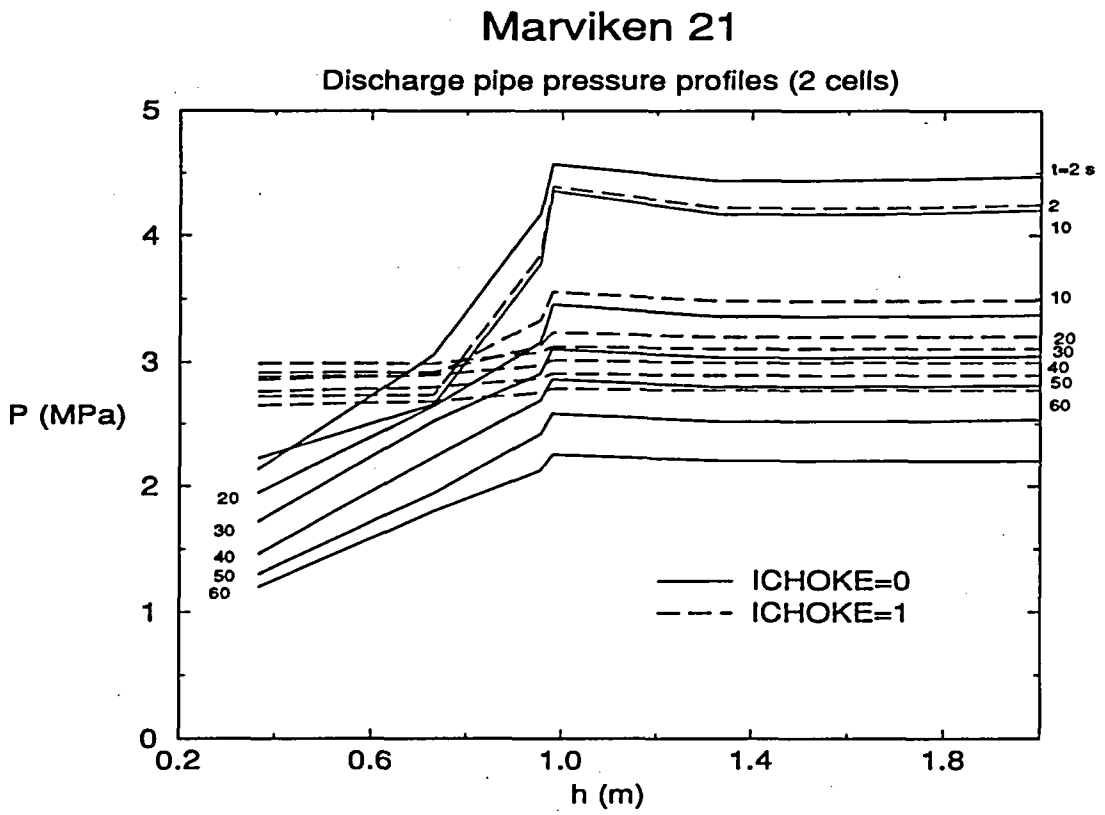

Figure 26

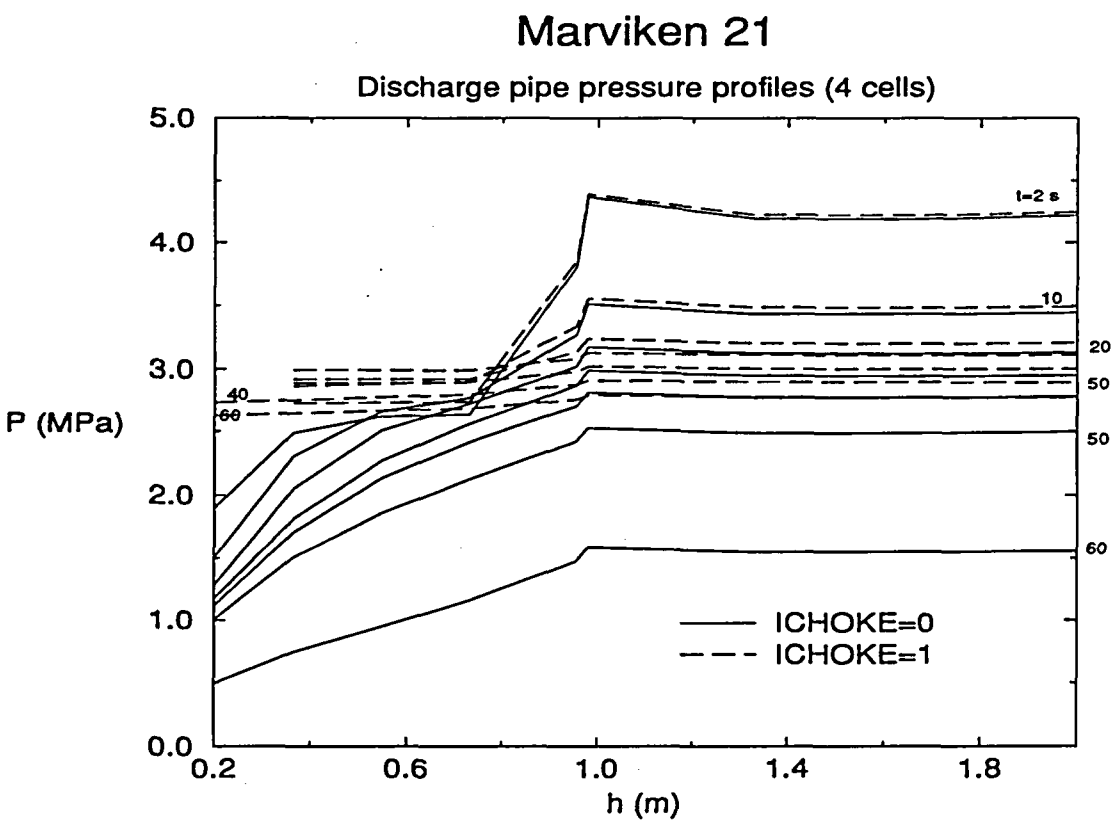

Figure 27

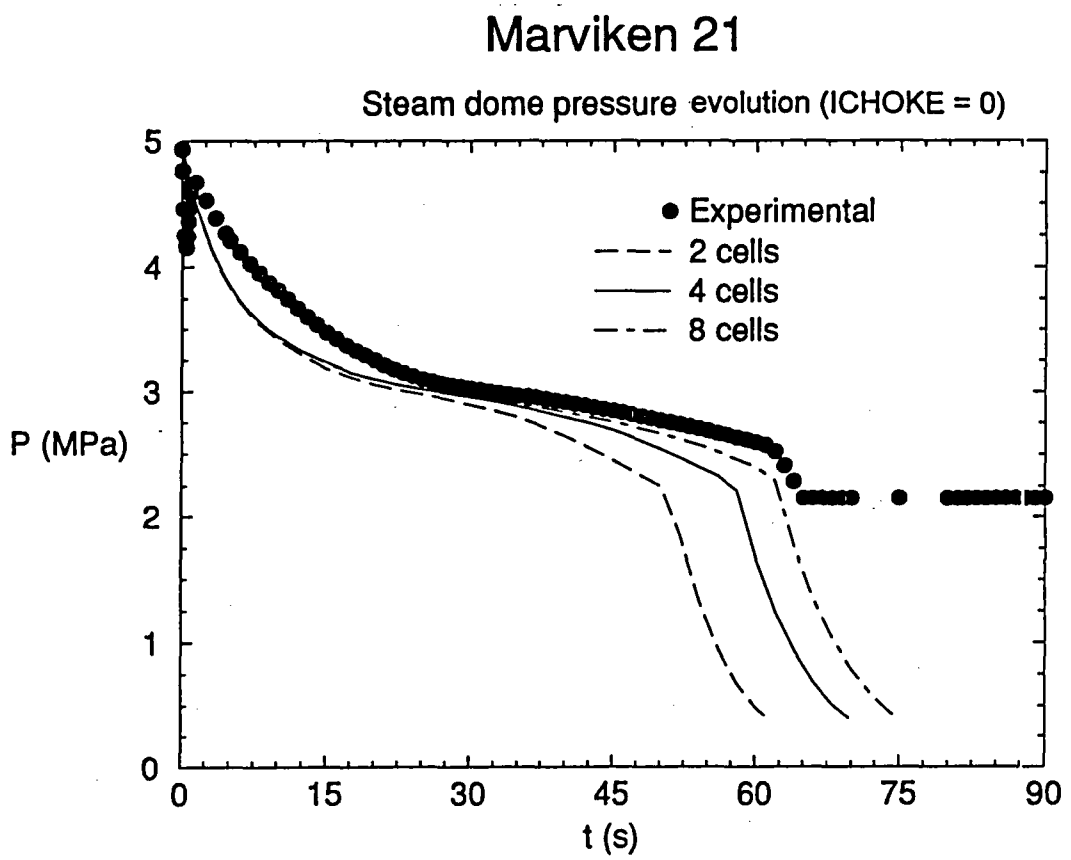

Figure 28

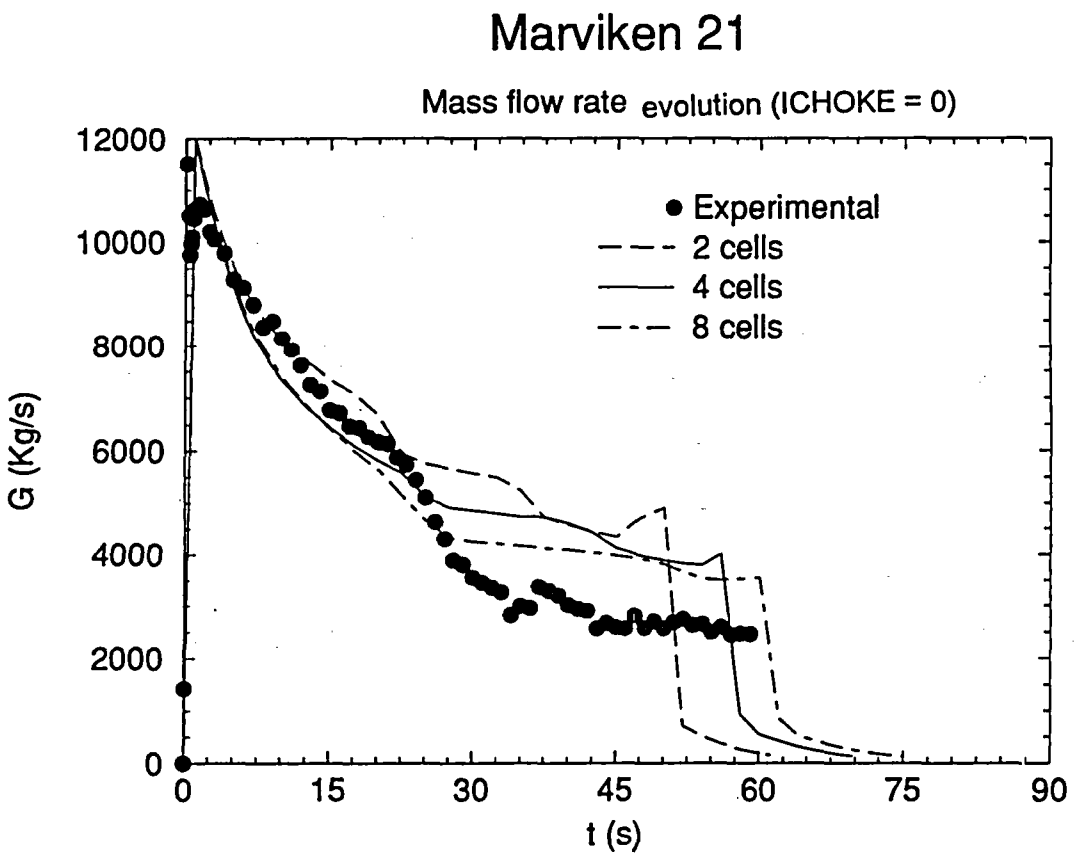

Figure 29

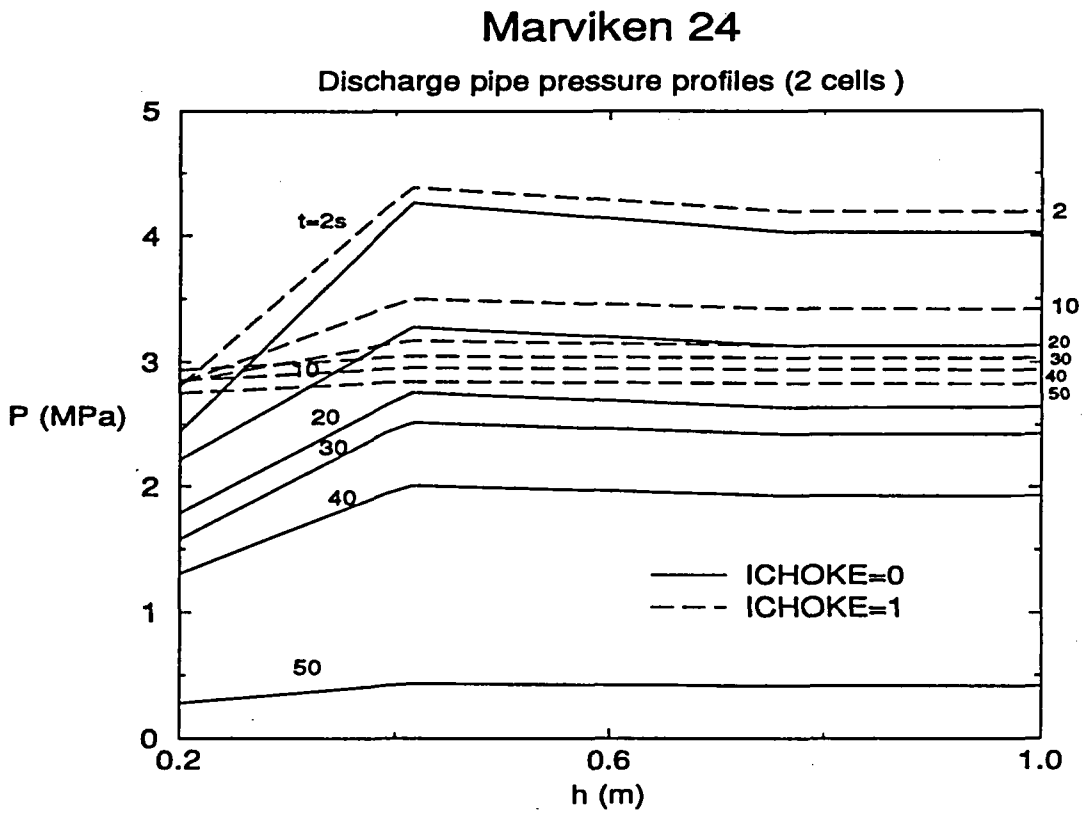

Figure 30

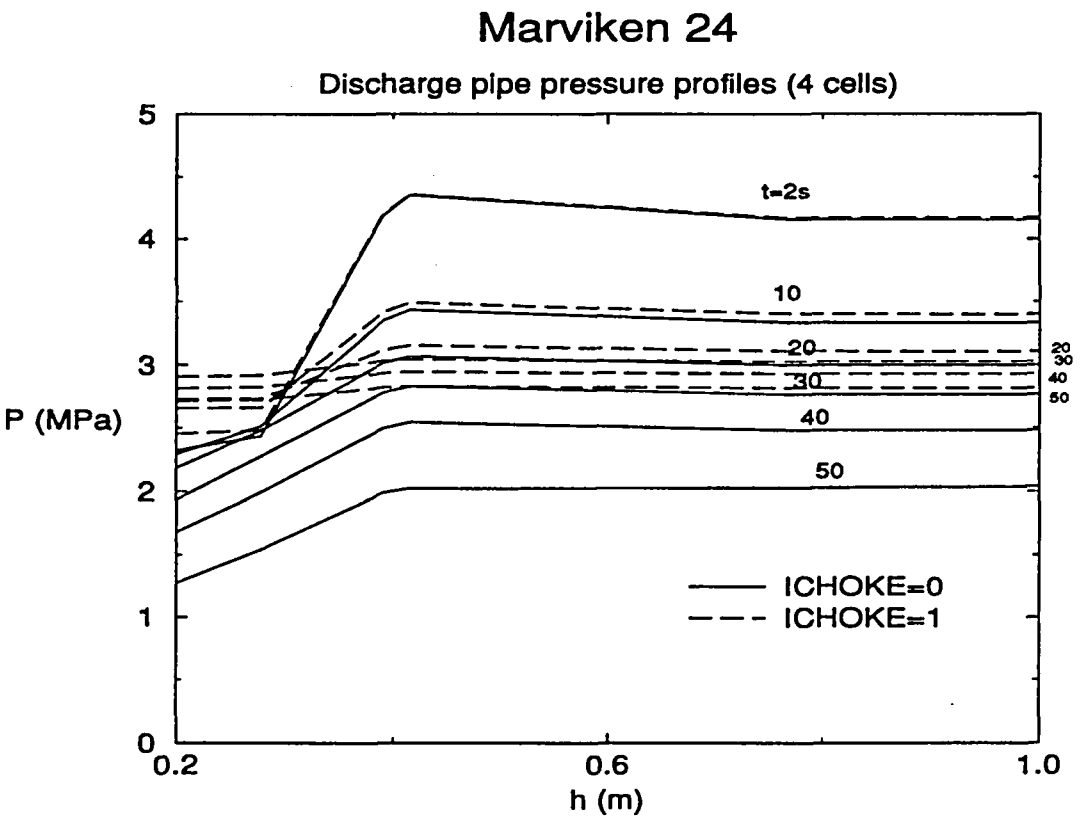

Figure 31

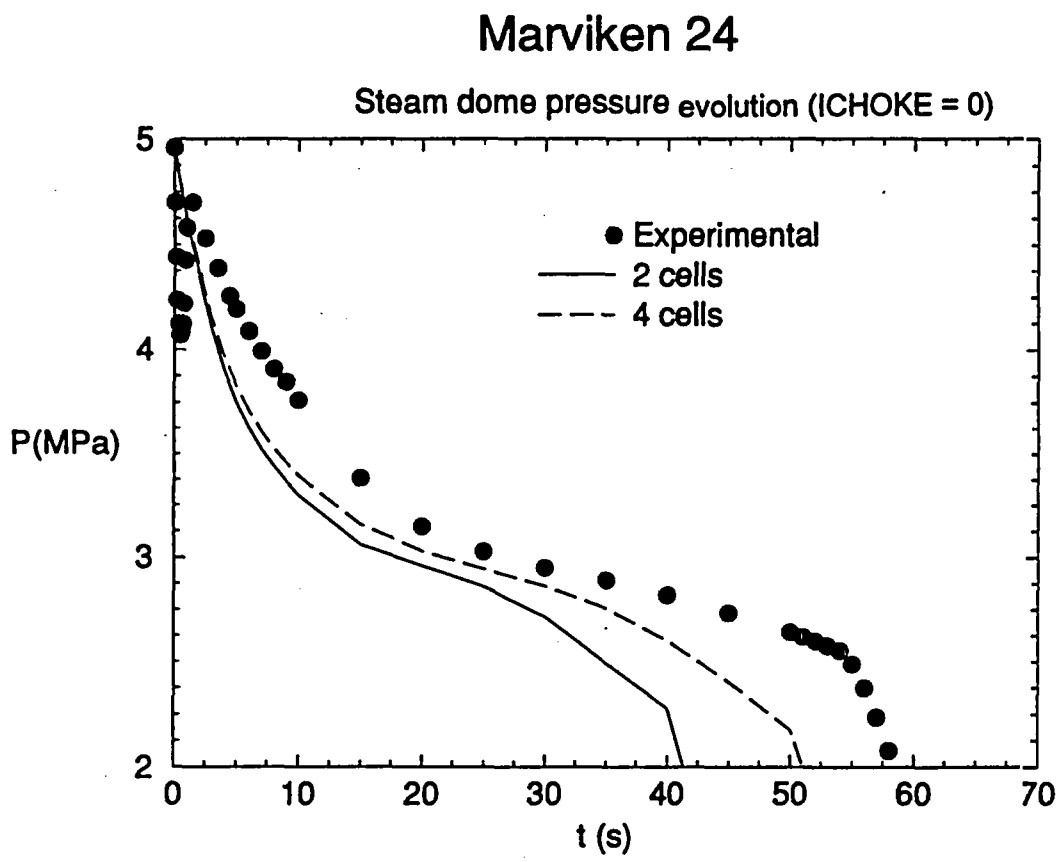

Figure 32

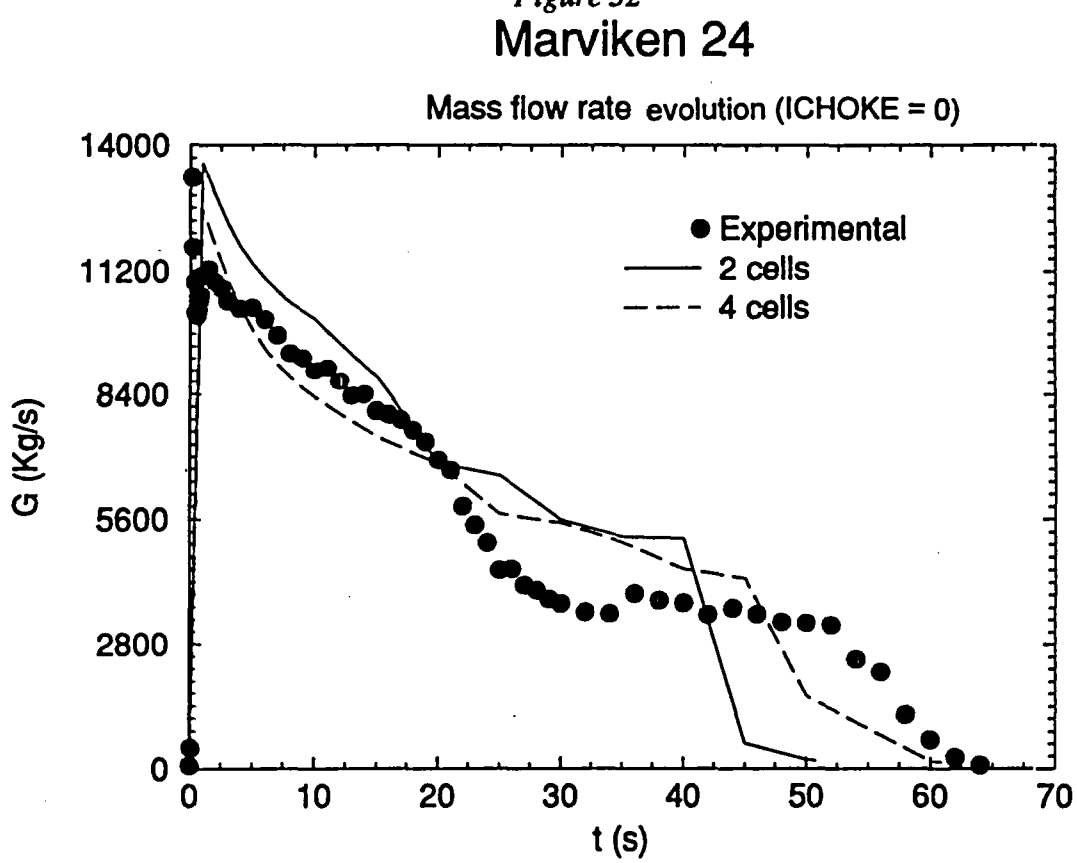

Figure 33

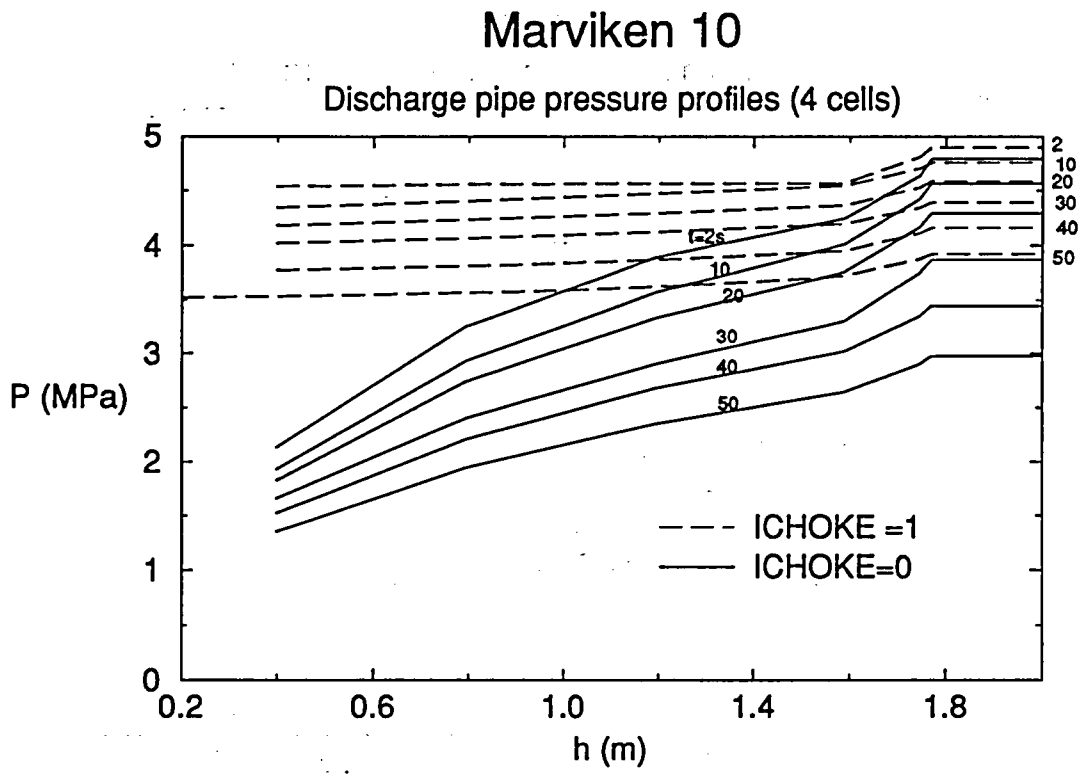

Figure 34

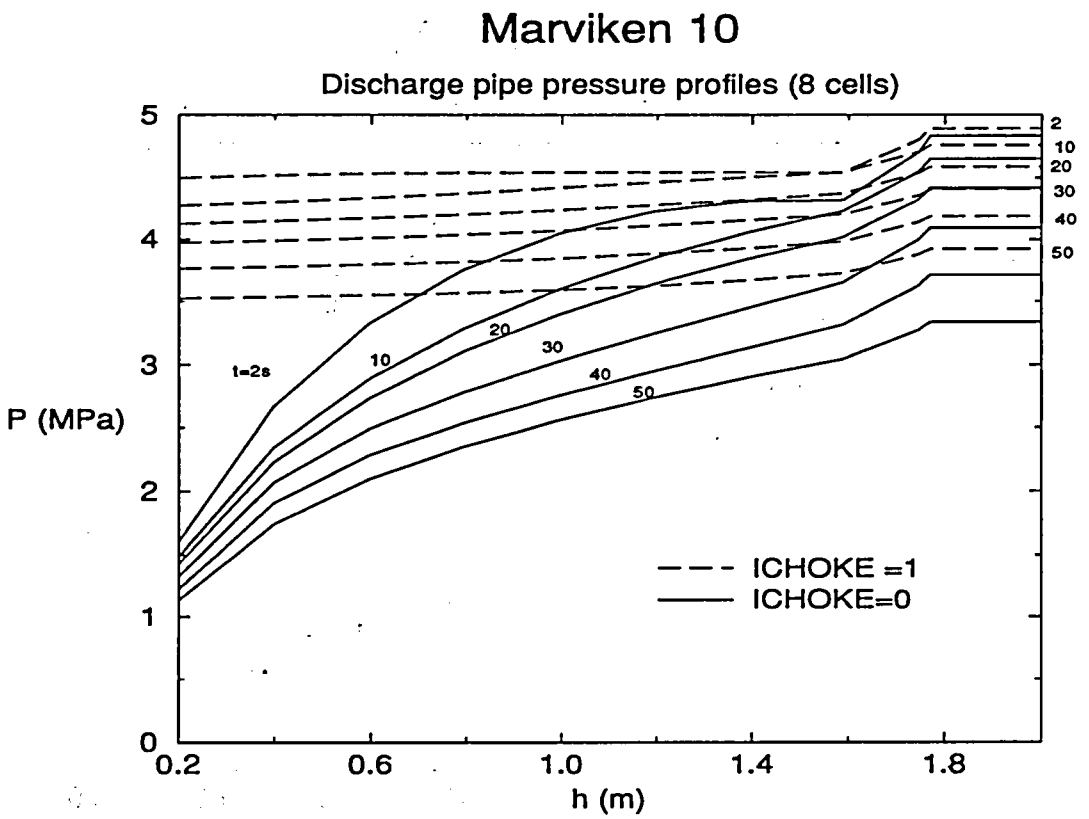

Figure 35

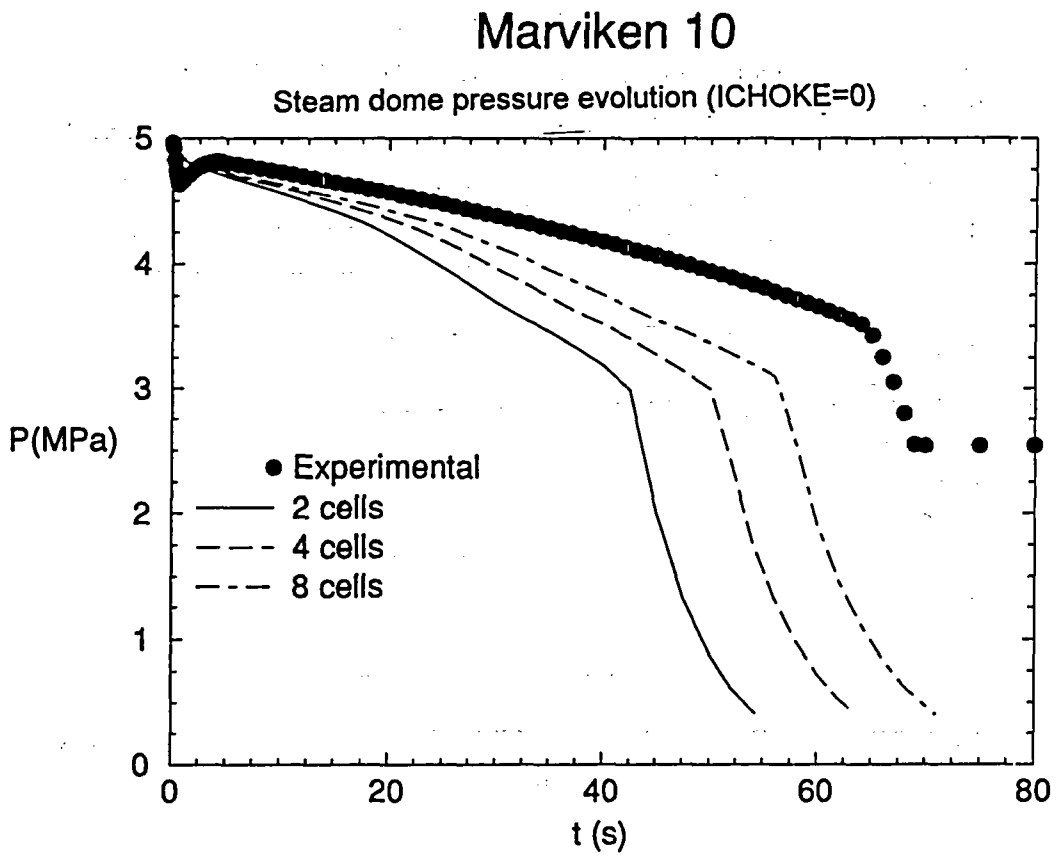

Figure 36

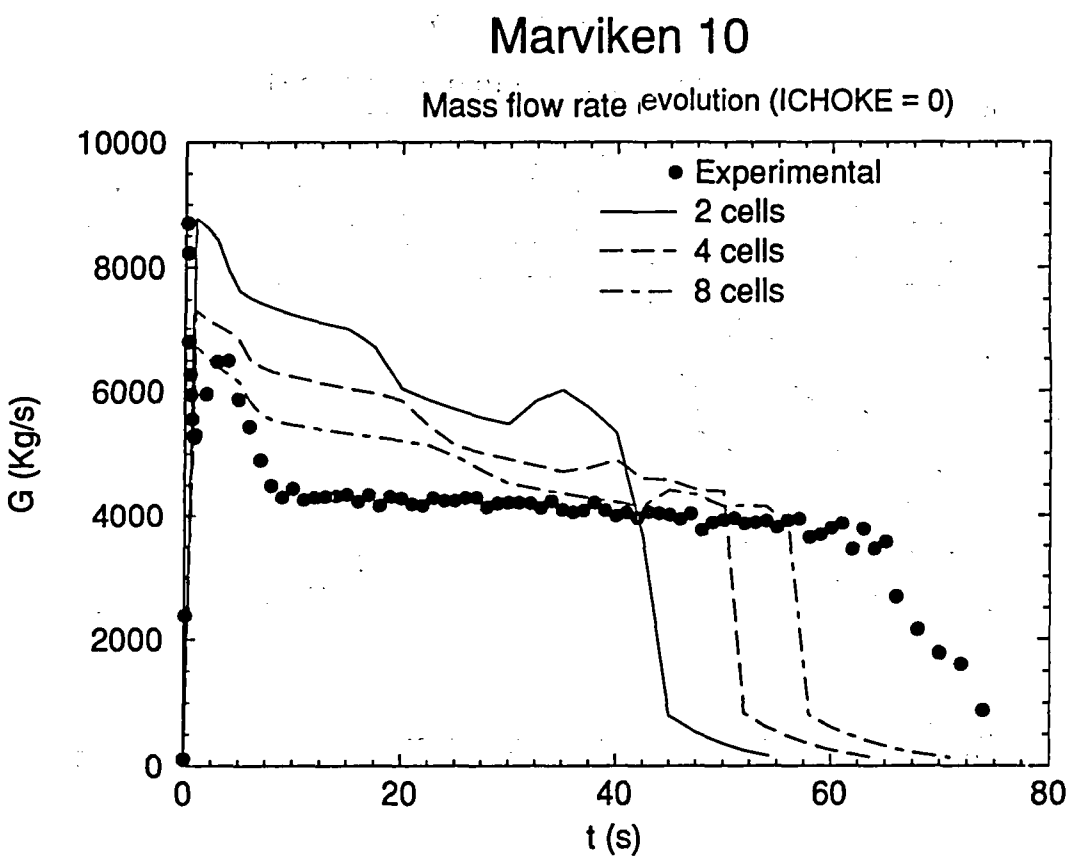

Figure 37

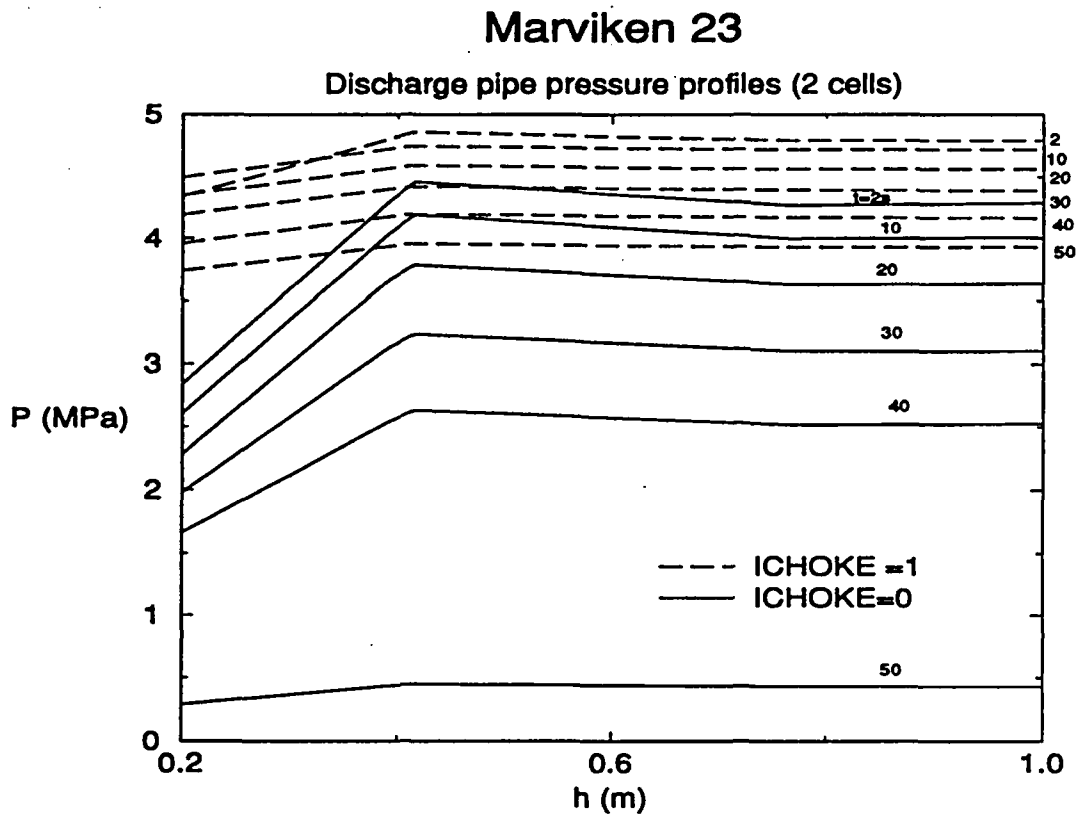

Figure 38

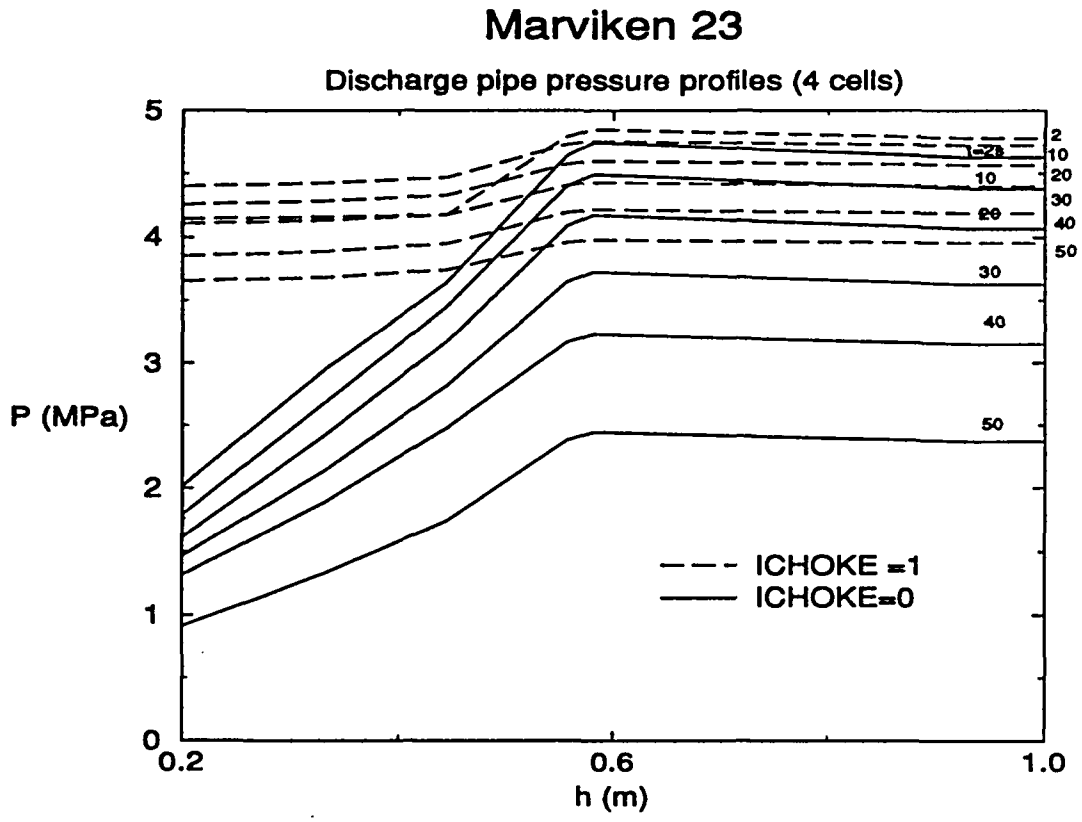

Figure 39

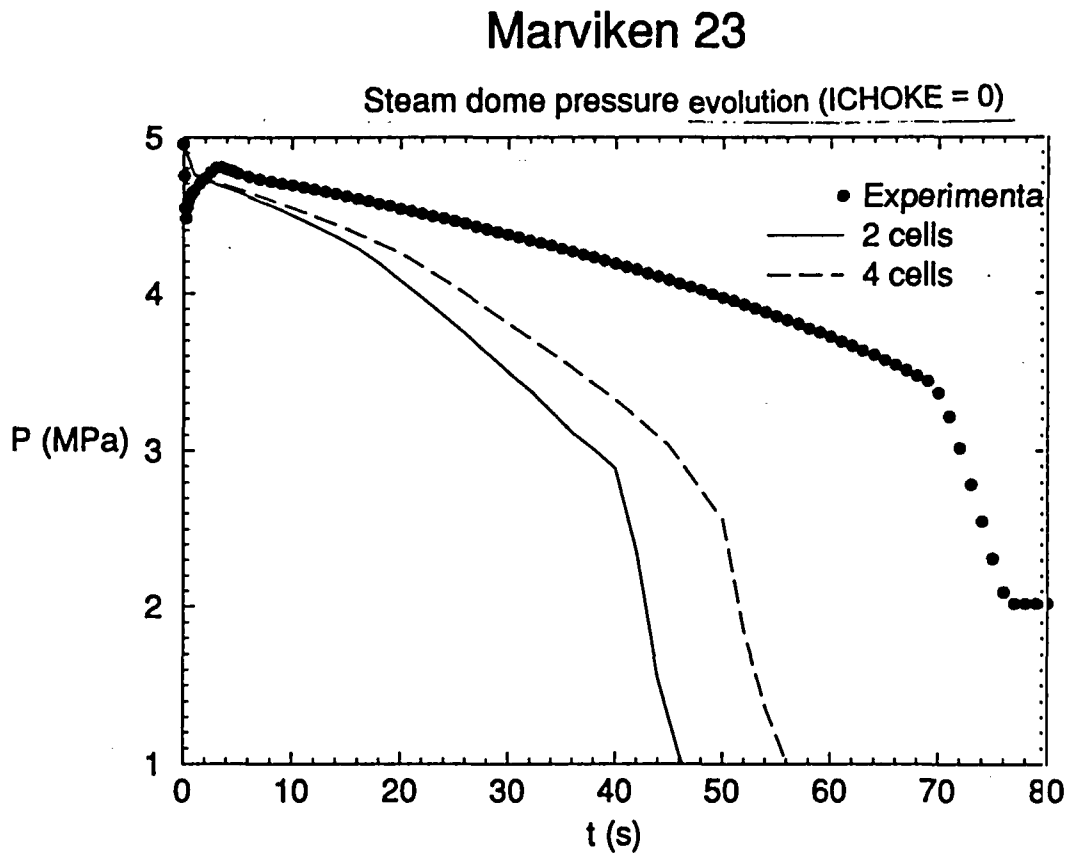

Figure 40

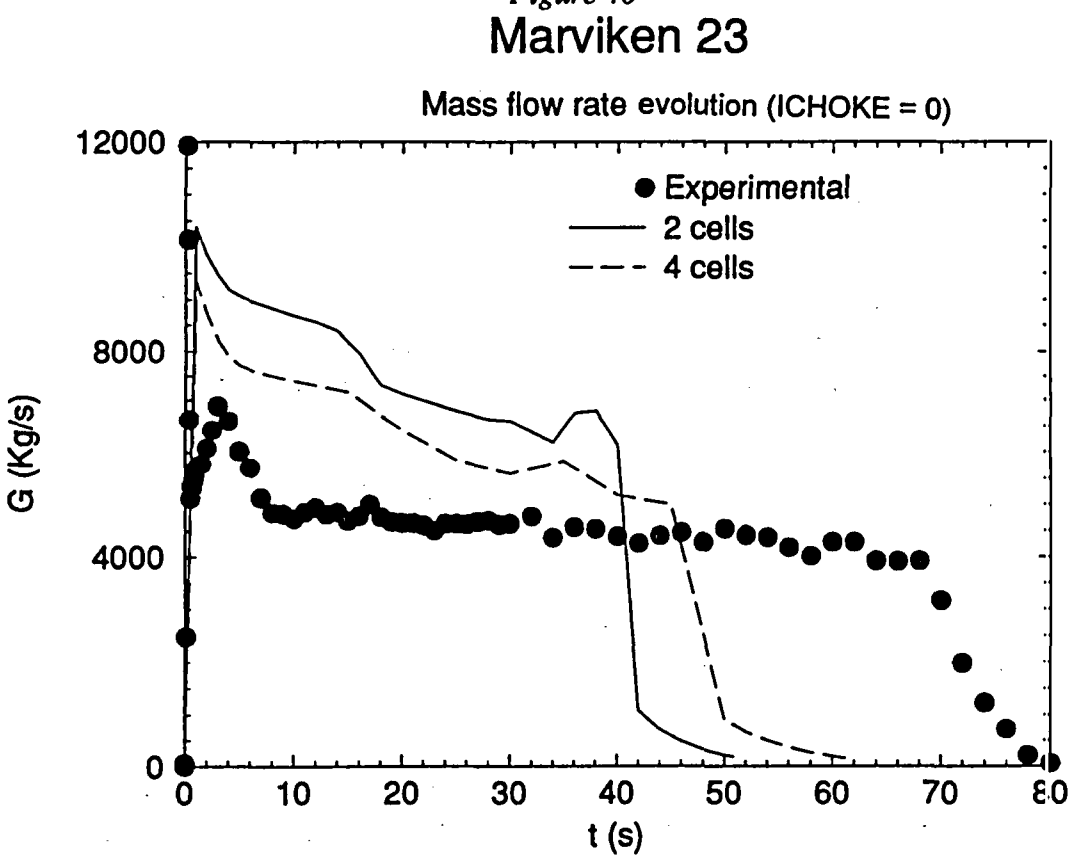

Figure 41

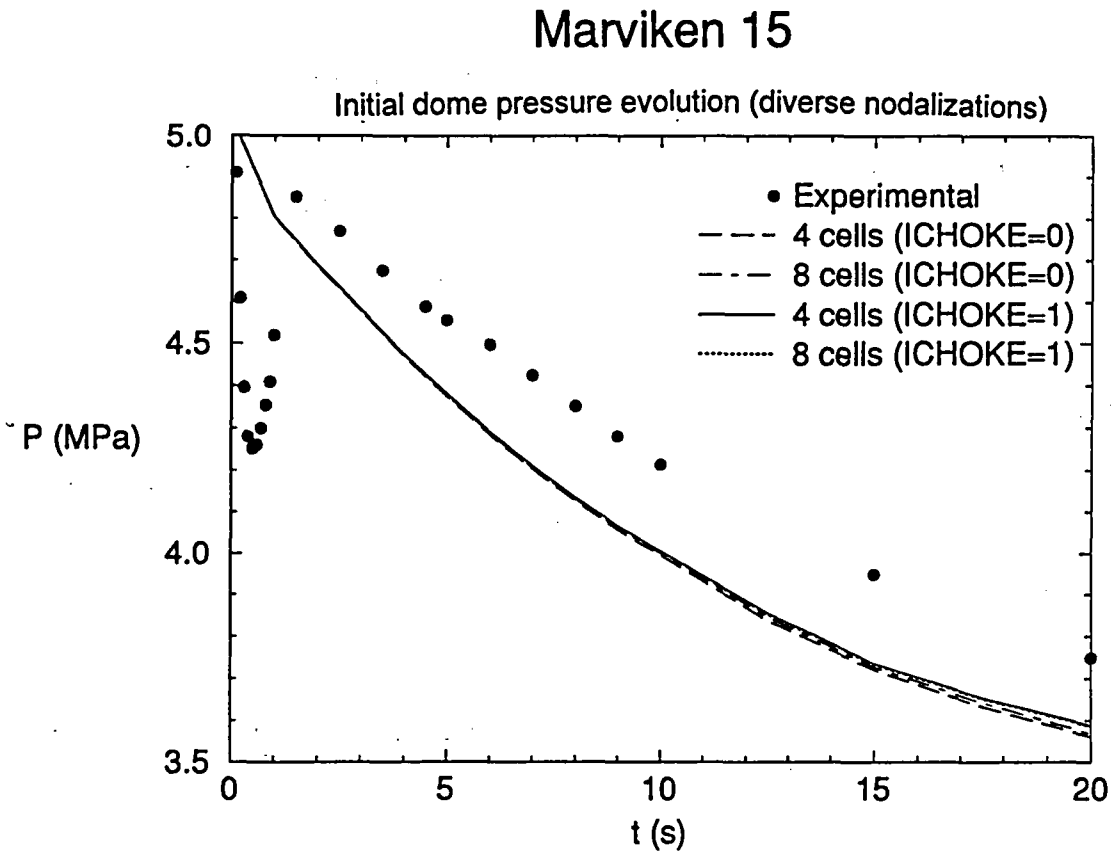

Figure 42

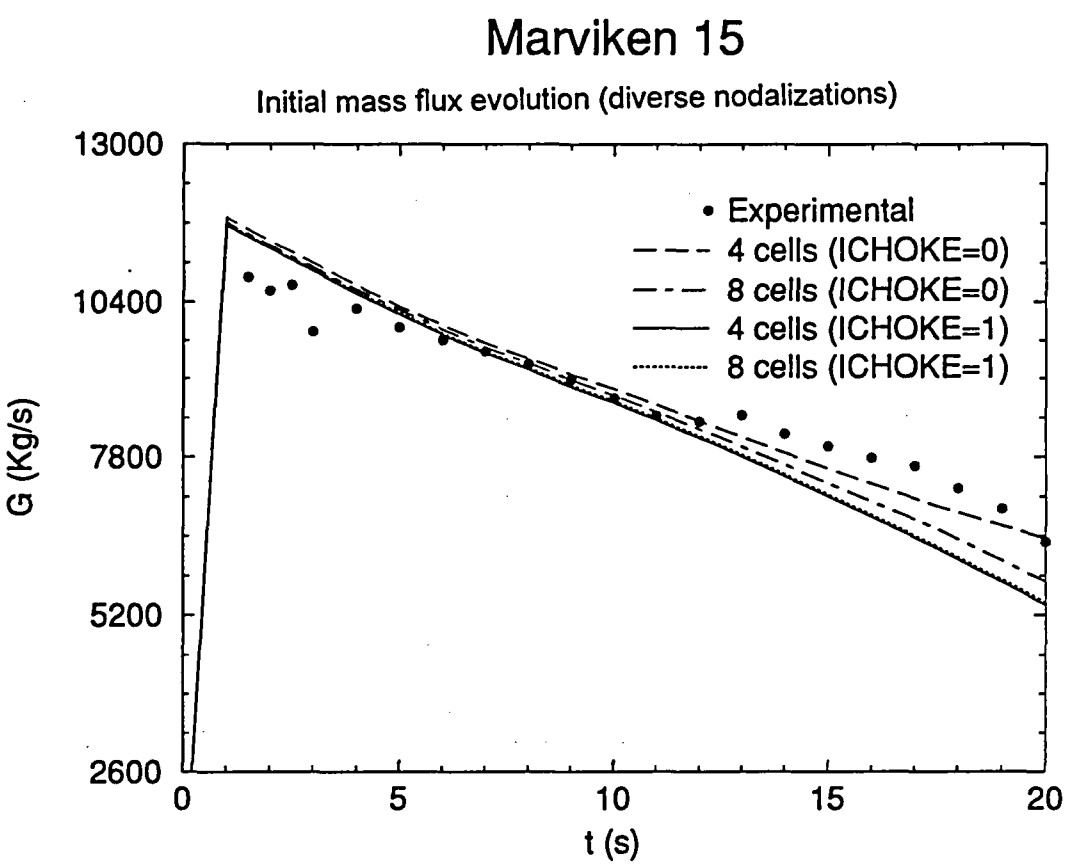

Figure 43

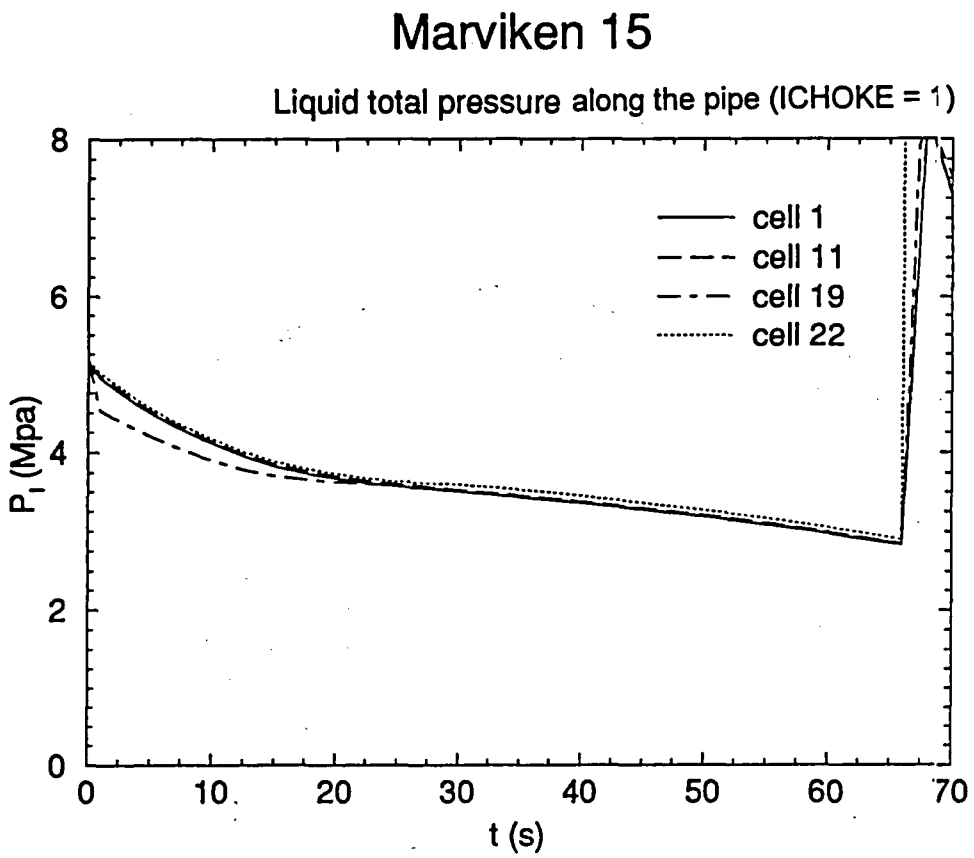

Figure 44

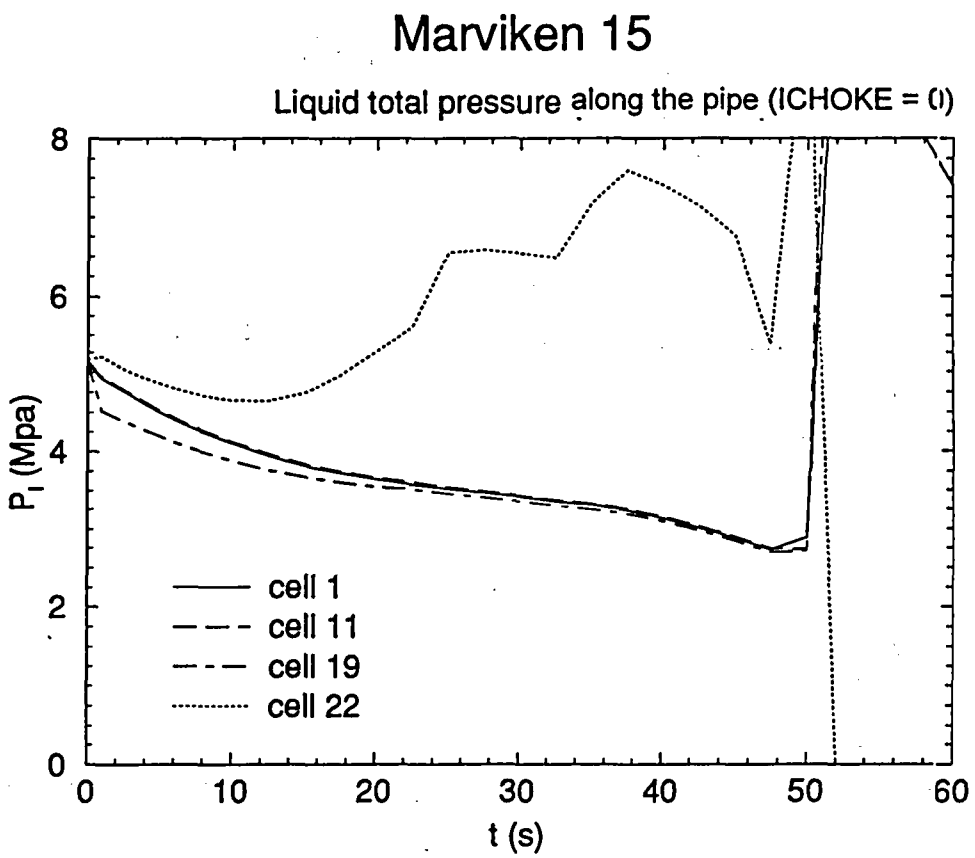

Figure 45

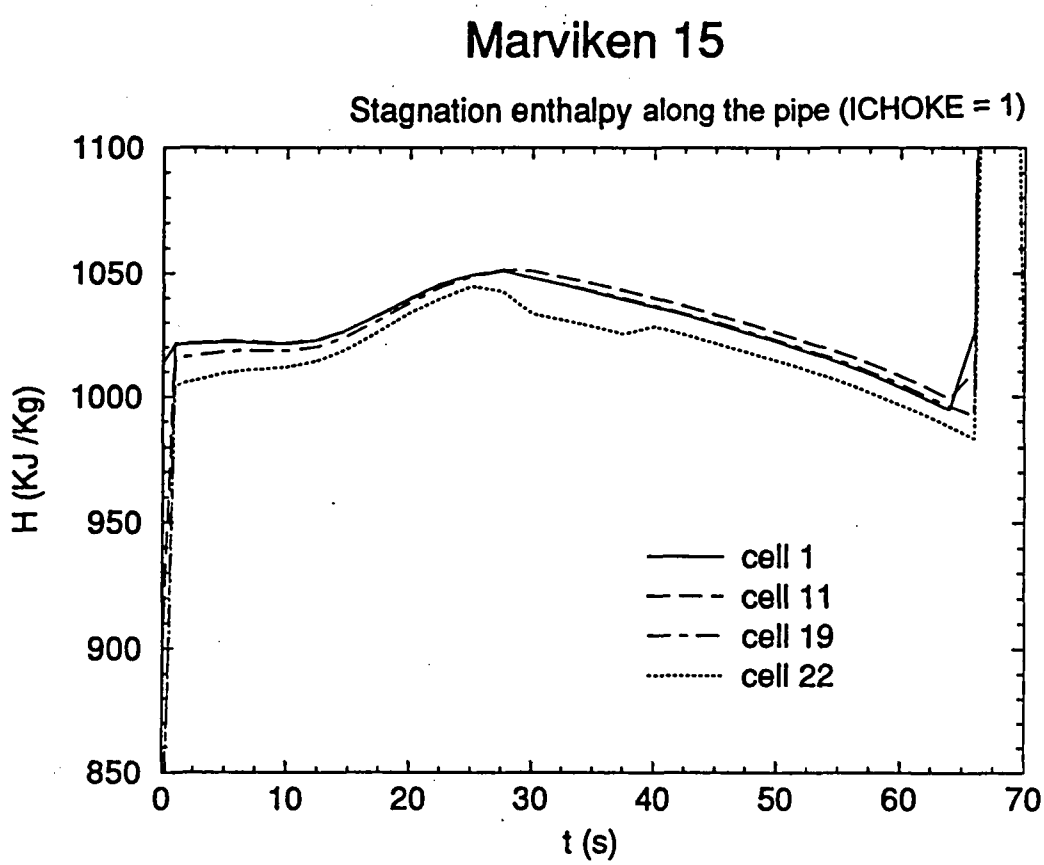

Figure 46

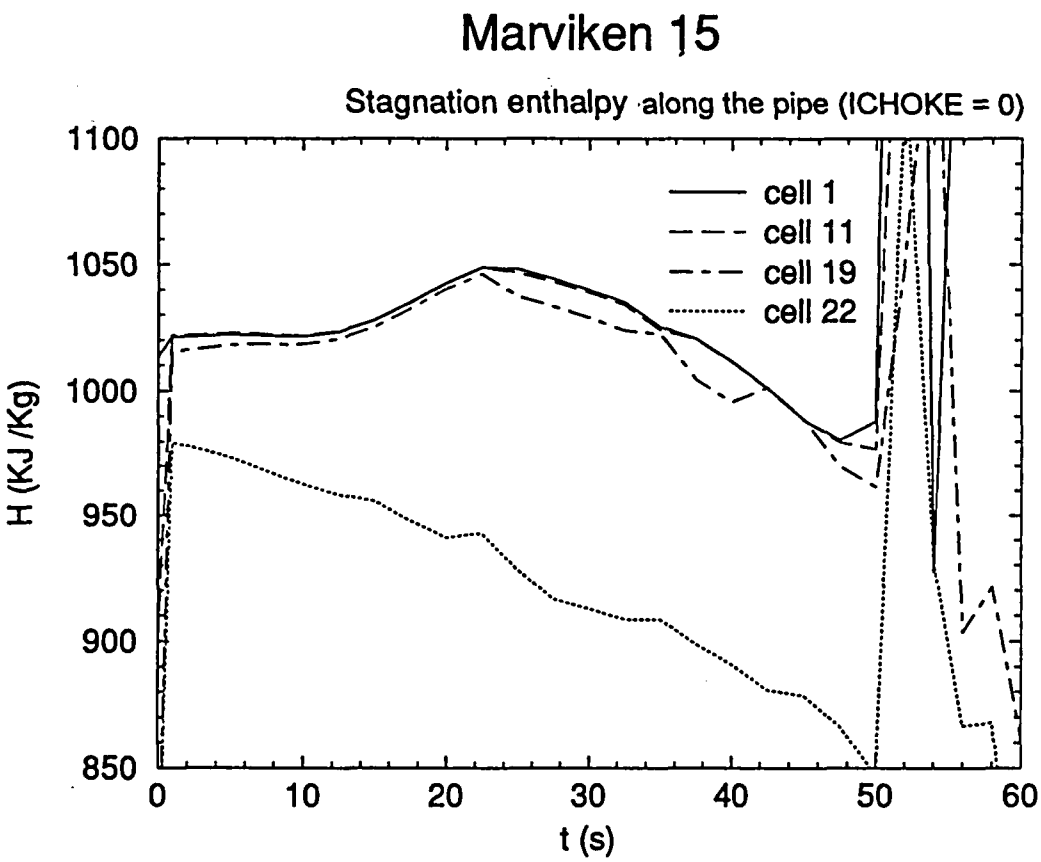

Figure 47

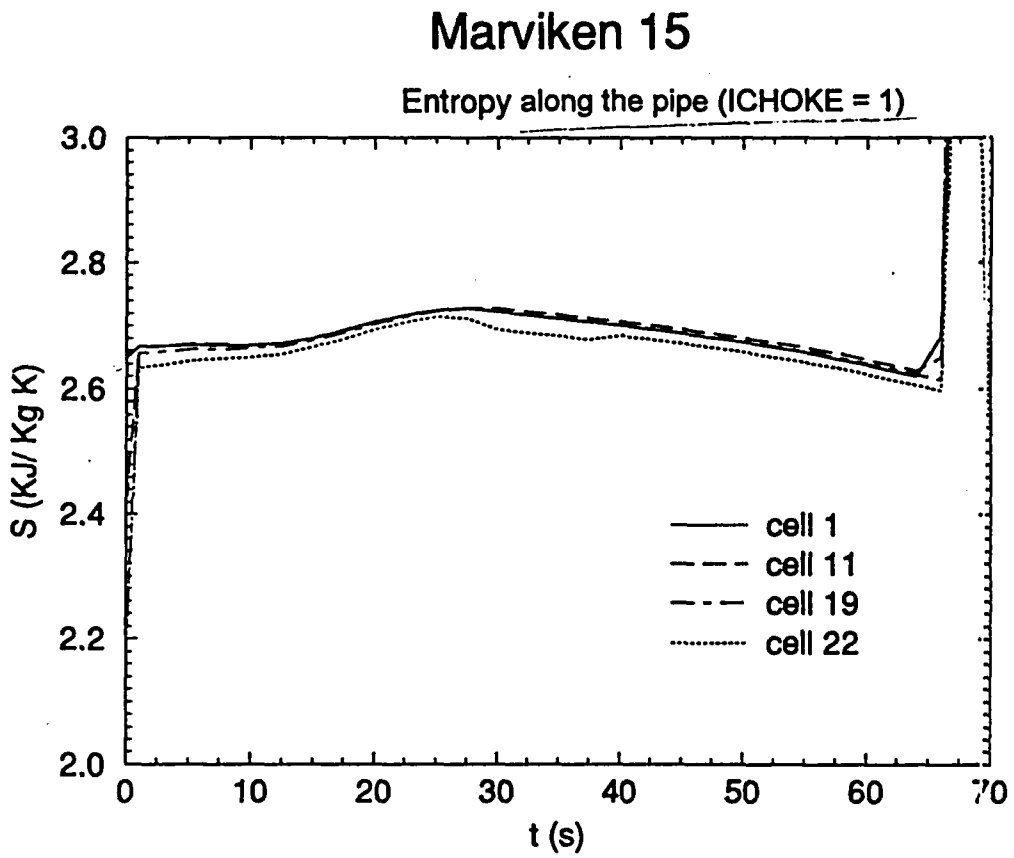

Figure 48

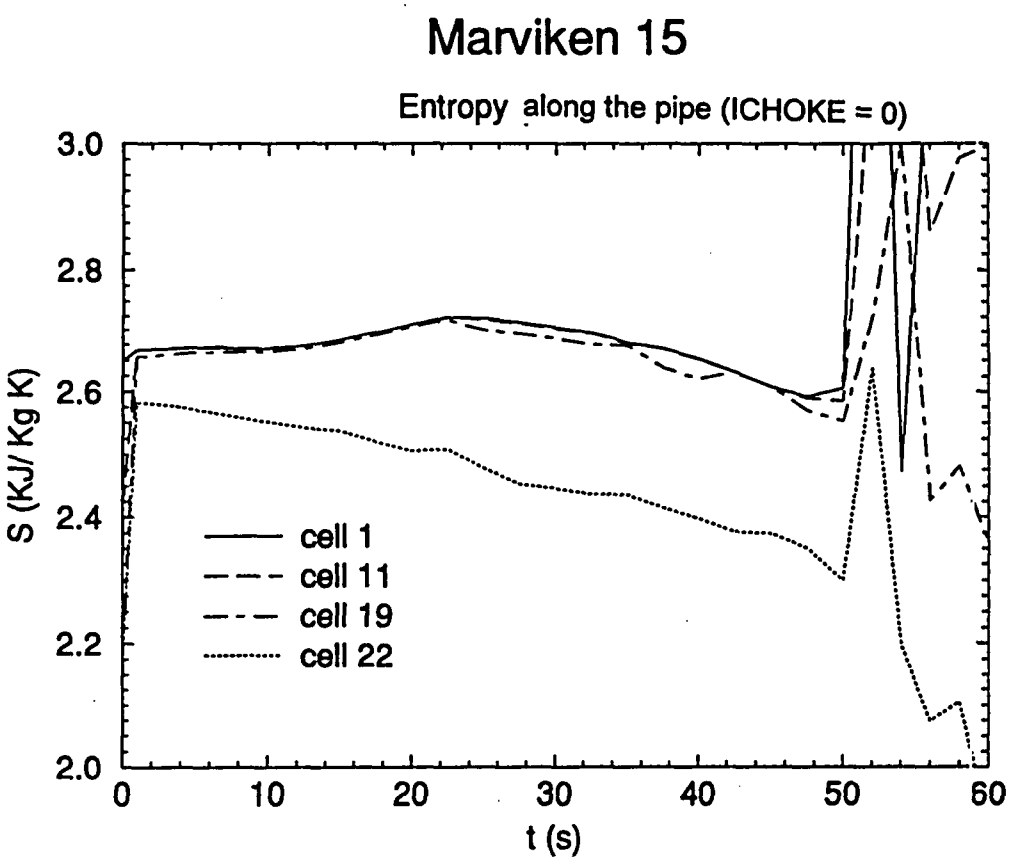

Figure 49

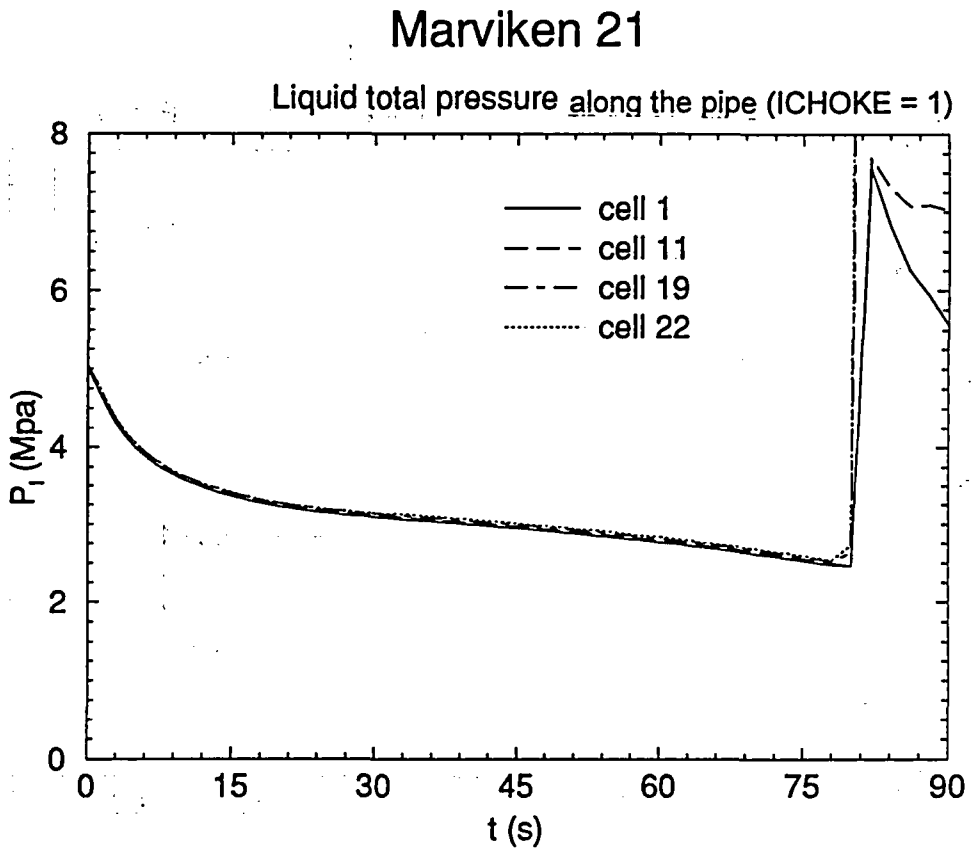

Figure 50

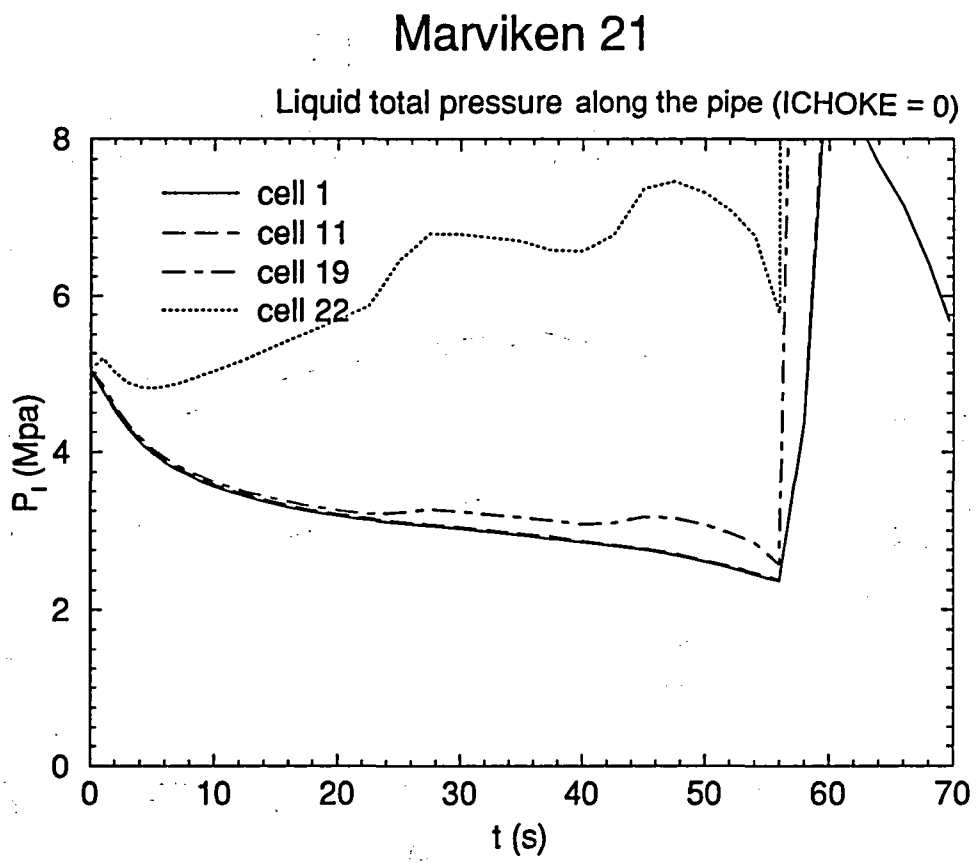

Figure 51

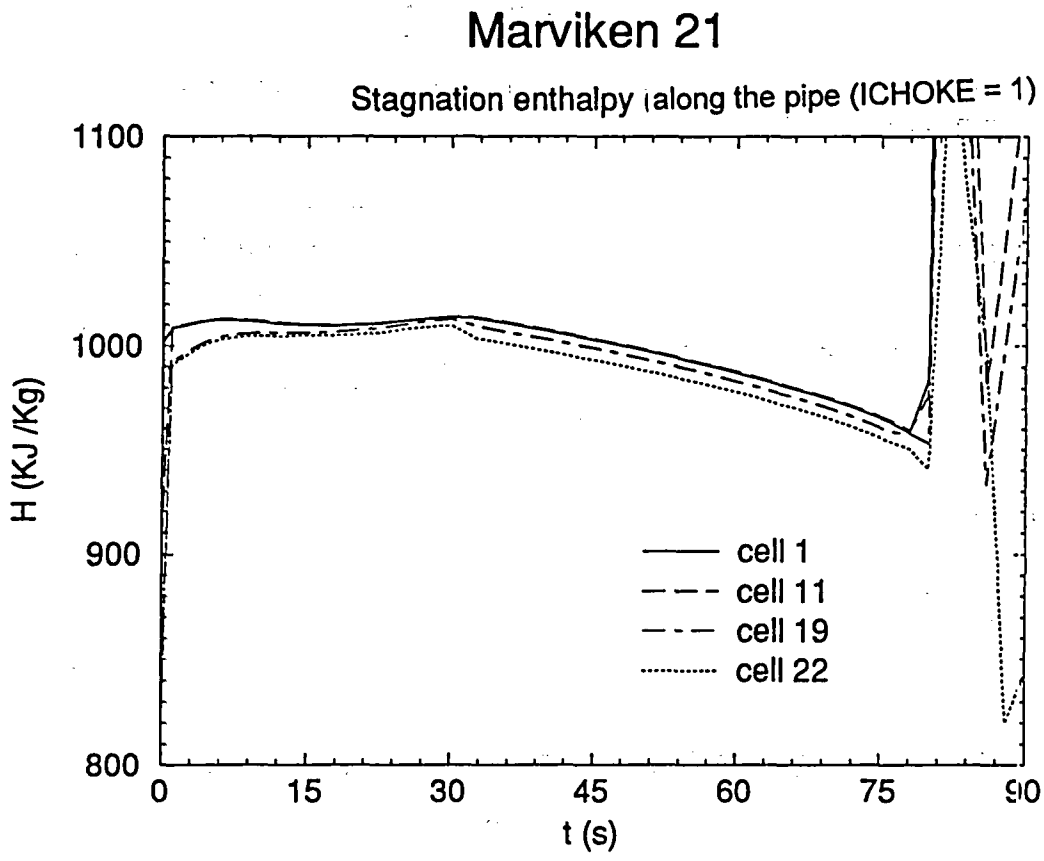

Figure 52

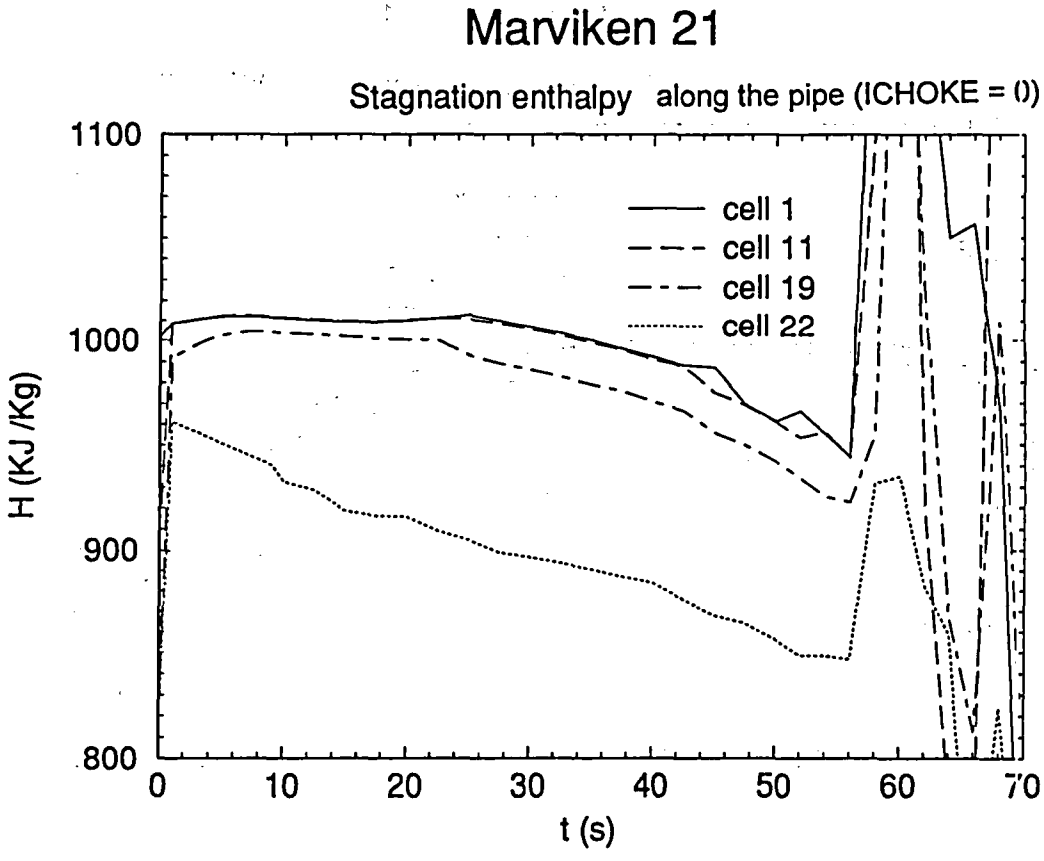

Figure 53

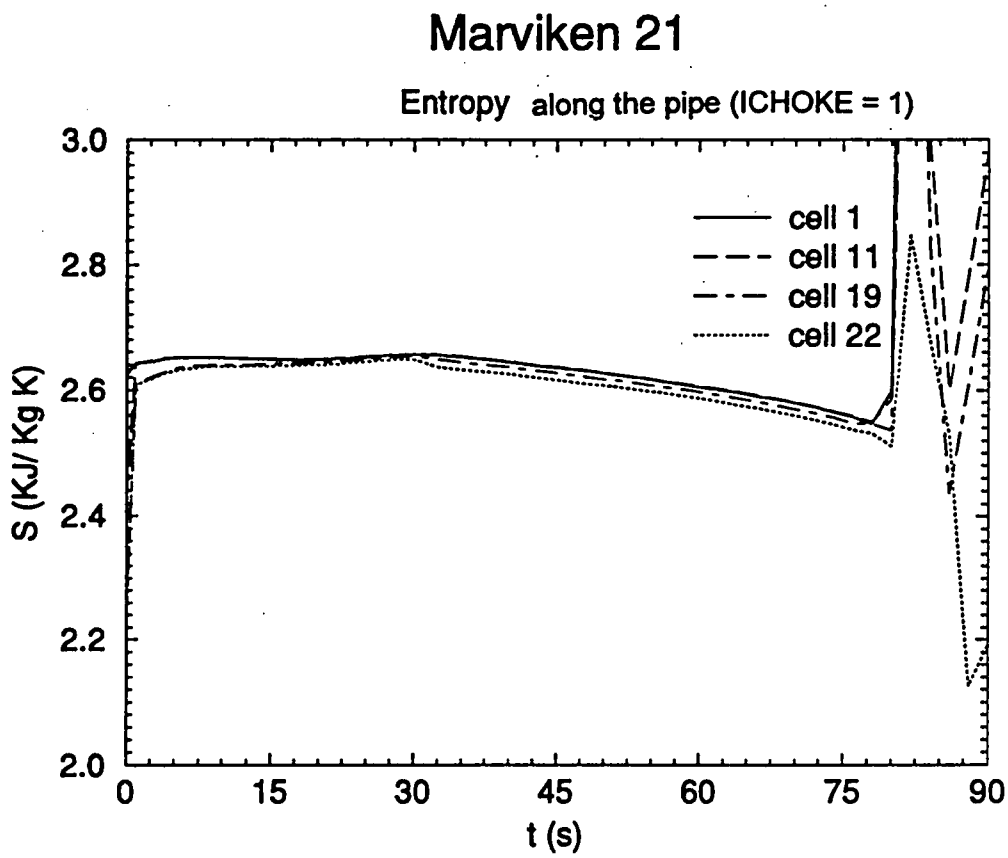

Figure 54

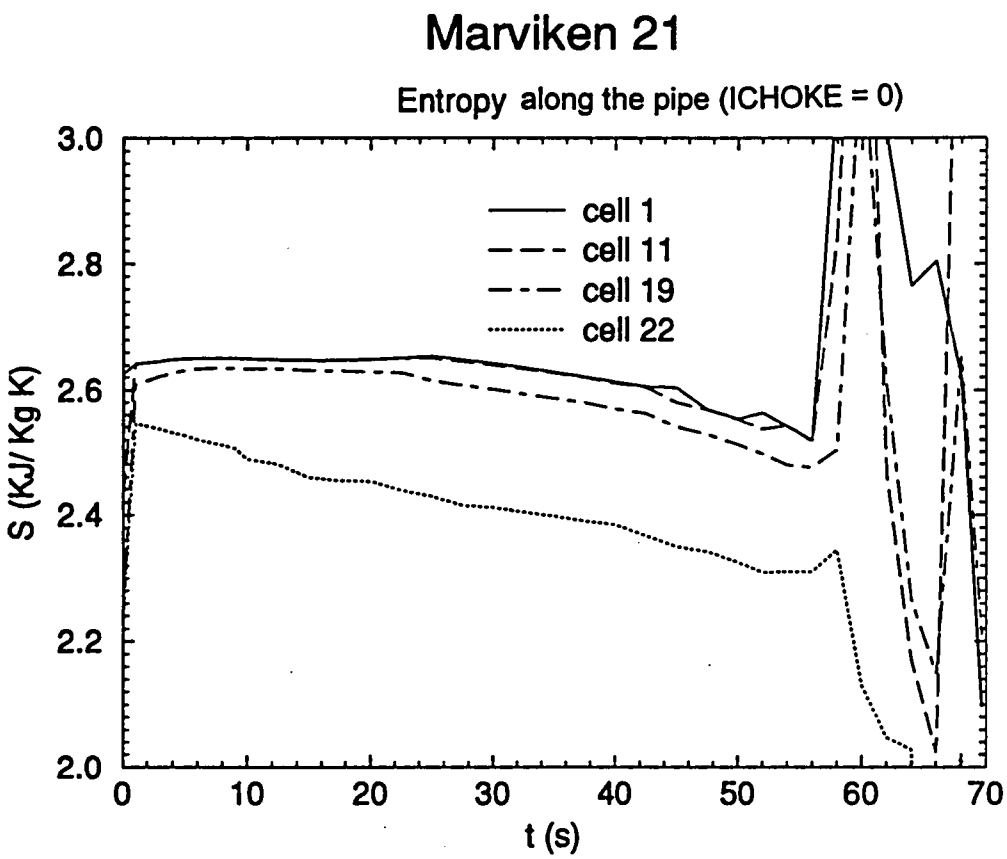

Figure 55

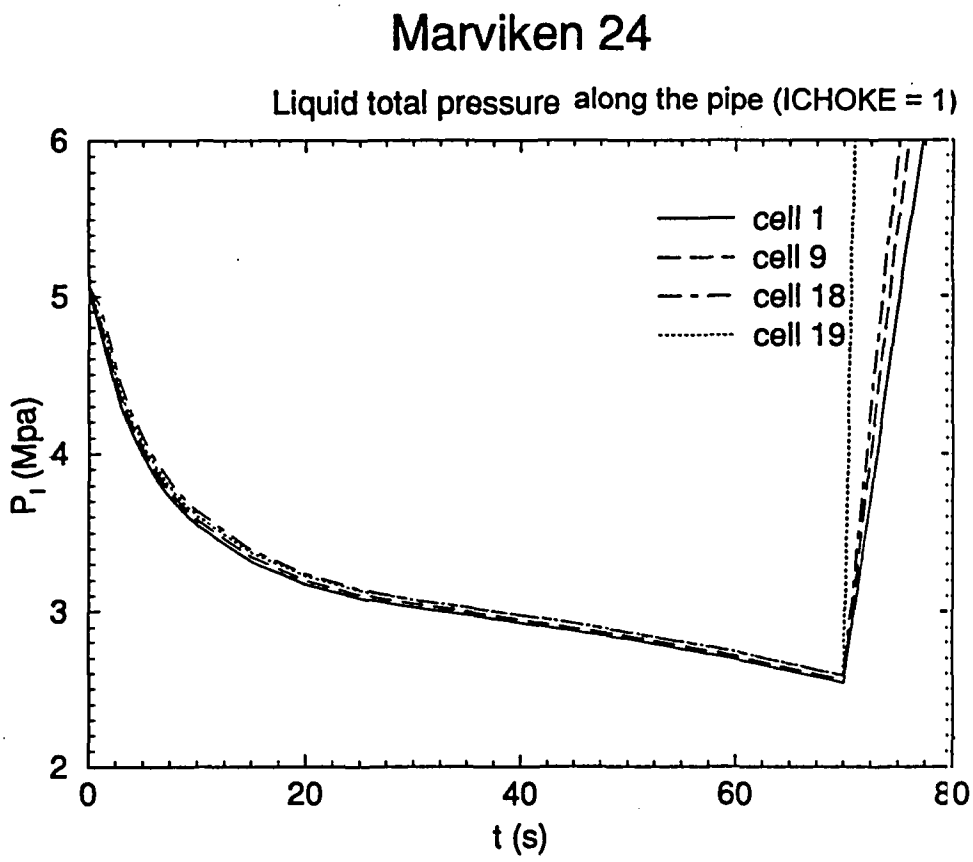

Figure 56

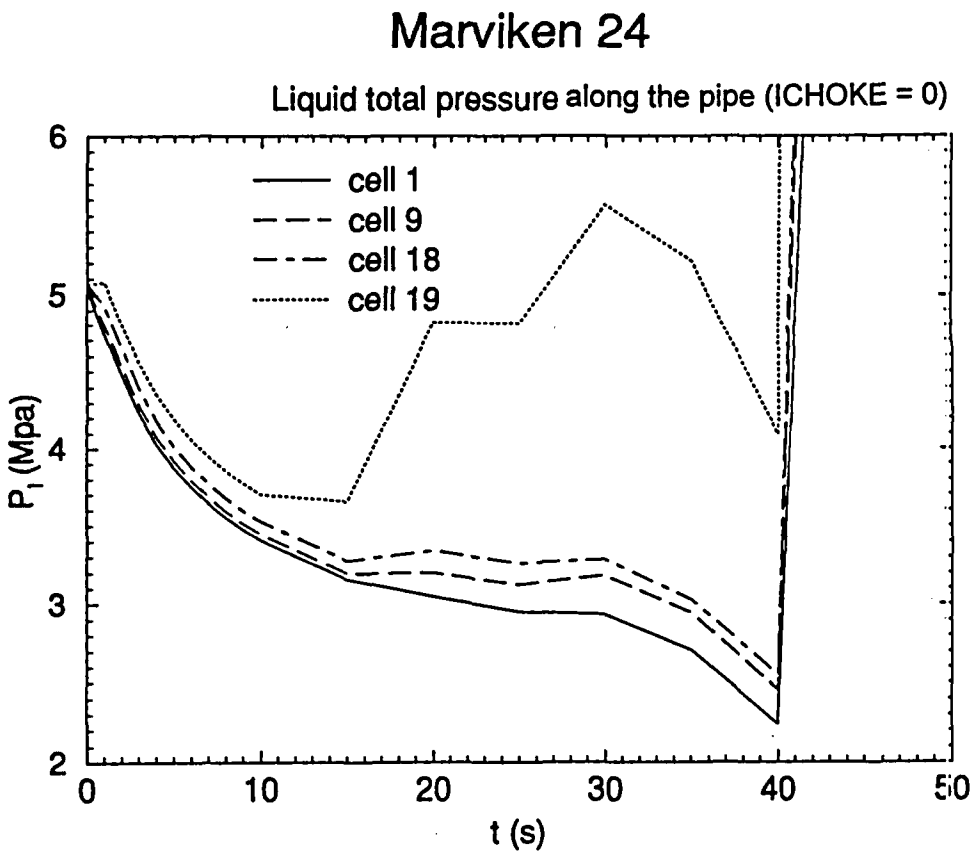

Figure 57

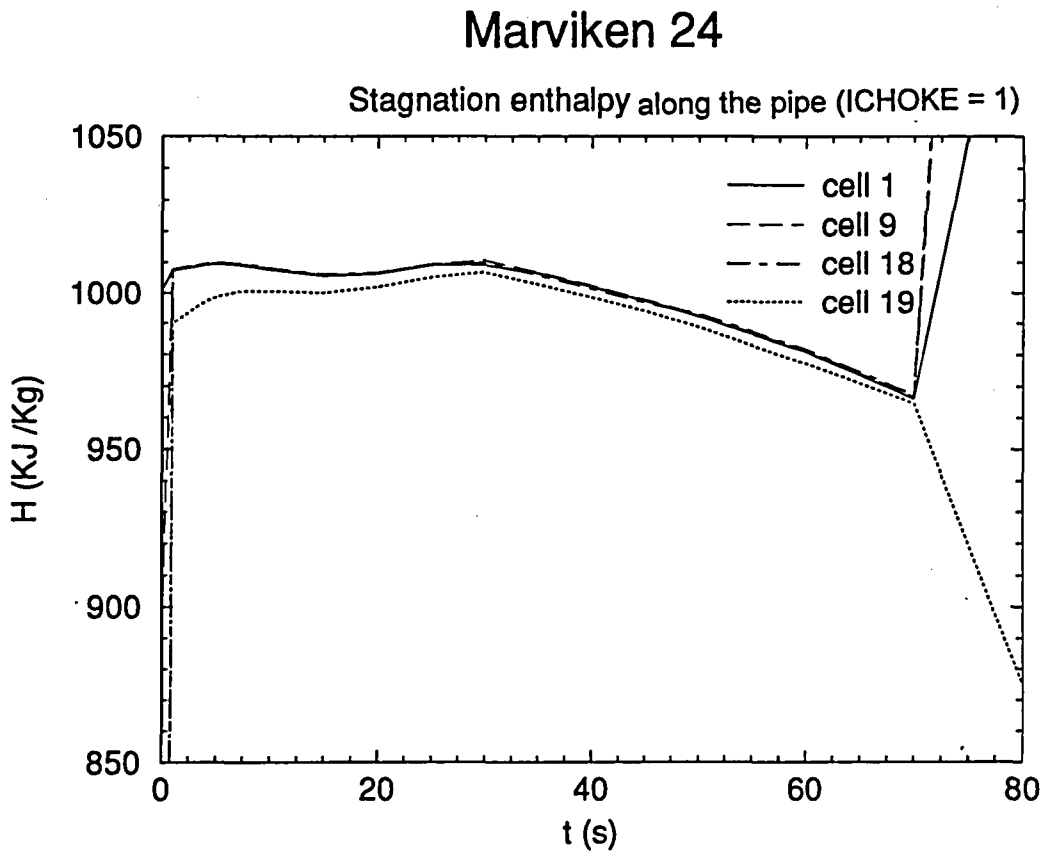

Figure 58

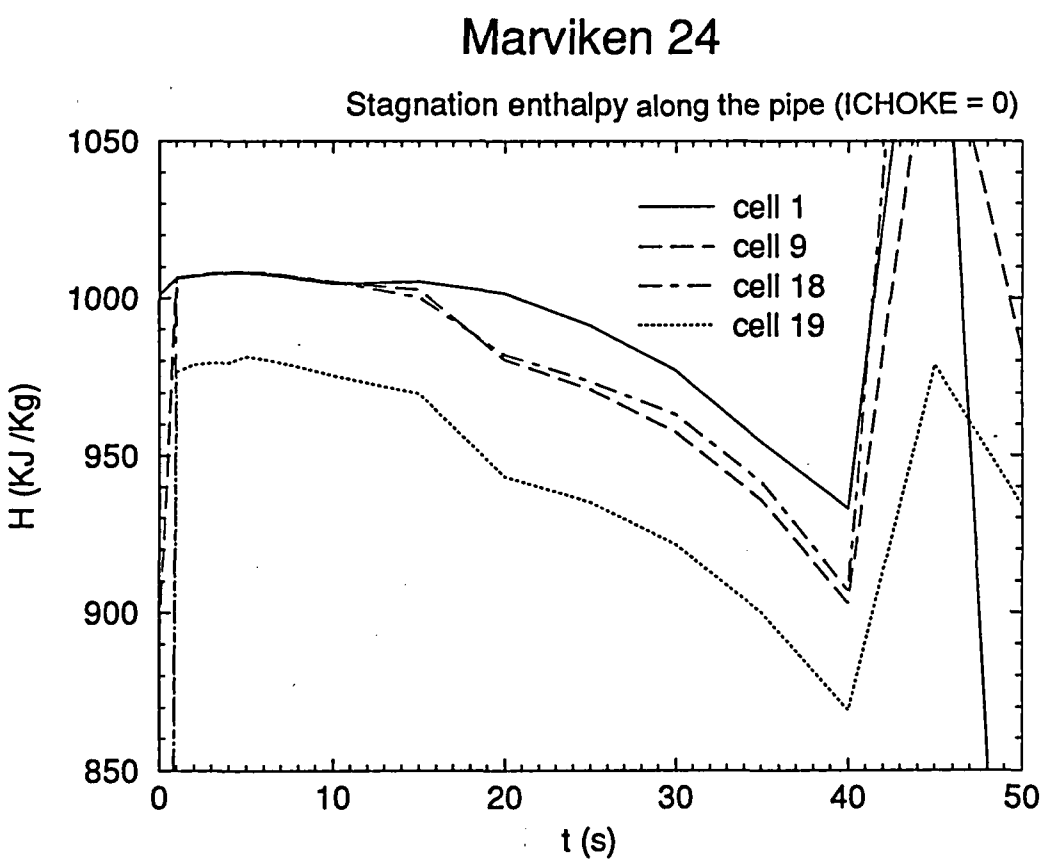

Figure 59

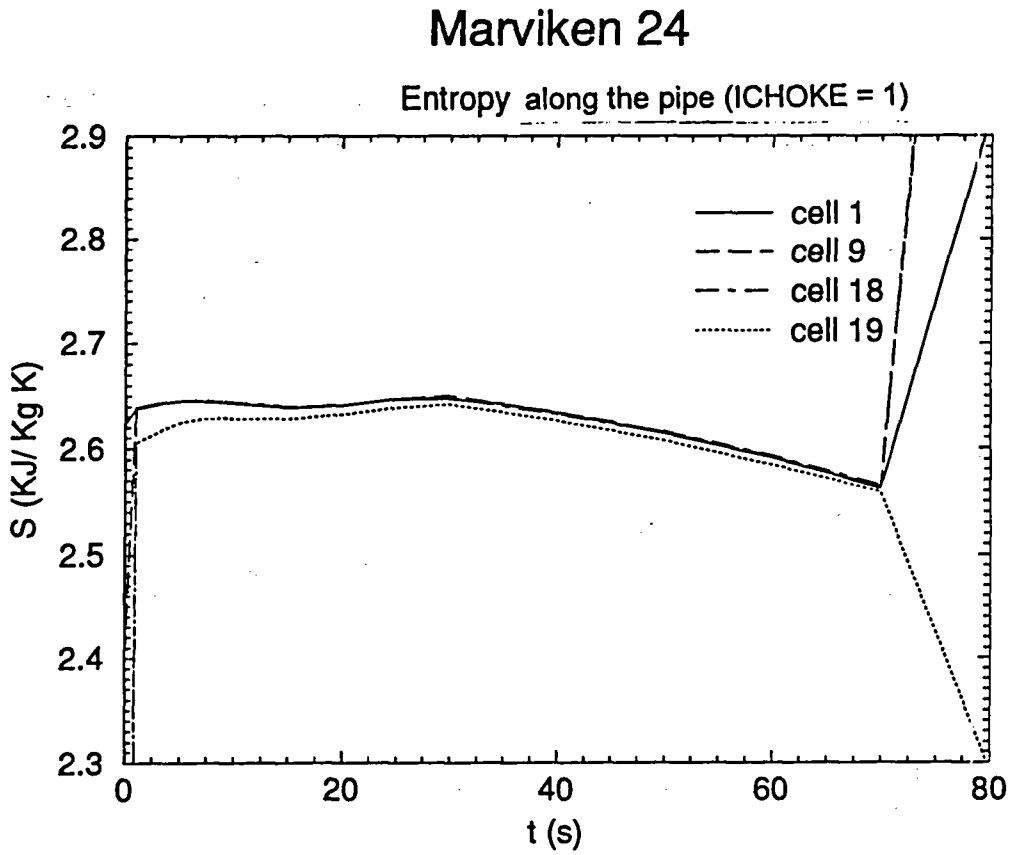

Figure 60

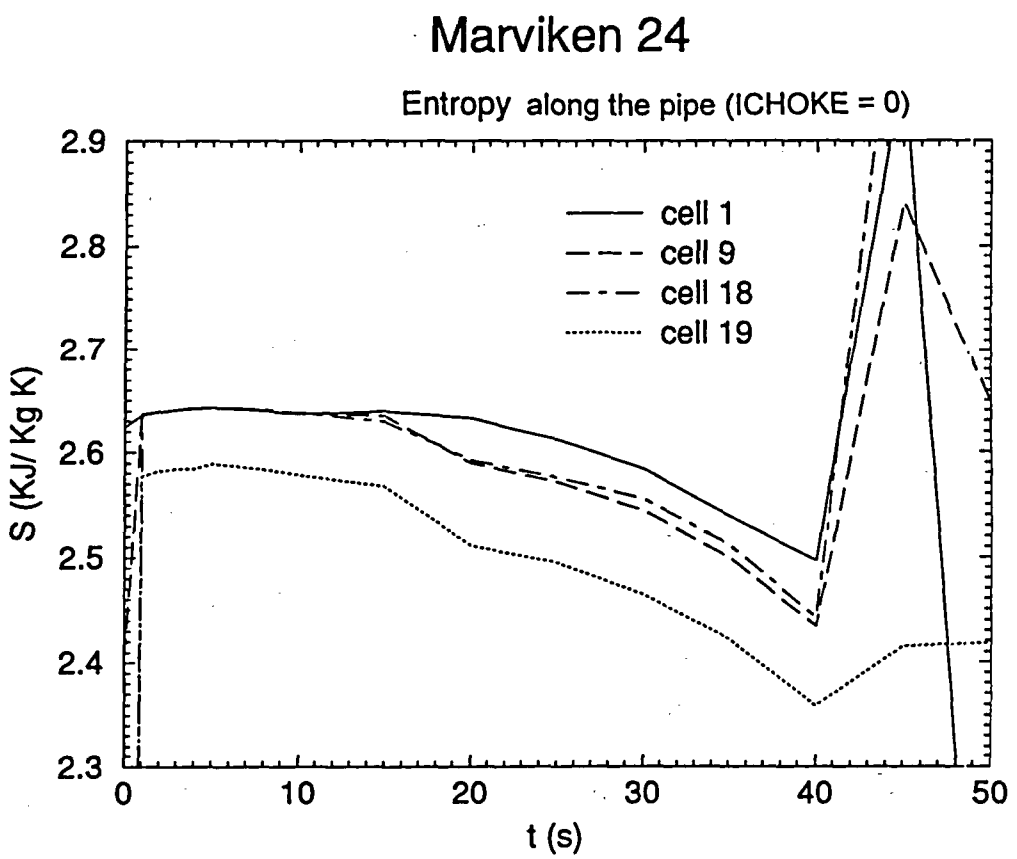

Figure 61

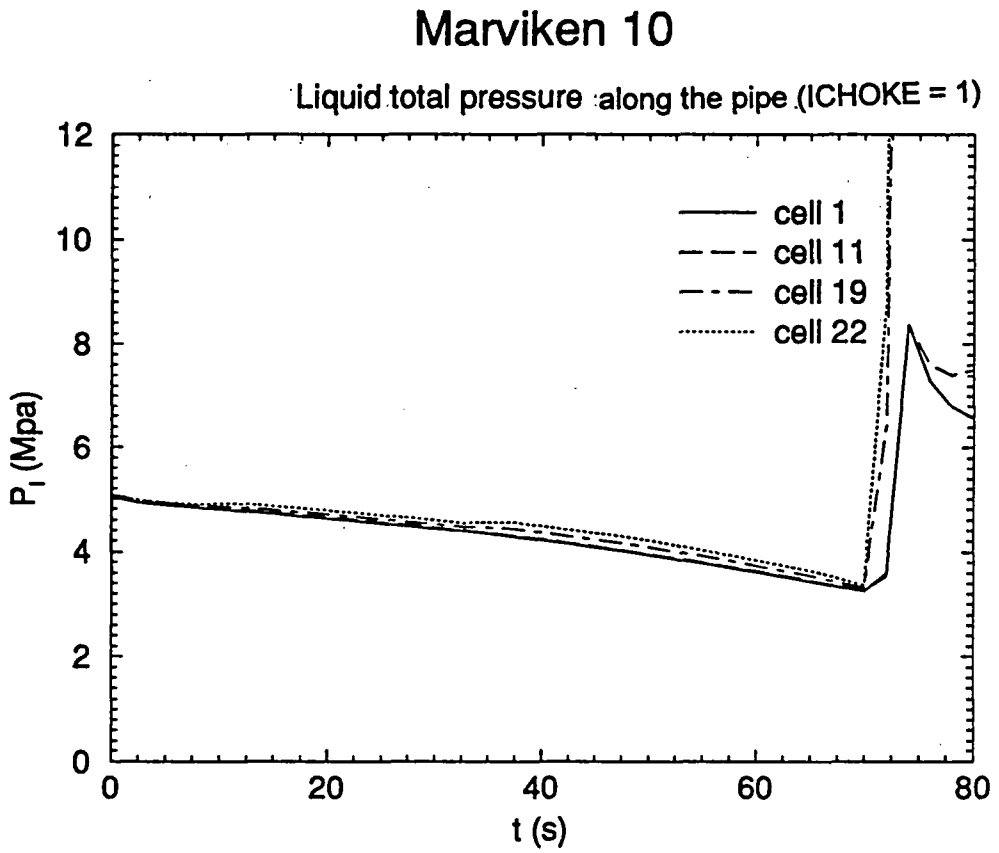

Figure 62

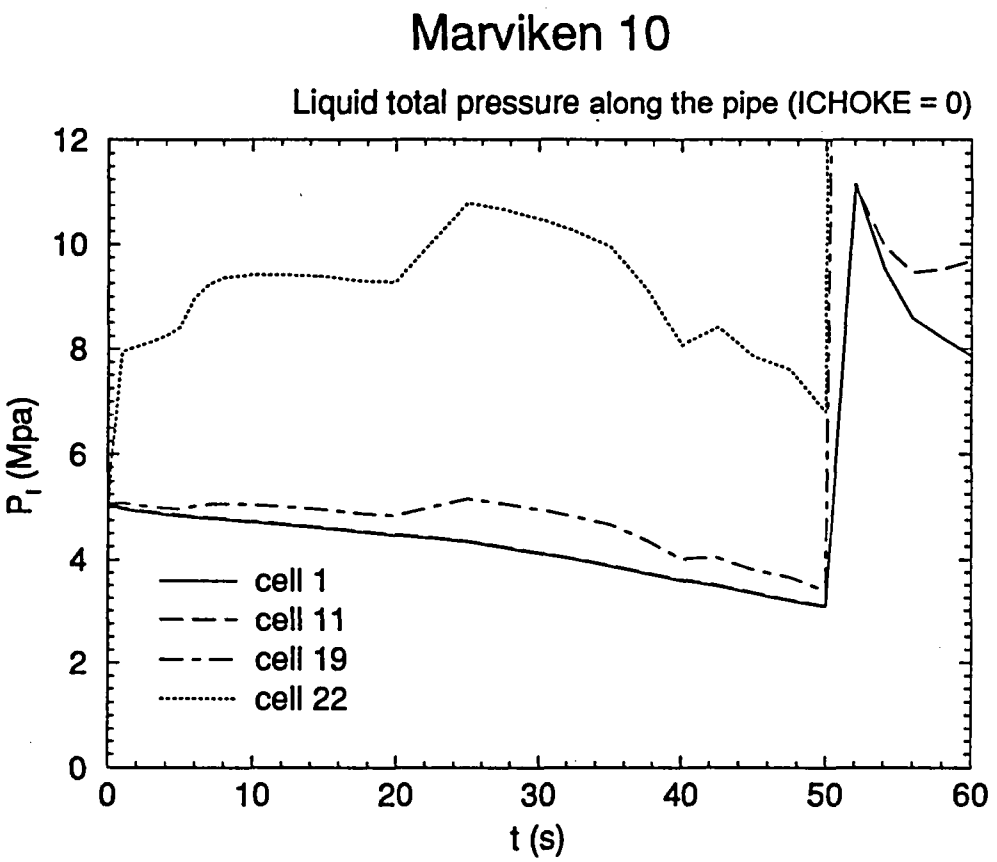

Figure 63

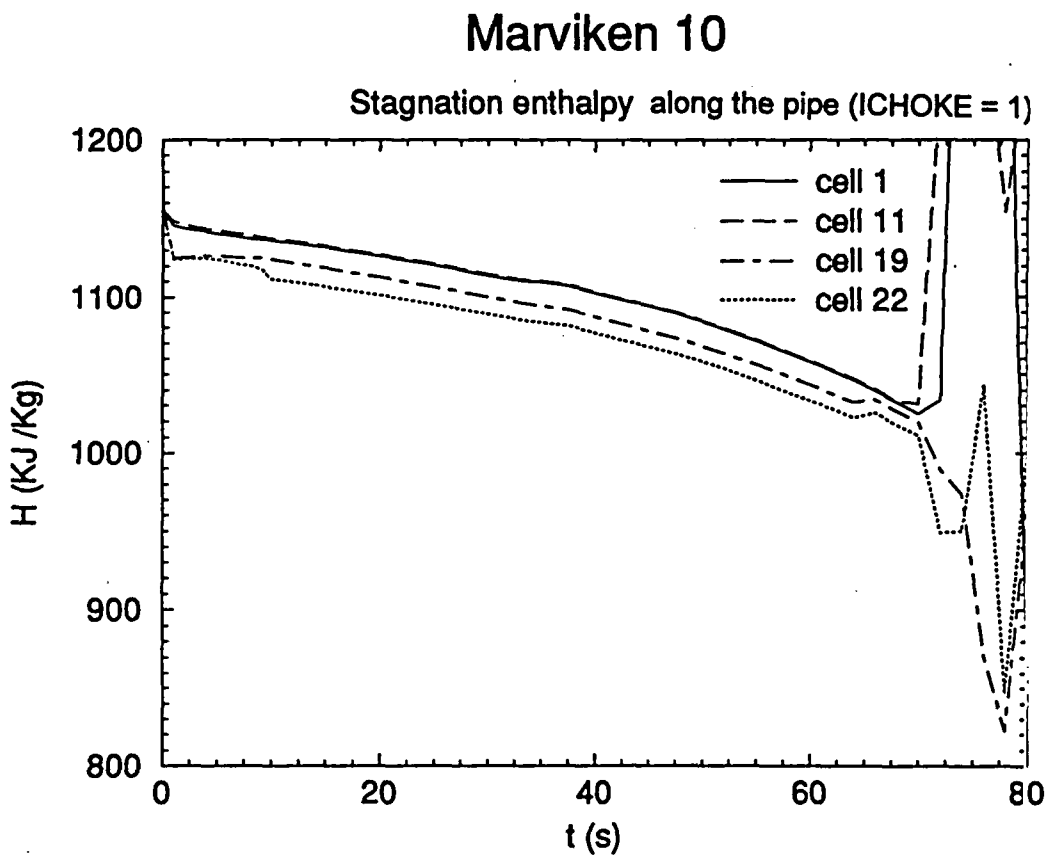

Figure 64

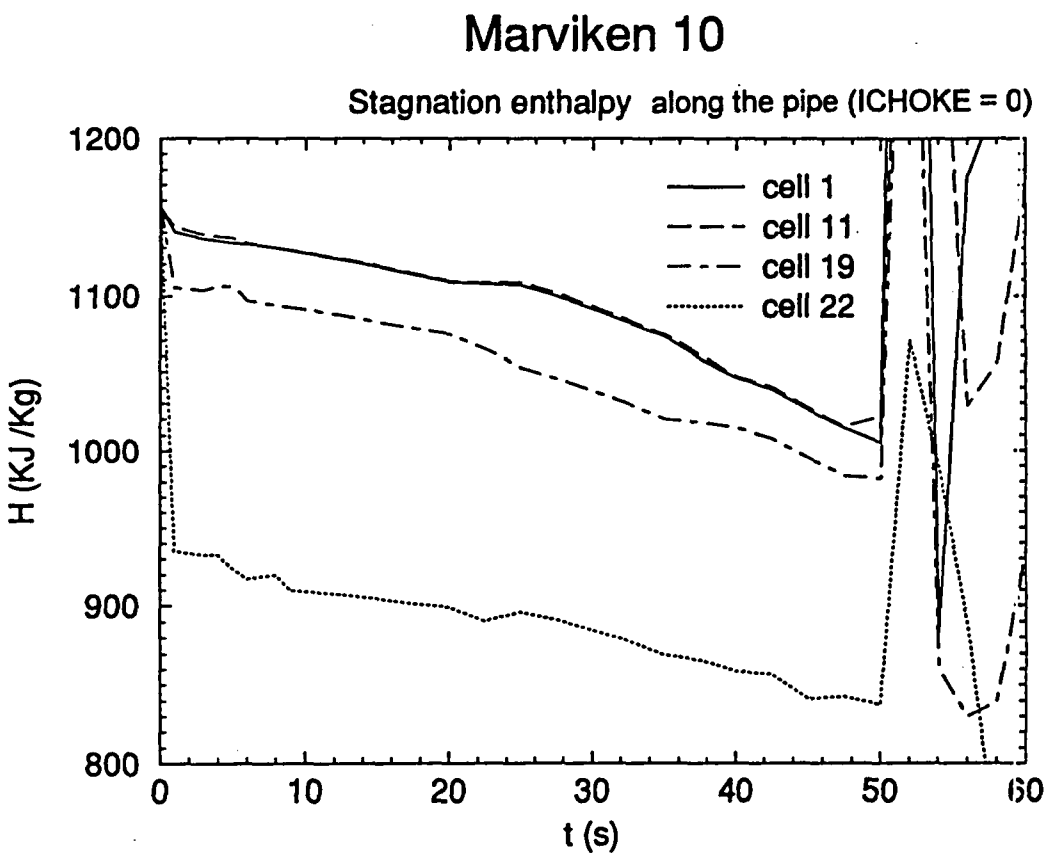

Figure 65

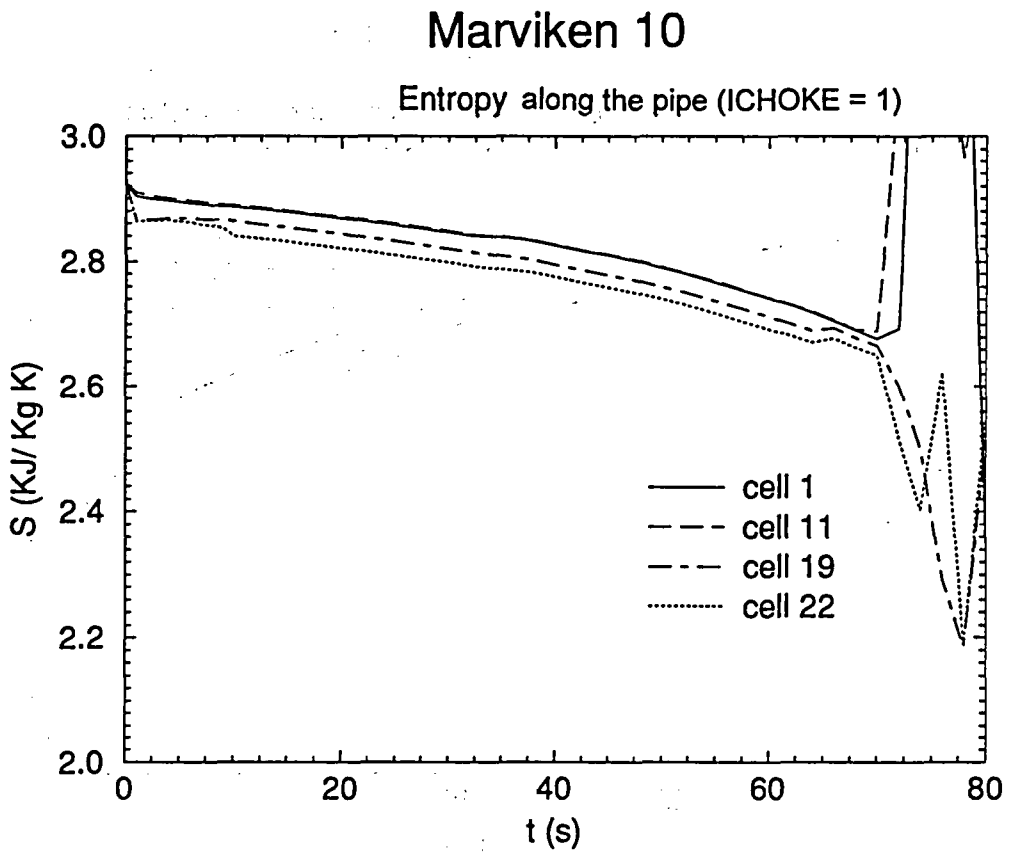

Figure 66

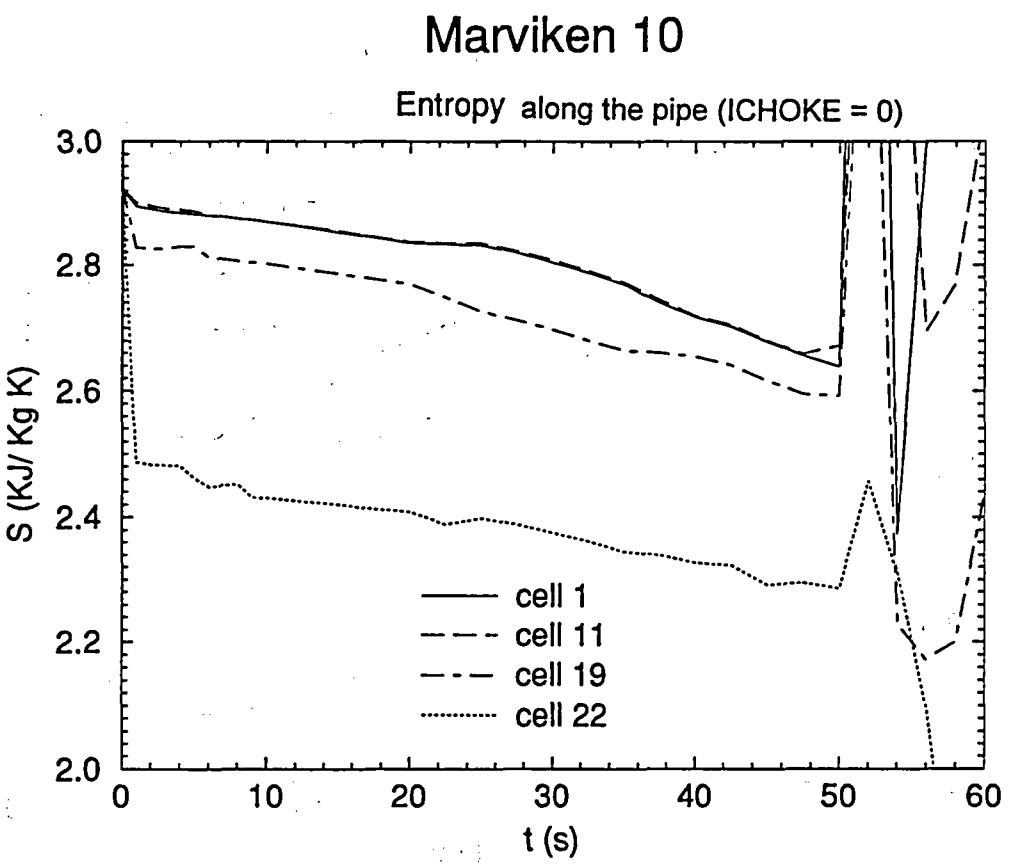

Figure 67

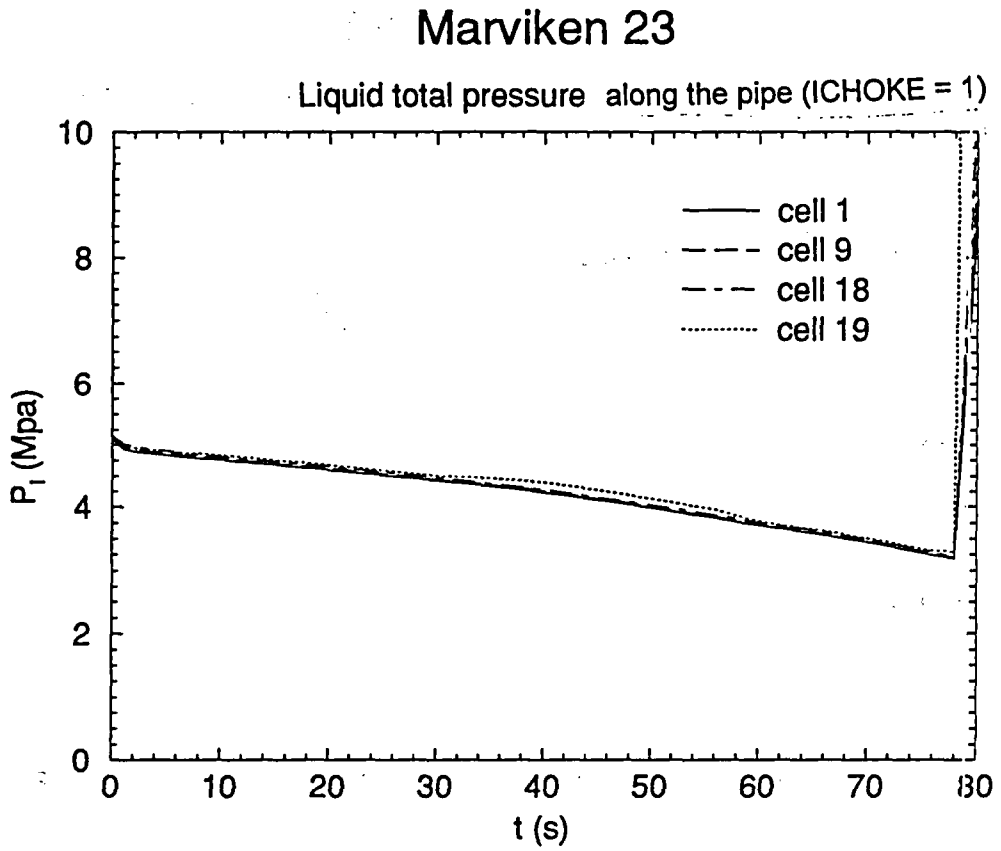

Figure 68

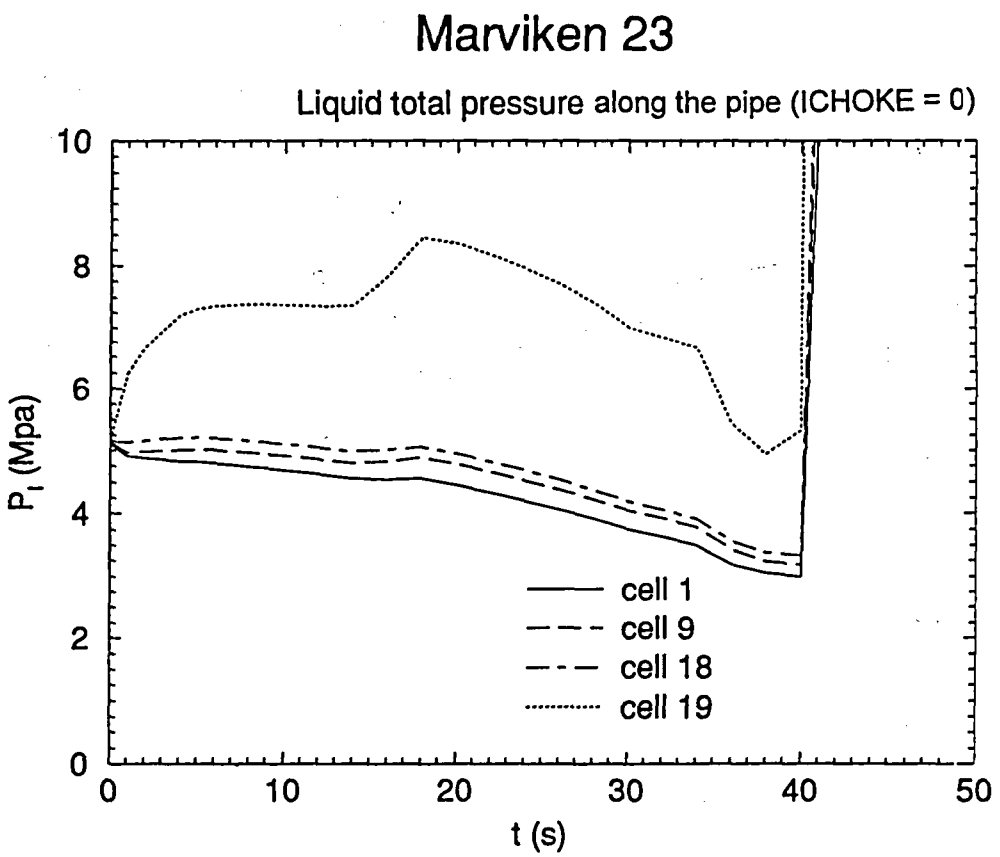

Figure 69

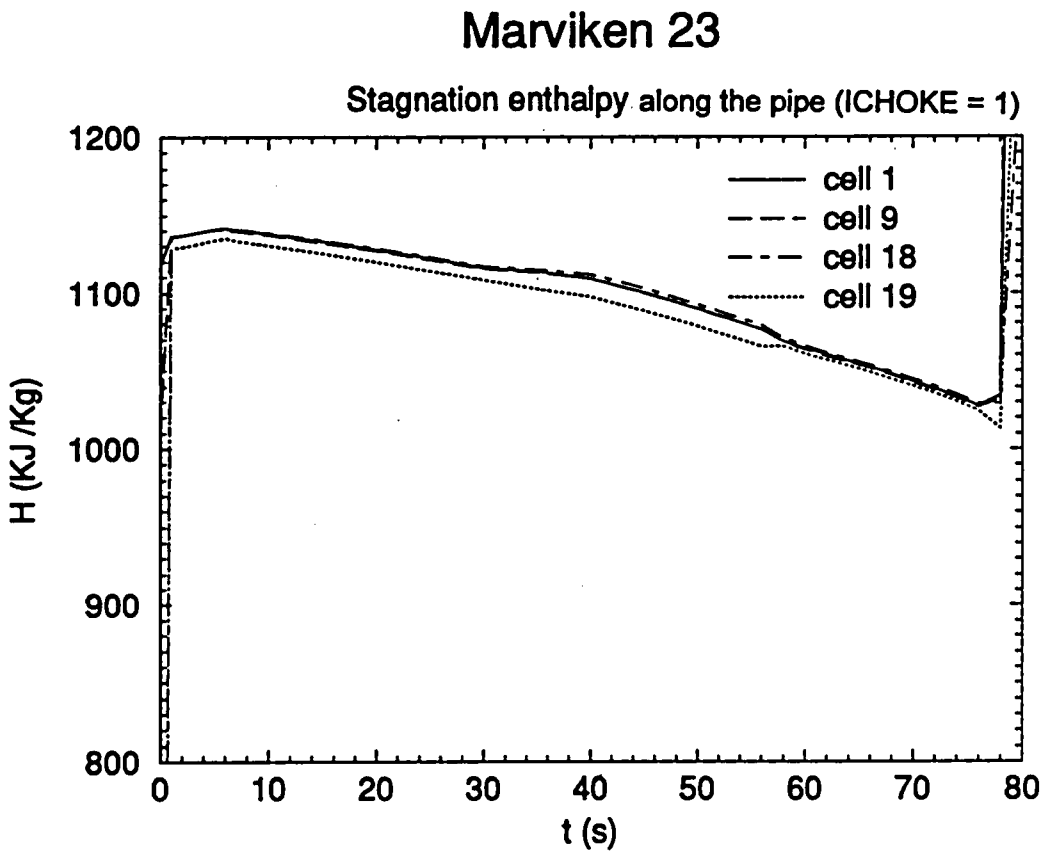

Figure 70

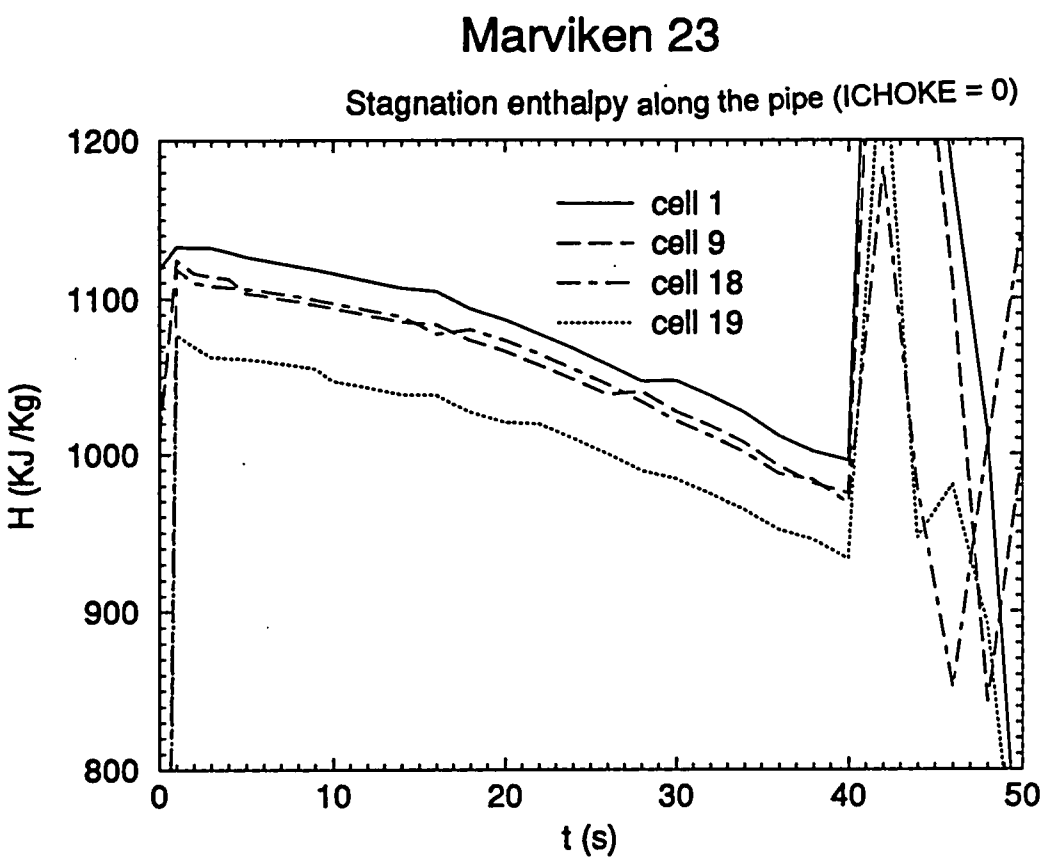

Figure 71

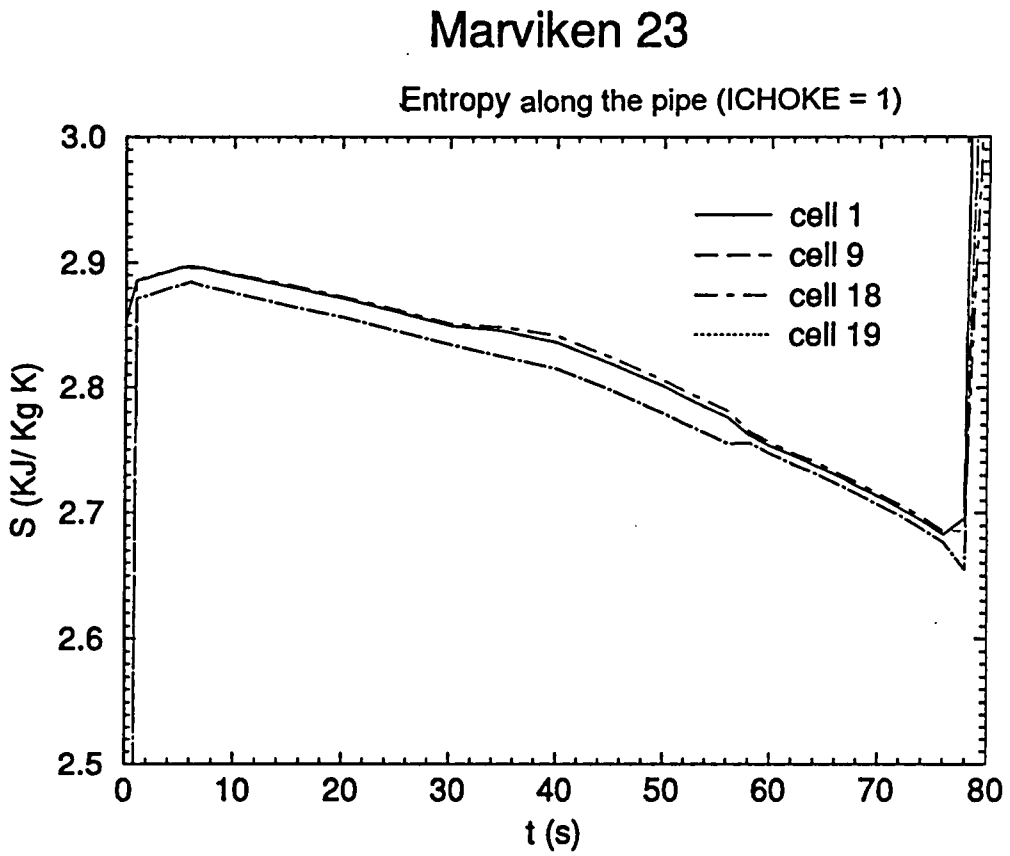

Figure 72

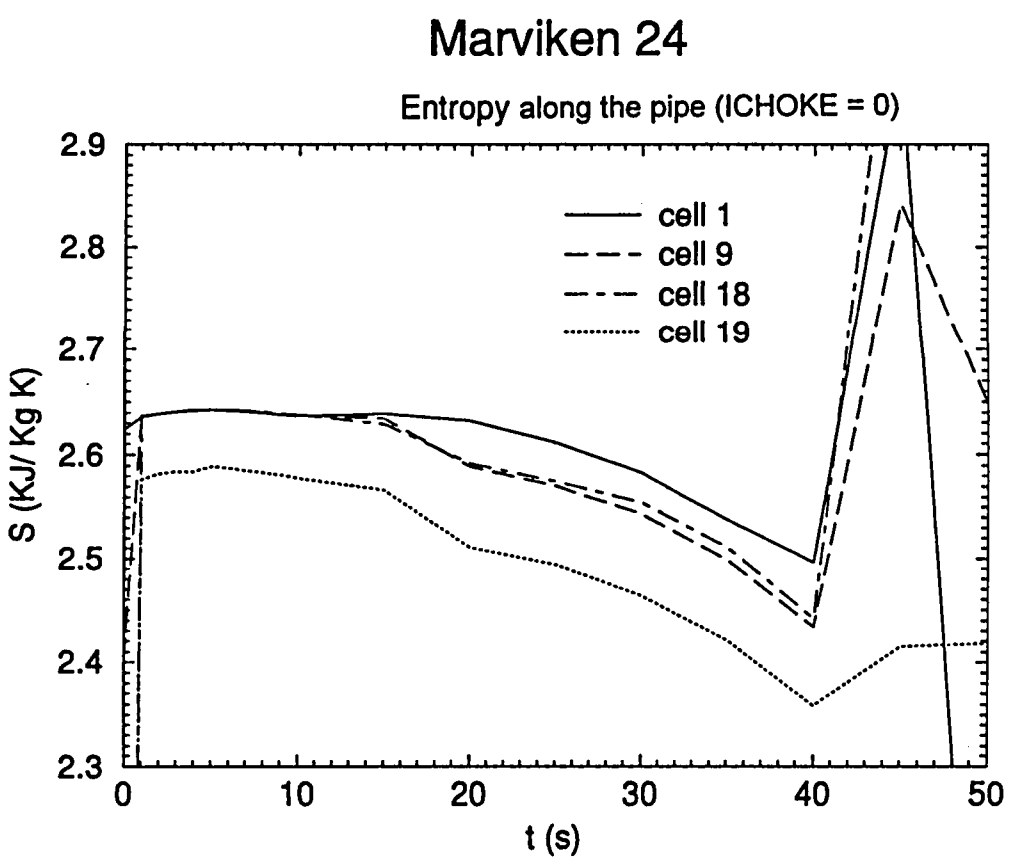

Figure 73

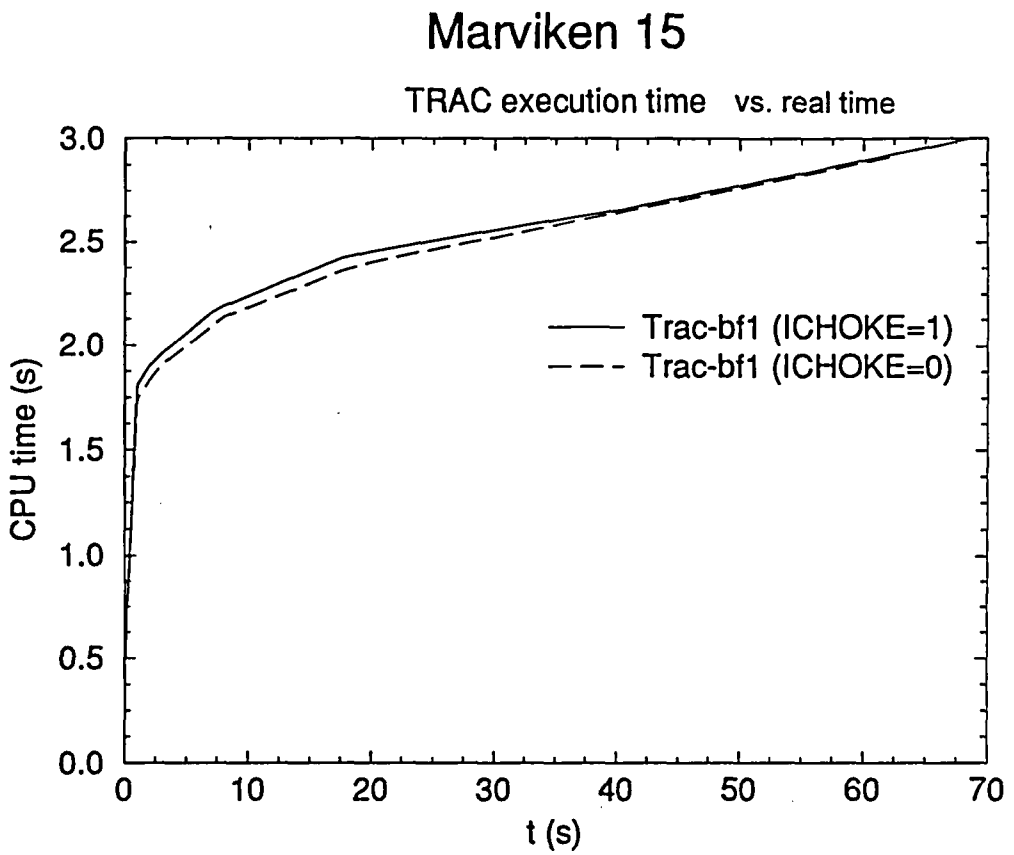

Figure 74

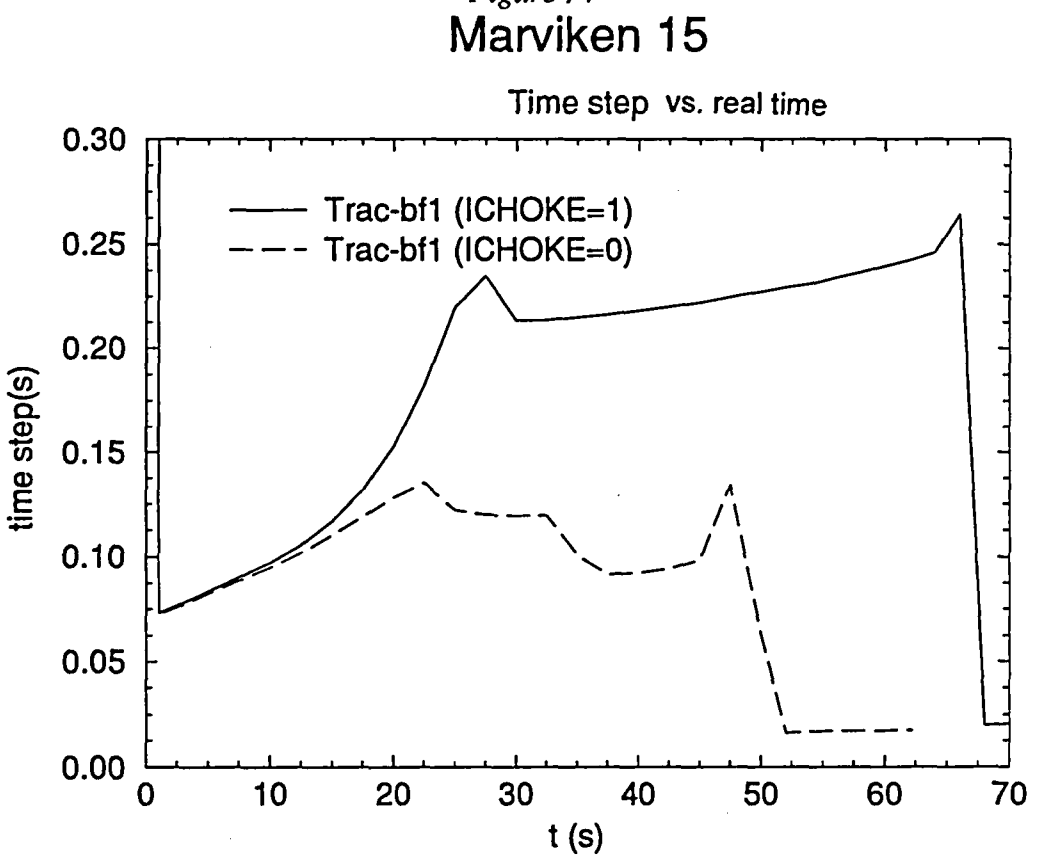

Figure 75

NRC FORM 335 (2-89) NRCM 1102, 3201, 3202

U.S. NUCLEAR REGULATORY COMMISSION

BIBLIOGRAPHIC DATA SHEET

(See instructions on the reverse)

1. REPORT NUMBER (Assigned by NRC, Add Vol., Supp., Rev., and Addendum Numbers, if any.)

NUREG/IA-0160

2. TITLE AND SUBTITLE

ANALYSIS OF THE CRITICAL FLOW MODEL IN TRAC-BF1

3. DATE REPORT PUBLISHED

MONTH	YEAR
May	1999

4. FIN OR GRANT NUMBER

5. AUTHOR(S)

M. Gomez, E. Valero, and I. E. Parra

6. TYPE OF REPORT

Technical

7. PERIOD COVERED *(Inclusive Dates)*

8. PERFORMING ORGANIZATION - NAME AND ADDRESS *(If NRC, provide Division, Office or Region, U.S. Nuclear Regulatory Commission, and mailing address; if contractor, provide name and mailing address.)*

UNIVERSIDAD POLITECNICA DE MADRID, Department of Applied Mathematics and Statistics
CONSEJO DE SEGURIDAD NUCLEAR, SPAIN

9. SPONSORING ORGANIZATION - NAME AND ADDRESS *(If NRC, type "Same as above"; if contractor, provide NRC Division, Office or Region, U.S. Nuclear Regulatory Commission, and mailing address.)*

Office of Nuclear Regulatory Research
U.S. Nuclear Regulatory Commission
Washington, DC 20555-0001

10. SUPPLEMENTARY NOTES

T. Lee, NRC Project Manager

11. ABSTRACT *(200 words or less)*

The critical flow model in TRAC-BF1 is assessed against five Marviken tests that include saturated and subcooled blowdowns under critical conditions with length-to-diameter ratio at the exit nozzle ranging from 0.3 to 3.6.

Results of this study indicate that the numerical scheme of TRAC-BF1 does not have critical solutions such as those described by the equilibrium analytical model; the critical condition must be imposed externally in the code using the semi-empirical model, CHOKE. When CHOKE is activated, the code calculates acceptable results although CHOKE still introduces certain intrinsic errors.

Both the CHOKE model and the analytical model fail to reproduce non-equilibrium effects arrising from transition from monophasic liquid to boiling mixture. Critical mass flow rates are generally underpredicted in subcooled blowdowns and discharges through very short nozzles.

When CHOKE is not activated, the code calculates erroneous results. A subcritical pressure is calculated at the nozzle exit. Pressure gradients and mass fluxes at the nozzle are generally overestimated. Erroneous behaviors are observed regarding conservation of quantities. Specifically, code calculations indicated that the second law of thermodynamics with regard to entropy could be violated.

12. KEY WORDS/DESCRIPTORS *(List words or phrases that will assist researchers in locating the report.)*

Assessment of the Critical Flow model, TRAC-BF1, Marviken tests

13. AVAILABILITY STATEMENT

unlimited

14. SECURITY CLASSIFICATION

(This Page)

unclassified

(This Report)

unclassified

15. NUMBER OF PAGES

16. PRICE

Printed on recycled paper

Federal Recycling Program

UNITED STATES
NUCLEAR REGULATORY COMMISSION
WASHINGTON, DC 20555-0001

OFFICIAL BUSINESS
PENALTY FOR PRIVATE USE, $300

SPECIAL STANDARD MAIL
POSTAGE AND FEES PAID
USNRC
PERMIT NO. G-67